



<https://theses.gla.ac.uk/>

Theses Digitisation:

<https://www.gla.ac.uk/myglasgow/research/enlighten/theses/digitisation/>

This is a digitised version of the original print thesis.

Copyright and moral rights for this work are retained by the author

A copy can be downloaded for personal non-commercial research or study,
without prior permission or charge

This work cannot be reproduced or quoted extensively from without first
obtaining permission in writing from the author

The content must not be changed in any way or sold commercially in any
format or medium without the formal permission of the author

When referring to this work, full bibliographic details including the author,
title, awarding institution and date of the thesis must be given

Enlighten: Theses

<https://theses.gla.ac.uk/>
research-enlighten@glasgow.ac.uk

SEISMIC STRATIGRAPHY OF THE ATTAHADDY FIELD
CONCESSION 6, SIRTE BASIN, LIBYA

BY
FAUZI AGELI SHALADI

THESIS SUBMITTED FOR THE DEGREE OF M.Sc.

IN THE

DEPARTMENT OF GEOLOGY
UNIVERSITY OF GLASGOW

DECEMBER 1990

ProQuest Number: 11007561

All rights reserved

INFORMATION TO ALL USERS

The quality of this reproduction is dependent upon the quality of the copy submitted.

In the unlikely event that the author did not send a complete manuscript and there are missing pages, these will be noted. Also, if material had to be removed, a note will indicate the deletion.



ProQuest 11007561

Published by ProQuest LLC (2018). Copyright of the Dissertation is held by the Author.

All rights reserved.

This work is protected against unauthorized copying under Title 17, United States Code
Microform Edition © ProQuest LLC.

ProQuest LLC.
789 East Eisenhower Parkway
P.O. Box 1346
Ann Arbor, MI 48106 – 1346

CONTENTS

page number

List of figures

List of tables

List of enclosures

Acknowledgments..... i

Summary..... ii

CHAPTER ONE : INTRODUCTION..... 1

1.1 Regional Geology and structural
setting of the Sirte Basin..... 1

1.2 Regional stratigraphy..... 4

1.2.1 Introduction..... 4

1.2.2 Northwestern Libya..... 7

1.2.3 Central Sirte Basin..... 10

1.2.4 Northeastern Libya..... 12

1.2.5 The intra-Cretaceous Unconformity..... 14

1.3 Tectonic and sedimentary model..... 14

1.4 The Attahaddy Field..... 17

1.4.1 Introduction..... 17

1.4.2 Field location..... 17

1.4.3 Geology..... 20

1 . 5 Previous work..... 22

1 . 6 Aims of the present research..... 29

CHAPTER TWO : GEOPHYSICAL AND GEOLOGICAL DATA USED IN THE STUDY..... 30

2 . 1 Data available..... 30

2 . 2 Seismic survey and processing..... 30

2 . 2 . 1 Data acquisition..... 30

2 . 2 . 2 Data processing..... 32

2 . 3 Wells used for the study..... 32

2 . 4 Description of well logs..... 32

CHAPTER THREE : SEISMIC INTERPRETATION..... 41

3 . 1 Number of seismic sections and examples..... 41

3 . 2 Horizons used for reflection identification..... 41

3 . 3 Seismic ties to well data..... 50

3 . 4 Seismic mapping..... 50

3 . 4 . 1 Time structure maps..... 56

3 . 4 . 2 Depth conversion..... 57

3 . 4 . 3 Depth structure maps..... 59

3 . 4 . 4 Average velocity maps..... 60

3 . 4 . 5 Isopach maps (in time)..... 60

3 . 5 Results..... 60

	<u>page number</u>
<u>CHAPTER FOUR</u> : SEISMIC STRATIGRAPHY.....	63
4 . 1 Introduction.....	63
4 . 2 Relevant aspects of seismic strati- graphy.....	64
4 . 3 The Eocene carbonate sequence.....	64
4 . 4 The Palaeocene shale sequence.....	67
4 . 5 The Upper Cretaceous units.....	71
4 . 6 Electric log correlation.....	79
4 . 7 Palaeogeographic evolution.....	79
<u>CHAPTER FIVE</u> : GENERAL INTERPRETATION AND CONCLUSIONS	84
5 . 1 Geophysical interpretation.....	84
5 . 2 Geological interpretation.....	85
5 . 3 Conclusion.....	87
5 . 4 Recommendations for further work.....	88
REFERENCES.....	90
APPENDIX I Well data used for the study.....	94
APPENDIX II Seismic two-way travel time values.....	111
APPENDIX III Average velocity and depth values for the reservoir horizon (Bahi/Gargaf).....	127

List of figures

	<u>page number</u>
Fig. 1.1 Sirte Basin with areal extent of basement, Cambro-Ordovician and younger Palaeozoic rocks.....	2
Fig. 1.2 Regional structure of the Sirte Basin.....	3
Fig. 1.3 The Upper Cretaceous-Tertiary formations of northern Libya.....	8
Fig. 1.4 Tectonic and sedimentation model, (after Yarborough, 1978).....	15
Fig. 1.5 Concession map.....	18
Fig. 1.6 Well location map.....	19
Fig. 1.7 Generalized columnar section of Attahaddy Field.....	21
Fig. 1.8 Isopach map of Bahi Formation, (after McDowell, 1988).....	23
Fig. 1.9 Isopach map of Socna Formation, (after McDowell, 1988).....	24
Fig. 1.10 Isopach map of Zmam Formation, (after McDowell, 1988).....	25
Fig. 1.11 Geological cross-section, (after Kardoes, 1986).....	27
Fig. 2.1 Side-label showing field parameters.....	31
Fig. 2.2 Side-label showing processing parameters.....	33
Fig. 2.3 FF6-6 composite log (Attahaddy Field).....	34
Fig. 3.1 Base map of the Attahaddy Field.....	42
Fig. 3.2 Seismic line V87-412.....	43
Fig. 3.3 Seismic line V87-410.....	44

	<u>page number</u>
Fig. 3.4 Seismic line V87-413.....	45
Fig. 3.5 Seismic line V87-415.....	46
Fig. 3.6 Seismic lines V87-406 and V87-407 at the point of intersection with well FF4-6.....	47
Fig. 3.7 Seismic line V87-402.....	48
Fig. 3.8 Seismic lines V87-406 showing a summary of the geological and geophysical data, in linking between well and seismic data.....	51
Fig. 3.9 Seismic lines V87-407 showing a summary of the geological and geophysical data, in linking between well and seismic data.....	53
Fig. 3.10 Seismic ties around a closed loop.....	55
Fig. 3.11 Average velocity to top Bahi/Gargaf as function of two-way time.....	58
Fig. 4.1 Seismic facies map showing reflection patterns, and relation to upper and lower boundaries of the Eocene carbonate sequence.....	65
Fig. 4.2 General depositional model of the Eocene carbon- ate sequence, with examples of reflection attitude- and continuity at positions A, B and C in the model.....	66
Fig. 4.3 Minor top lap at the top of the Eocene sequence.....	68
Fig. 4.4 Seismic reflection patterns of the Palaeocene shale, displaying two types.....	69
Fig. 4.5 Palaeocene lower shale sequence showing onlapping relation to the lower boundary.....	70

Fig. 4.6	Seismic facies map showing reflection patterns, and relation to upper and lower boundaries of the Palaeocene shale sequence.....	72
Fig. 4.7	Diagrammatic illustration showing the three models to explain the thickness variations of the Upper Cretaceous units.....	74
Fig. 4.8	Seismic facies map showing reflection patterns, and relation to upper and lower boundaries of the Upper Cretaceous units.....	75
Fig. 4.9	Seismic line V87-421 showing seismic configuration and geological model of the Upper Cretaceous units.....	76
Fig. 4.10	Map showing area where Socna Formation is absent.....	78
Fig. 4.11	Electric log correlation between wells (FF7,FF13, and-FF12), using gamma-ray and sonic tools, showing thickness variation of the Upper Cretaceous units.....	80
Fig. 4.12	Electric log correlation between wells (FF14,FF4, and-FF5), using gamma-ray and sonic tools, showing thickness variation of the Upper Cretaceous units.....	81
Fig. 4.13	Diagrammatic illustration of the erosional and depositional process creating the Upper Cretaceous units.....	82

List of Enclosures

- Enclosure 1. NW-SE geological cross-section.
- Enclosure 2. Top Sheghega TWT structure contour map.
- Enclosure 3. Top Heira TWT structure contour map.
- Enclosure 4. Top Zmam TWT structure contour map.
- Enclosure 5. Top Bahi/Gargaf TWT structure contour map.
- Enclosure 6. Depth structure map to the top Bahi/Gargaf.
- Enclosure 7. Average velocity map to top Bahi/Gargaf.
- Enclosure 8. Heira/Sheghega time isopach map.
- Enclosure 9. Zmam/Heira time isopach map.
- Enclosure 10. Structural cross-section through wells FF4-6, FF3-6 and FF9-6.
- Enclosure 11. Structural cross-section through wells FF14-6, FF1-6, FF8-6, and FF7-6.

ACKNOWLEDGEMENTS

I wish to record my deep thanks to my supervisor, Professor D. K. Smythe for his guidance, continued advice and help during the execution of this project, for his kind assistance in getting the data from the National Oil Corporation of Libya, and for interrupting his work to solve a problem when I knocked on his door.

I would like to thank Professor B. E. Leake as Head of Department, for his kind co-operation and help. I am grateful also to Dr B. Doody and Dr D. Watts for their help and useful discussion at various stages, and wish particularly to thank Professor M. Russell for his kind encouragement.

Thanks are due to Mr D. Maclean for his kind help in photographing sections, Mrs S. Hall for her help in tracing work, and Mr R. Morrison for his kind supply of important facilities for the project. I am also thankful to all the staff, Technicians and research students of the Geology Department for their help.

I am grateful to all people of Jawaby Oil Service in London for their care and help.

I would like to express my deep thanks to Mr A. Fatiss, Dr S. Kumati and all the staff members of the National Oil Corporation of Libya. I also thank the National Oil Corporation training Department for financial support.

Lastly, I am very grateful to all members of my family, especially my wife, for their moral support.

SUMMARY

The Attahaddy Field is a giant gas field discovered in 1964. It covers approximately 43,300 acres. Several exploration and outpost wells were drilled, displaying very good producibility in the field. This encouraged the company to drill numerous development wells. The total number of wells that have been drilled to date is 16, however, the development work is still continuing at the present time.

Seismic coverage over the Attahaddy Field comprises an area of approximately 200 km², of 12-30 and 48 fold Vibroseis seismic data acquired in 1980, 1983, 1984 and 1985 in the Concession 6 Area. The addendum incorporates an additional 270 km² of 30 fold Vibroseis data recorded in 1987.

The final interpretation presented in this study was carried out using only the 1987 data. This is due to the unresolvable seismic time misties between the different vintages caused by the use of different acquisition and processing parameters. The 1987 data, which provides adequate coverage for mapping, forms a seismic grid with the lines oriented in a NW-SE and NE-SW direction with approximately 2.5 km line spacing.

The stratigraphy of the Attahaddy Field starts at the top from the undifferentiated Oligocene-Miocene which consists of a mixture of deep-shallow marine shales and limestones with some interbedded clastic deposits of loose sand, which occurred during the transgression and regression of the sea during that time. Deeper in the section, the sedimentation of the Lower Eocene is dominated by carbonates, which have good porosity. It is believed that due to the lack of the source and cap rocks, no hydrocarbon accumulation has taken place.

The Palaeocene deep marine deposits (a very thick section of green shale) are believed to be the source rock for the underlying structural traps in most of Concession 6. In addition, a lot of problems have been encountered as the shale was penetrated, due to the stickiness and softness of the shale, resulting in the drill bit sticking during drilling, and thereby slowing the drilling time.

The Palaeocene shale has been subdivided into two seismic sequences, in which the lower part is characterized by layers truncated at the boundary with the upper part. This seismic stratigraphic subdivision is a new result from the present study. The upper part of the subdivided sequence is characterized by parallel layers that show a concordant relation to the upper bounding surface.

The Upper Cretaceous units consist mainly of sandy limestone and occasionally in some parts of the field consist of calcareous sand, underlain by the deep marine deposits of the Socna shale/limestone, which is absent in some places of the field as a result of the intra-Cretaceous unconformity.

As a result of the intra-Cretaceous unconformity, the deep marine deposit (Heira shale) of Palaeocene age was laid down above the Upper Cretaceous shallow carbonate deposits (Zmam Formation) which are separated from the Upper Cretaceous clastic deposits (Bahi Formation) by the early Cretaceous unconformity.

The thick underlying Cambro-Ordovician metamorphic section consists of highly fractured, massive, dense quartzitic sandstones and quartzite which form the hydrocarbon pay zone of the Attahaddy Field.

CHAPTER ONE

INTRODUCTION

1.1 Regional Geology and structural setting of the Sirte Basin

The Sirte Basin or embayment (Conant & Goudarzi, 1967), is one of several sediment-filled troughs which formed on the African foreland between the stable cratonic shield and the mobile Tethys belt (Klitzsch, 1971). It covers an onshore area of approximately 375,000 km², and contains 16 giant oil and gas fields.

The onshore portion of the Sirte Basin, with an estimated sedimentary area of 300,000 km², encompasses much of the northeast quadrant of Libya. To the northeast lies the Cyrenaica platform; to the south and to the west lie the Palaeozoic basins of Al-Kufrah, Murzuq and Ghadamis. The Sirte Basin is a cratonic rift, resulting from crustal extension of an old eroded basement and Palaeozoic uplift.

An excess of 8 km of predominantly marine late Mesozoic and Tertiary sediments have accumulated in the deeper segments of the basin. Although Palaeozoic deposition was generally widespread across the northern portion of the African continent, within the Sirte Basin only a meagre record of that era remains after the erosion during the Hercynian orogeny. Five major crustal uplifts, the Nafusah and Al Gargaf in western Libya, the Tibisti in Southern Libya, and the Sirte and Kalanshiyu arches of central and eastern Libya were strong positive features by the end of this orogeny. Some of the older basins date from Palaeozoic times and developed through several cycles of uplift and subsidence with various structural trends.

The Sirte Basin, however, was initiated in late Cretaceous times and has probably continued to subside, although with decreasing intensity, to recent times. Development commenced with the collapse of an eroded basement uplift (the Tibisti-Sirte uplift; Fig. 1.1), to form a series of tilted horsts and grabens generally trending NW-SE or E-W (Fig. 1.2). Early sedimentation was highly differentiated with deposition of shales in the grabens and carbonates on the horsts, but as transgression continued, Cretaceous sedimentation became more uniformly argillaceous.

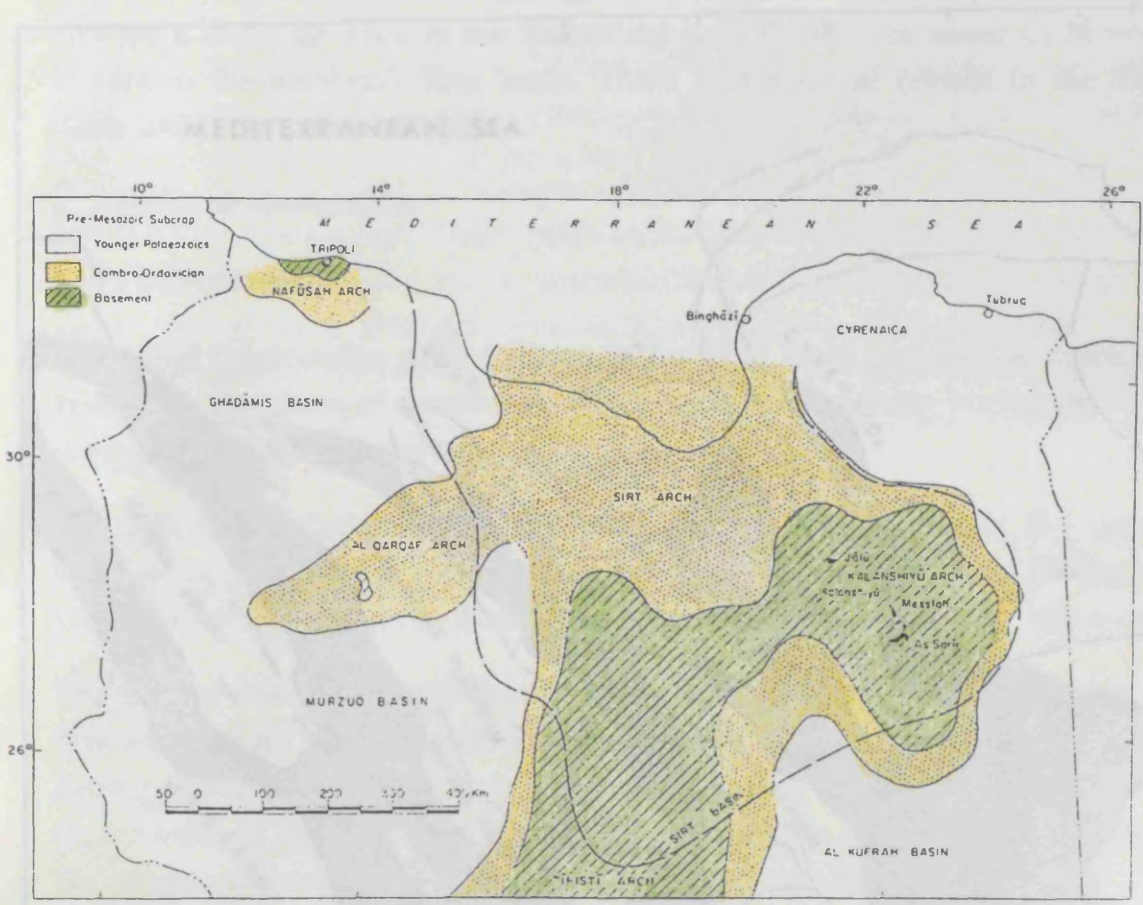


Fig. 1.1 Sirte Basin with areal extent of basement, Cambro-Ordovician and younger Palaeozoic rocks.

Fig. 1.2 Regional structure of the Sirte basin.

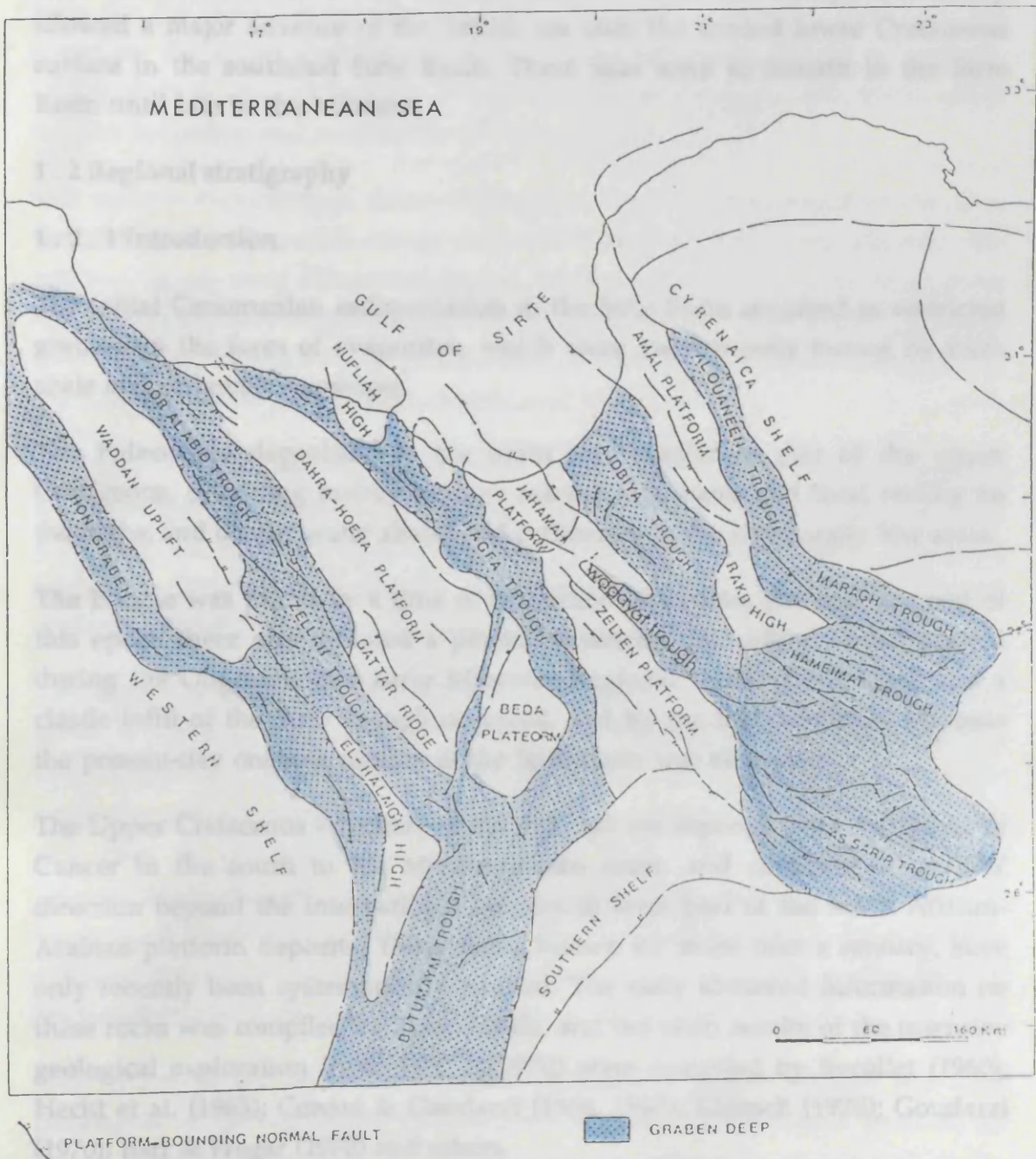


Fig. 1.2 Regional structure of the Sirte basin.

During the early Cenomanian the Sirte Basin developed structurally in the form that is presently recognized. At this time there occurred a collapse of the Sirte and Tibisti arches, and the rejuvenation of the Kalanshiyu downwarp allowed a major advance of the Tethys sea onto the eroded lower Cretaceous surface in the southeast Sirte Basin. These seas were to remain in the Sirte Basin until late in the Miocene.

1.2 Regional stratigraphy

1.2.1 Introduction

The initial Cenomanian sedimentation in the Sirte Basin occurred in restricted grabens in the form of evaporites, which were subsequently buried by thick shale and carbonate sequences.

The Palaeocene deposition in the basin was similar to that of the upper Cretaceous, providing mainly shallow marine carbonates and local reefing on the highs, and deeper water shales and carbonates in the structurally low areas.

The Eocene was primarily a time of carbonate deposition, but near the end of this epoch there was initiated a period of tectonic instability, which peaked during the Oligocene and early Miocene. Regional uplift of the basin and a clastic infill of the Sirte Trough occurred, and by the Middle-Upper Miocene the present-day onshore portion of the Sirte Basin was emergent.

The Upper Cretaceous - Tertiary strata in Libya are exposed from the Tropic of Cancer in the south to the Mediterranean coast, and continue in an E-W direction beyond the international borders to form part of the north African-Arabian platform deposits. These rocks, known for more than a century, have only recently been systematically studied. The early scattered information on these rocks was compiled by Desio (1943), and the main results of the intensive geological exploration (from 1955 to 1970) were compiled by Burollet (1960); Hecht et al. (1963); Conant & Goudarzi (1964, 1967); Klilzsch (1970); Goudarzi (1970); Barr & Wegar (1972) and others.

Comprehensive data on the Upper Cretaceous-Tertiary formations of Libya has recently been collected by the Industrial Research Centre (IRC), which was initiated in 1970. During the progress of regional geological mapping the IRC teams encountered a number of stratigraphical problems, caused by erroneous

transcriptions of local Arabic names previously used, incomplete descriptions and casual mention of stratigraphic terms; as well as the use of more than one term for the same lithostratigraphic unit by different authors. Generally 134 terms for the upper Cretaceous-Tertiary formations were named in northern Libya; of these only 45 formally introduced lithostratigraphic unit terms of the rank of formation and member have been adopted.

The surface exposures of these rocks in Al hamada al hamra and the Sirte Basin (NW Libya) exhibit nearly uniform lithological characters, allowing the unification of their lithostratigraphic nomenclature. However, the Upper Cretaceous-Tertiary strata exposed in Al jabal al akhdar and the Cyrenaica platform (NE Libya) are separated from the former by a wide stretch of late Tertiary-Quaternary cover (undifferentiated Miocene).

However, in both areas the Upper Cretaceous-Tertiary formations are made up of a carbonate, clay and calcilutite association with very minor evaporites, and a varying degree of dolomitization. The fauna suggest deposition mostly in neritic to littoral, with locally developed lagoonal, and rarely, bathyal environment of deposition (Megerisi & Mamgain, 1980).

The nature of the Cretaceous-Tertiary boundary is well known throughout much of Libya. In the Sirte Basin, where both Maastrichtian-Danian sediments are exceptionally well developed, exposures of their contact are found only along the western margin of the basin (Jordi & Lonfat, 1963; Gohrbandt, 1966; and Barr & Weegar, 1972, pp.171-173). There the Cretaceous-Tertiary (Maastrichtian-Danian) contact falls within the Zmam Formation, probably at the base of the Socna Formation. Although microfossils from these exposures indicate that there was a marked shallowing of the seas at the end of Maastrichtian time, no break in deposition is recognized.

Over much of the Sirte Basin, the Maastrichtian-Danian contact has been penetrated in the subsurface by hundreds of wells. In the deeper parts of the basin, there appears to be no interruption of deposition at the end of the Cretaceous. Often, however, there is an abrupt lithological change at this contact, reflecting a widespread and sudden change in depositional environment. This is the result of a shallowing of the late Maastrichtian seas, bringing the Cretaceous to a close, and then a strong transgressive surge at the beginning of the Danian (Barr, 1972a). In contrast, the Cretaceous-Tertiary

contact in Al Jabal al akhdar region (NW Libya) is usually marked by a major unconformity. Exposures are often poor and evidence is sparse in this region, making a detailed reconstruction of the tectonic and depositional history of this transitional period difficult.

Palaeocene

Palaeocene sediments are widespread through much of NW Libya. Limestone and marls of the Palaeocene Shurfah Formation cap hundreds of square kilometres of Al hamada al hamra area, although usually attaining a thickness of less than a couple of hundred metres. In the Sirte Basin Palaeocene seas also covered the entire basin, where they were deposited as a thick sequence of shales, marls and carbonates. A variety of lithofacies, representing varied depositional environments, are recognized in the subsurface of this basin, covering thousands of square kilometres. In some of the deeper troughs, up to a thousand metres of dark organic shales (Khalifa and Heira shales) are present. Some of these shales are considered to be important hydrocarbon source rocks. Along the eastern half of the basin, the Palaeocene sequence becomes predominantly a shelf carbonate facies.

Although the Palaeocene has been of wide distribution and importance in the Sirte Basin, very little is known of it from NE Libya. Early field studies of Al Jabal al akhdar recognized the well-exposed Eocene formations, but Palaeocene rocks were not recognized or documented until 1968, by the Petroleum Exploration Society of Libya field trip to northern Cyrenaica (Barr, 1968, p.138).

Because of structural complexities and the poor quality of the exposures in this area, contact relationships are uncertain. It appears, however, that the Eocene Apollonia limestone may unconformably overlies the Palaeocene chalk. It has been suggested that the Wadi dukhan Formation might overlie Al uwayliah chalk.

Eocene

Eocene strata are absent from most of northern Libya; however, much of the Sirte Basin contains a thick sequence of Eocene carbonates and evaporites. The lower Eocene (Ypresian) sequence of the Sirte Basin is principally assigned to

the Gir Formation (Domran equivalent), whereas the Middle Eocene (Lutetian) is referred to the Gialo limestone (Sheghega equivalent). The Upper Eocene (Priabonian) of the Sirte Basin is usually referred to as the Augila Formation (Etel equivalent). The Upper Eocene formation is the result of a regional shallowing of the seas which brought the Eocene cycle to a close - the Augila Formation is unconformably overlain by sands of the Oligocene Arida (Muailah) Formation.

Oligocene

Following the definitions of Barr & Weegar (1972), the base of the Oligocene has been taken at the top of the upper Eocene Augila Formation, and the upper boundary has been drawn at the base of the thin shale which immediately overlies the uppermost beds of the Diba Formation (Muailah equivalent).

The stratigraphic nomenclature adopted for NW and NE Libya is presented in Fig. 1.3, along with its correlation with the subsurface of the Attahaddy Field in the Sirte Basin.

1.2.2 Northwestern Libya

Upper Cretaceous

The thickness of surface exposures of Upper Cretaceous formations in NW Libya averages around 870 m (Megerisi & Mamgain, 1980), but exceeds 1800 m in the subsurface. They are divisible into the following lithostratigraphic units.

Sidi as side Fm (Cenomanian) Forming the base of the marine Upper Cretaceous succession, the lower part of the Formation is characterized by limestone and dolomitic limestone, and the upper part is characterized by a clay -marl-evaporite sequence. The Formation is exposed all along the Jabal Nafusa escarpment, increasing in thickness from 65 m in the west to 380 m in the east.

Nalut Fm (Cenomanian-Turonian) It is characterized by grey to cream coloured, hard, crystalline dolomitic limestone and dolomite, with common chert concretions in the upper part. The thickness varies from 40 m in the west to 200 m in the eastern part.

ERA	PERIOD	EPOCH	AGE	STRATIGRAPHIC SEQUENCE IN AL HAMADA-WESTERN SIRTE BASIN(MAGRISI&MAMGAIN, 1980)	SUB-SURFACE SEQUENCE IN SIRTE BASIN (ATTAHADDY FIELD)	STRATIGRAPHIC SEQUENCE IN AL JABAL AL AKHDAR, EAST (MAGRISI&MAMGAIN,1980)									
CENOZOIC	TERTIARY	NEOGENE	PALAEOGENE	AL KHUMS FORMATION	UNDIFFERENTIATED	AR RAJMAH FM.									
							PLIO.	ZANCL- PLACENZ	MIocene	AL FAIYDIAH FM.					
							U	TORTON- MESSIN							
							M	SERRAVA- LINE LANGHIAN							
							L	AQUITAN- BURDHGH							
							U	CHATTIAN			MUAILAH FM.				
							L	RUPELIAN			ETEL FM.				
							U	PRIABONI- NIAN			SHEGHEGA FM.				
							M	LUTETIAN			DOMRAN FM.				
							L	YPRESIAN			RUAGA FM.				
							U	LANDENIAN			HEIRA FM.				
							M	MONTIAN			ZMAM FM.				
							L	DANIAN			SOCNA FM.				
							MESOZOIC	CRETACEOUS			UPPER	PALAEO.	SHURFAH FM.	BAHI FM.	AL UWAYLIAH FM.
CAMPANIAN	FM.	AL MAJAHIR FM.													
SANTONIAN	?	AL BANYAH FM.													
CONIACIAN		QASR AL AHRAR FM.													
TURONIAN															
CENOMAN.															
	SIDI AS SID FM.														
	NALUT FM.														
	QASR TIGRINNAH FM.														

Fig. 1.3 The Upper Cretaceous-Tertiary Formations of northern Libya.

Qasr Tigrinnah Fm (Turonian-Coniacian) It is characterized by greenish-grey marls, gypsiferous in the lower part, whereas the upper part is made up of white porous chalky limestone and marl, The thickness varies from 30-130 m.

Mizdah Fm (Santonian-Campanian) The lower part is characterized by yellowish-white to pink crystalline limestone; the upper part consists of white chalky and thinly bedded limestone. It varies from 5-30 m in thickness.

Zmam Fm (Campanian-Maastrichtian) It is a claystone, marl, limestone and dolomitic limestone sequence. The exposed thickness varies from 40-190 m, and it marks the end of the upper Cretaceous marine succession.

Tertiary

The Tertiary outcrops averages 700 m in thickness, which is exceeded by the 4800 m in the subsurface. They are divisible into the following lithostratigraphic units.

Shurfah Fm (Palaeocene) The marlstone, chalk and chalky limestone sequence is divisible into three members, with a maximum exposed thickness of 100 m, The lower part consists of thinly bedded limestone - marlstone at the base followed by platy claystone and white to cream chalky limestone. The middle part is characterized by chalk and chalky limestone, and the upper part by well-bedded dolomitic limestone with a few marl intercalations.

Bishimah Fm (Lower Eocene) The lower part is characterized by greenish-buff marl and nodular to dolomitized limestone, which straddles the Palaeocene-Eocene boundary, overlain by chalky limestone. The upper part is characterized by massive thick-bedded chalky and dolomitic limestone. The Formation varies in thickness from 30-120 m, and mostly represents Ypresian age.

Al Jir Fm (Middle Eocene) It is characterized by white chalk and chalky limestone in the lower part, and medium-grained limestone in the upper part. The thickness varies from 35 - 65 m.

Wadi Thamat Fm (Middle-Upper Eocene) It is divisible into three parts ; the lower part consists of greenish to buff marly limestone; the middle part consists of massive white argillaceous limestone and indistinctly bedded

brown weathering chalk; the upper part consists of yellow to cream coloured limestone alternating with marls. The average thickness of this formation is 250 m.

Umm Addahiy Fm (Lower Oligocene) It is characterized by alterations of organodetrital limestone, marl and marlstone. The thickness of this formation averages around 40 m.

Bu Hashisha Fm (Upper-Oligocene) It is characterized by white to brownish and cream coloured limestone, followed by the alternations of dolomitic limestone and marlstone, averaging 40 m in thickness.

Mazul Ninah Fm (Lower to Upper Oligocene) It represents the 30-60 m thick lagoonal to lacustrine deposits of the Oligocene Epoch. The lower member consists of alterations of greenish-brown to reddish-brown clay and claystone, with gypsum. The upper member is formed of chalky and marly limestone grading into crystalline limestone.

Tarab Fm (Lower to Upper Oligocene) It is characterized by a 6 m thick sequence of thinly bedded claystone, marlstone and calcilutite.

1.2.3 Central Sirte Basin

Upper Cretaceous

The thickness of the subsurface Upper Cretaceous formations in the area of the Attahaddy Field averages around 300 m. They are divisible into the following lithostratigraphic units.

Bahi Fm (Cenomanian) The Bahi Formation consists of interbedded sandstone, siltstone, conglomerate and shale. Sandstone and pebbly sandstone are the most common lithologies. The Bahi Formation occurs in the northwestern part of the Sirte Basin and is especially well developed in the Bahi Field (Concession 32) area. The thickness of the Bahi Formation varies from a few metres to a maximum of over 100 m. The Formation unconformably overlies a Lower Palaeozoic formation of probable Cambro-Ordovician age.

Socna Fm (Campanian-Maastrichtian) This Formation consists of a shale sequence with thin limestone interbeds; the shales range in colour from dark grey to mainly dark brown, they are carbonaceous and calcareous for the most part, and grade into shaly limestone, and they become increasingly silty and sandy towards the base. The thickness of Socna Formation averages around 120 m in the central and western Sirte Basin. The Formation rests on rocks as old as the Bahi Formation, where the unconformity is present, whereas in the eastern Sirte Basin, the time equivalent of the Socna Formation becomes calcareous in the lower part. In this Field, however, the name Socna is restricted to the upper shale sequence.

Zmam Fm (Maastrichtian-Lower Palaeocene) The Zmam Formation consists predominantly of white, tan or grey limestone, argillaceous calcilutite, with some dark grey calcareous shale interbeds. Occasionally the upper part of the Formation becomes calcarenitic. In the eastern Sirte Basin the Zmam Limestone becomes white and increasingly chalky, which is quite similar to that of the Atrun Limestone. The thickness ranges from about 30-120 m. Although this Formation occurs over much of the Sirte Basin, it is not normally a reservoir, but since it is a tight micrite, it makes a good seismic reflector which was used for mapping the top Cretaceous.

Tertiary

Heira Fm (Lower Palaeocene) This Formation consists mainly of a shale sequence with occasional thin limestone interbeds. The shale is dominantly grey, soft to medium hard, calcareous, fossiliferous and slightly silty in part. Occasional beds of light brownish grey, very calcareous clay occur in association with the shales. The limestone beds, which are more common in the upper part of the Formation, are grey, tan and brown, very fine grained, hard and dense. The top of the Formation is marked by a characteristic reduction in electric log resistivity at a sub-sea depth of -4064 ft (-1220 m), while the base is placed at a similar characteristic increase in resistivity at -5880 ft (-1765 m). The Heira Formation makes a cap-rock for the various older reservoir sediments.

Ruaga Fm (Upper Palaeocene) The Ruaga Formation consists predominantly of a limestone sequence with very subordinate amounts of shale. The limestone is dark brown, hard, argillaceous, calcilutite and sometimes calcarenite with thin stringers of grey-green pyritic shale. The thickness of this

Formation ranges from 60-90 m, which remains fairly constant over a large area where it is typically developed.

Domran Fm (Lower Eocene) The lower part of the Domran Formation consists mainly of thin bedded, tan, chalky calcarenite layers, which contains dark grey chert nodules in every two to three metres. The middle and upper portions of the Formation consist of alternating thin beds of soft, white, chalky calcilutite and harder tan calcilutite. Chert nodules are less common in the upper part of the Formation. The thickness of this Formation ranges from 240-300 m.

Sheghega Fm (Middle Eocene) The Sheghega Formation consists of a thick sequence of grey or tan to brown, shallow marine limestone. It is highly fossiliferous, containing concentrations of several species of nummulites, which in parts of the sequence make up a high percentage of the limestone. Portions of this Formation are chalky and very friable. The Formation is widespread in the subsurface of the Sirte Basin, and its thickness ranges from 300-360 m.

Etel Fm (Lower Oligocene) The Etel Formation consists mainly of a soft, light grey to dark green shale, which is sometimes silty. The thickness of this Formation varies from about 120-180 m.

Muailah Fm (Upper Oligocene) The Muailah Formation consists of an alternating sequence of thick sandstone units and thin shales, while a few sandy limestone beds are present at the very lower part of the Formation. The shale is soft, silty, and grey to green in colour. The Formation varies in thickness from 100-165 m.

1.2.4 Northeastern Libya

Upper Cretaceous

The surface exposures of the Upper Cretaceous rocks in Al Jabal al akhdar average 980 m in thickness and are divisible into the following lithostratigraphic units.

Qasr al ahrar Fm (Cenomanian) It is characterized by green to yellow marl with rare intercalations of marly limestone. The exposed thickness varies from 20-30 m.

Al banyah Fm (Cenomanian-Coniacian) It is characterized by marly limestone, intercalated with dolomitic limestone. The thickness varies from 35-600 m, due to pre-Campanian erosional intensity.

Al majahir Fm (Campanian) It is represented by light grey marls, followed by fine-grained marly to chalky limestone, thick bedded and dolomitic in the middle and upper part. The thickness varies from 70-200 m.

Wadi dukhan Fm (Maastrichtian) It consists of dark grey to brown dolomite and vuggy dolomitic limestone, which is massive.

Tukrah Fm (Senonian) It is characterized by light grey, well-bedded compact limestone with chert nodules. The exposed thickness averages a few tens of metres.

Al hilal Fm (Cenomanian-Coniacian) These are the brownish and greenish-grey thinly bedded marl exposed for a few tens of metres.

Al athrun Fm (Maastrichtian) Is the tan white microcrystalline limestone, with marly intercalations and lenses of brown chert, with an exposed thickness varying from 45-52 m.

Tertiary

The exposed thickness of Tertiary formations in Al jabal al akhdar and Cyrenaica region averages around 990 m, and has been differentiated into the following lithostratigraphic units.

Al uwayliah Fm (Palaeocene) It is characterized by greenish marl, whitish chalk and bedded chalky limestone, that extends for a few metres in thickness.

Apollonia Fm (Lower-Middle Eocene) It is represented by cream coloured microcrystalline limestone, with grey to brown lenses and nodules of chert.

Darnah Fm (Middle-Upper Eocene) It consists of massive, medium to coarse-grained, nummulitic limestone, and dolomitic limestone. The exposed thickness averages around 100 m.

Al bayda Fm (Lower Oligocene) It is marl and marly limestone in the lower part, and organodetrital limestone in the upper part. The exposed thickness averages around 40 m.

Al abrag Fm (Lower-Upper Oligocene) It is characterized by a limestone, dolomitic limestone, dolomite and marl sequence. It varies in thickness from 60-130 m.

Al faidiyah Fm (Oligocene-Miocene) It consists of greenish calcareous clay, marl and marly limestone; the thickness of this Formation varies from 10-100m.

1.2.5 The intra-Cretaceous Unconformity

The intra-Cretaceous unconformity, at the base of the marine Upper Cretaceous sequence, is present through the Sirte Basin and is of profound significance to the entrapment of the billions of barrels of petroleum in the underlying sandstone. As a generalization, the major clastic accumulation in the Sirte Basin occurs below this unconformity. The plane of the unconformity reflects the cessation of non-marine Mesozoic conditions and the incoming of an Upper Cretaceous sea in Cenomanian-Turonian times.

1.3 Tectonic and sedimentary model

The Sirte Basin is a late Mesozoic-Tertiary cratonic rift resulting from crustal extensions of older basement and Paleozoic rocks. The tectonic evolution of the Sirte Basin controlled the sedimentation and provenance of the sediment material that built the stratigraphic section in the study area. The formation of the Hagfa (Heira), Sirte (Socna), Sarir and Wadayat troughs and their associated platforms characterised the basin, and is responsible for the major plays in the Sirte Basin.

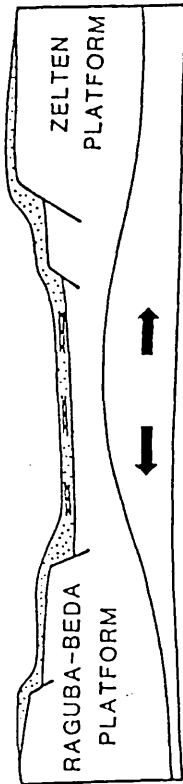
The evolution of the basin can be broken down into four major sequences of deformation and sedimentation (Yarborough, 1978), which is reflected in the Hagfa trough by the rift valley formation model (Fig. 1.4).

(1) Palaeozoic formation of the Sirte Arch: The extent of Palaeozoic sedimentation in the Sirte Basin is not known. Patches of Silurian rocks are known, but subsequent erosion has removed all but a few traces of Palaeozoic

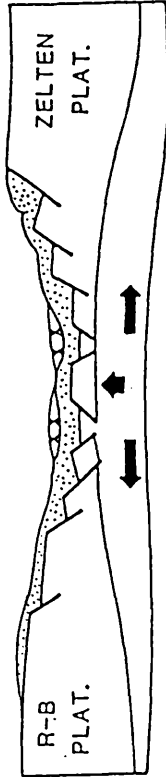
HAGFA TROUGH (RIFT VALLEY FORMATION) TECTONIC SEDIMENTATION

TECTONIC MOVEMENT

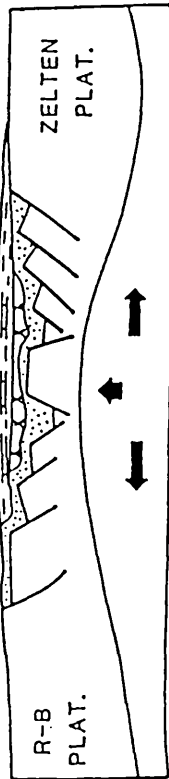
A. CRUSTAL THINNING
(FAULTING) PRE-RIFT STAGE



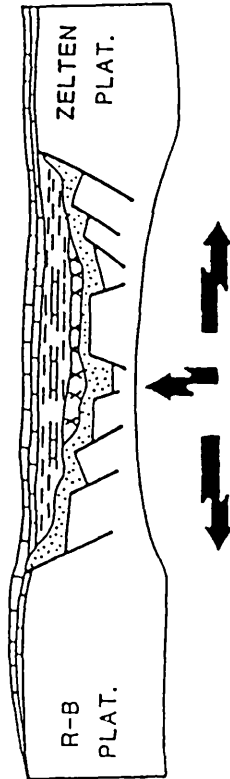
B. UPLIFT+EXTENSION
EARLY RIFTING
(AULACOGEN)(FORMATION)



C. MAXIMUM RIFTING
AND DEVELOPMENT
OF THE WADI-HORST



D. STABILIZING
THE TECTONIC ACTIVITY
AND SEDIMENTATION
FILLING OF LOW AREA.



A. ALLUVIAL STAGE
CLASTICS +

B. EVAPORITE STAGE
MAY BE ABSENT
EVAPORITE+LUCUSTRINE
+EARLY MARINE
PRECIPITATION
(SALT WAS TRACED ONLY
AROUND D4-NC149)

C. EARLY DEEP
MARINE STAGE

D. ULTIMATE
DEEP+SHALLOW
MARINE DEPOSITS
(CHALKS, MARLS,
REEFS, BLACK SHALE.)

Fig. 1.4 Tectonic and sedimentation model, (after Yarborough, 1978).

rocks. During the Palaeozoic a broad tectonic arch developed on the site of the Sirte Basin. Erosion removed virtually all sediments down to the Cambro-Ordovician Gargaf Formation, resulting in widespread deposition around the flank of the Arch of the Nubian formation (Upper Palaeozoic to Lower Cretaceous).

(2) This was followed in the Aptian-Albian by arch foundering and pre-Socna major block faulting. Extensional forces were enhanced by the continued uplifting of the basin (Calbick & Smith, 1967). This tectonic stage instigated the Cretaceous marine transgression and marked the termination of alluvial-lacustrine sedimentation, and as a result, a series of horst and grabens was developed. Sedimentation was mainly active in the subsiding grabens, while the horsts or platforms were emerging above sea level and acting as a source area for the early marginal clastic wedge developments. These were deposited on the downthrown sides of the major faults and caused a change in facies to evaporite/shale and/or shale/limestone sequences away from the platform margins. The clastic accumulation on the downthrown sides of the faults is found to be prospective in several parts of the basin (Williams, 1970). This graben-fill sedimentation of the Bahi and Waha clastics and the Cretaceous Socna shales was terminated by the deposition of widespread, argillaceous limestone of the Gheriat (Zmam) Formation at the end of Maastrichtian time.

(3) Following the deposition of the Gheriat (Zmam) Formation, regional subsidence occurred where a series of carbonate and shale units was deposited during the Palaeocene and Eocene. Lateral facies changes occurred in these units, reflecting not only the development of grabens but also the shifting of the sedimentation depocentre from one area to another. Due to this facies shift during the Lower to Middle Palaeocene the Heira shale changes to dolomite (Al uwayliah/ Sabil Formations) to the east of the Zelten Platform. Also the Heira developed several reefal buildups and carbonate banks, represented by the Ora, Meem and Mabruk Members. During the Eocene, block faulting rejuvenation of Sitra and Domran deposits created the final stage of this structural setting.

(4) Finally, the basin tilted to the north-east during late Eocene time owing to the development of the major depocentre in what is today the Agedabia Trough. Here, Oligocene/Miocene sediments are up to 3,900 m thick.

1. 4 Attahaddy Field

1. 4 . 1 Introduction

The Attahaddy Field (formerly Areada) is located in the NW part of Concession 6. The discovery well FF1-6 was drilled by Esso Standard Libya, Inc. in 1964, and tested gas from a thin Bahi section, and drilled 28 m into the Gargaf, but this section was not tested. The FF2-6 well was drilled 30 m into the Gargaf in 1967. It tested gas, but this test was not conclusive.

In 1985 FF3-6 was a big success, establishing a potential gas column in the Gargaf of over 640 m. This success formed the basis of an appraisal programme in the field.

Several exploration and outpost wells were then drilled, displaying very good producibility in the field. This encouraged the company to drill numerous development wells. The total number of wells that have been drilled to date is 16, however, the development work is still continuing, and more wells in the field are being drilled.

The Field is now owned by Sirte Oil Company, the third biggest oil company in the country, which belongs to the National Oil Corporation of Libya.

1. 4 . 2 Field location

The Attahaddy Field is located in the NW portion of Concession 6 (Fig. 1.5). It covers approximately 43,300 acres. The field is mainly located on the Menzella ridge of the Zelten Platform in the Sirte Basin, between the Hagfa Trough and Wadayat Trough (the Sirte Basin deep).

Despite the 16 appraisal and delineation wells that have been drilled already (Fig. 1.6), the NW sector of the Field has not yet been investigated. Well FF17-6 will fulfil that need.

The field comprises a main central block (Central horst), plus peripheral areas to the north and south.

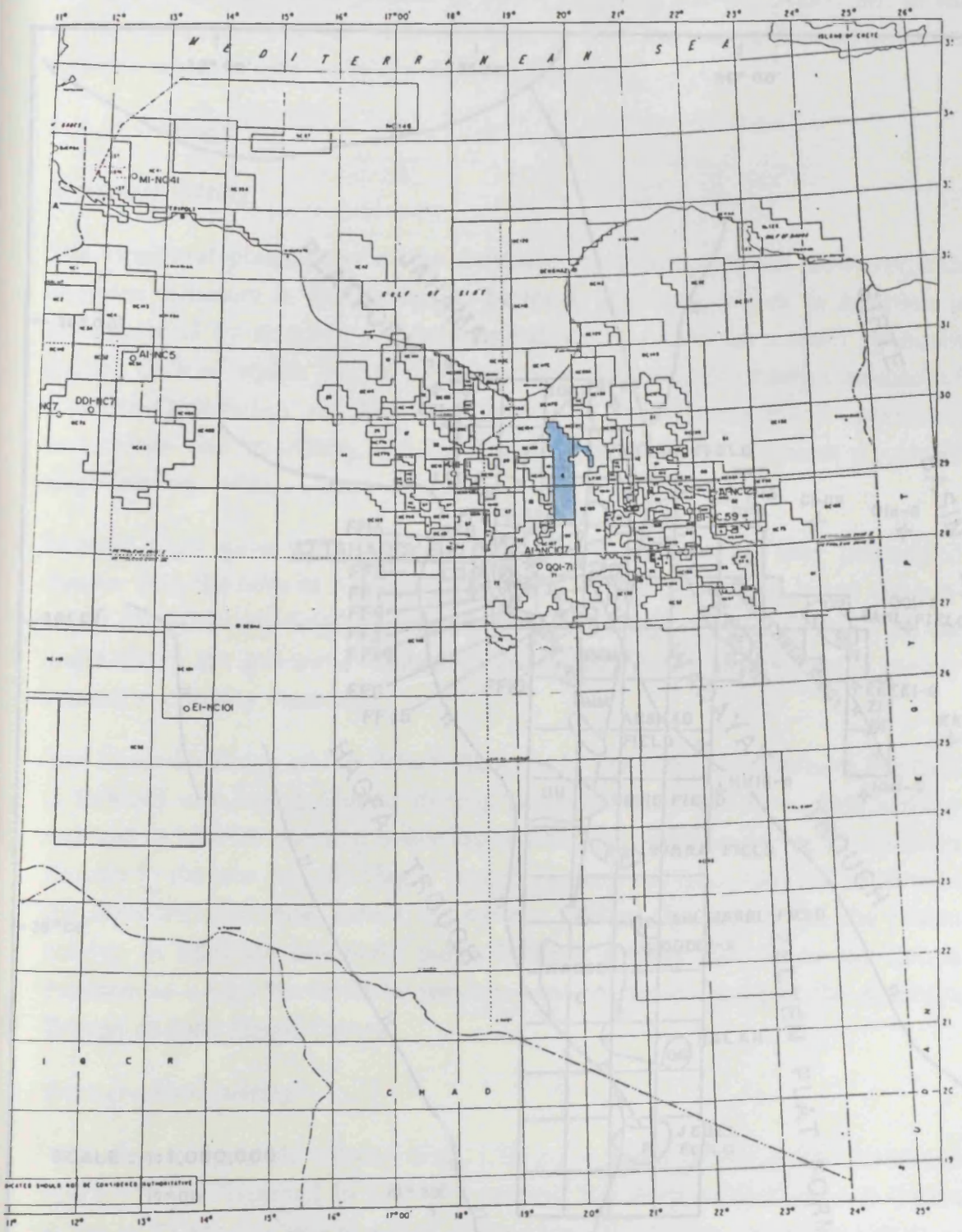


Fig. 1.5 Concession map.

The gas-water contact is present at about -12200 ft sub-sea (-3660 m), in the south-western part of the field. The base of the reservoir is formed by a red siltstone which is present below -12200 ft (-3660 m).

1.4.3 Geology

Structural setting

The structural phenomena of the field are quite complicated. However, this complex structure is understood to be block structure, which in addition is accompanied by dividing the field into different blocks (separated by major faults), each of which has its own structural features. The Early Cretaceous/Cambro-Ordovician faulting has produced highly fractured quartzitic sandstones and quartzite, and subdivided the area into different structural traps (Keskin, 1988).

Several wells have been drilled in different blocks, where they penetrated deeper than the ones in nearby blocks. Those which penetrated below the gas-water contact in the neighbouring blocks showed higher producibility than the wells above the gas-water contact of the field in other blocks, this is mainly related to porosity variation.

The Menzella Ridge of the Zelten Platform in the Sirte Basin (where the field is located) was highly faulted during Cambro-Ordovician time. This activity resulted in NW-SE trending major faults which extend parallel to the Ajdabiya Trough to the east and the Hagfa Trough to the west, from the Gulf of Sirte in the Mediterranean Sea, across the eastern part of the country to the Sudan border. In addition this early major faulting activity developed the Zelten Platform as a high bordered by two low areas of sedimentation, the Ajdabiya Trough and the Hagfa Trough.

Stratigraphical setting

See the stratigraphic column (Fig. 1.7). As a result of the intra-Cretaceous unconformity discussed in previous section, the deep marine deposit (Heira shale) of Palaeocene age was laid down above the Upper Cretaceous shallow carbonate deposits (Zmam Formation) which are separated from the Upper Cretaceous clastic deposits (Bahi Formation) by the Early Cretaceous unconformity.

**GENERALIZED COLUMNAR SECTION
ATTAHADDY GAS FIELD, CONCESSION 6**

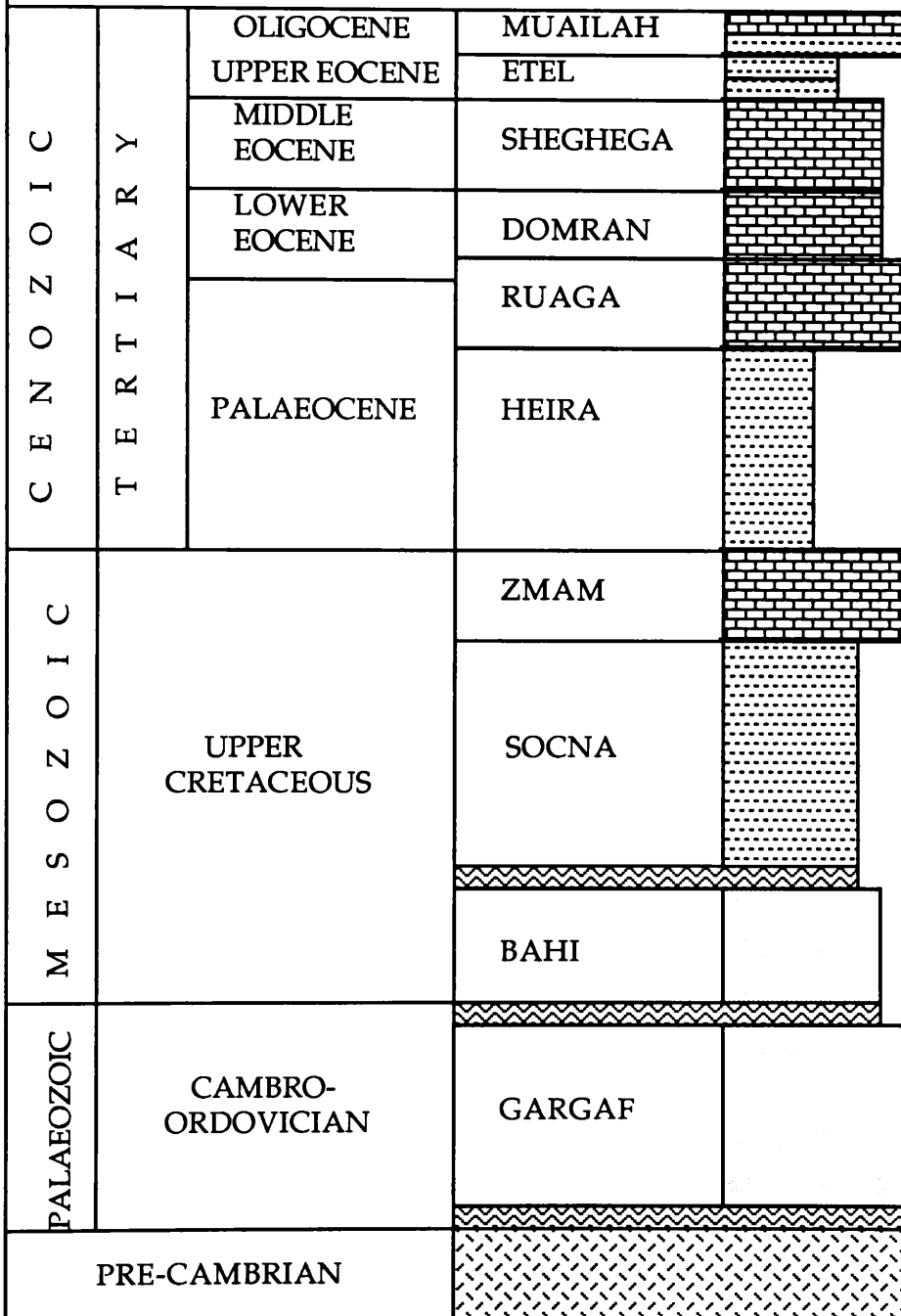
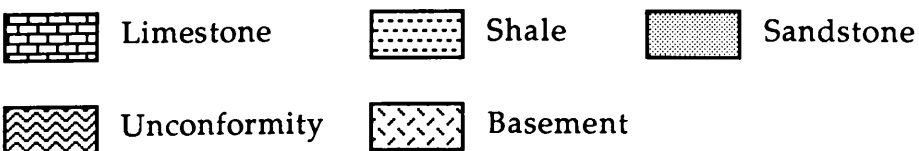


Fig. 1.7 Generalized columnar section of the Attahaddy Field.



In general, the stratigraphy of the field starts at the top from the undifferentiated Oligocene-Miocene which consists of a mixture of deep-shallow marine shales and limestones with some interbedded clastic deposits of loose sand, which occurred during the transgression and regression of the sea during that time. Deeper in the section, the sedimentation of the Lower Eocene is dominated by carbonates, which have good porosity. It is believed that due to the lack of the source and cap rocks, no hydrocarbon accumulation has taken place.

The Palaeocene deep marine deposits (a very thick section of green shale) are believed to be the source rock for the underlying structural traps. In addition, a lot of problems have been encountered as the shale was penetrated, due to the stickiness and softness of the shale, resulting in the drill bit sticking during drilling, and thereby slowing the drilling time.

The Upper Cretaceous carbonates consist mainly of sandy limestone and occasionally in some parts of the field consist of calcareous sand, underlain by the deep marine deposits of the Socna shale/limestone, which is absent in some places of the field as a result of the underlying unconformity.

The thick underlying Cambro-Ordovician metamorphic section consists of highly fractured, massive, dense quartzitic sandstones and quartzite which forms the hydrocarbon pay zone of the Attahaddy Field. Several intervals of core have been cut in each well. These displayed open fractures in the producible wells. On the other hand, however, very massive, tight quartzite was found in the dry holes.

1.5 Previous work

(a) A study project of Cretaceous rocks in Concession 6 was carried out in 1987 by Sirte Oil Company Exploration Department, involving a staff of seven people and other specialists as were needed (McDowell, 1988). The project objectives were revised with the specifications restricted to the construction of a series of isopach and lithofacies maps, locating growth faults and outlining the distribution of the various Cretaceous formations. The isopach maps of Bahi Formation (Fig. 1.8), Socna Formation (Fig. 1.9) and Zmam Formation (Fig. 1.10) were constructed at a scale of 1 : 100,000, and all their values were taken from records of the tops, or from data sheets of other workers in the area.

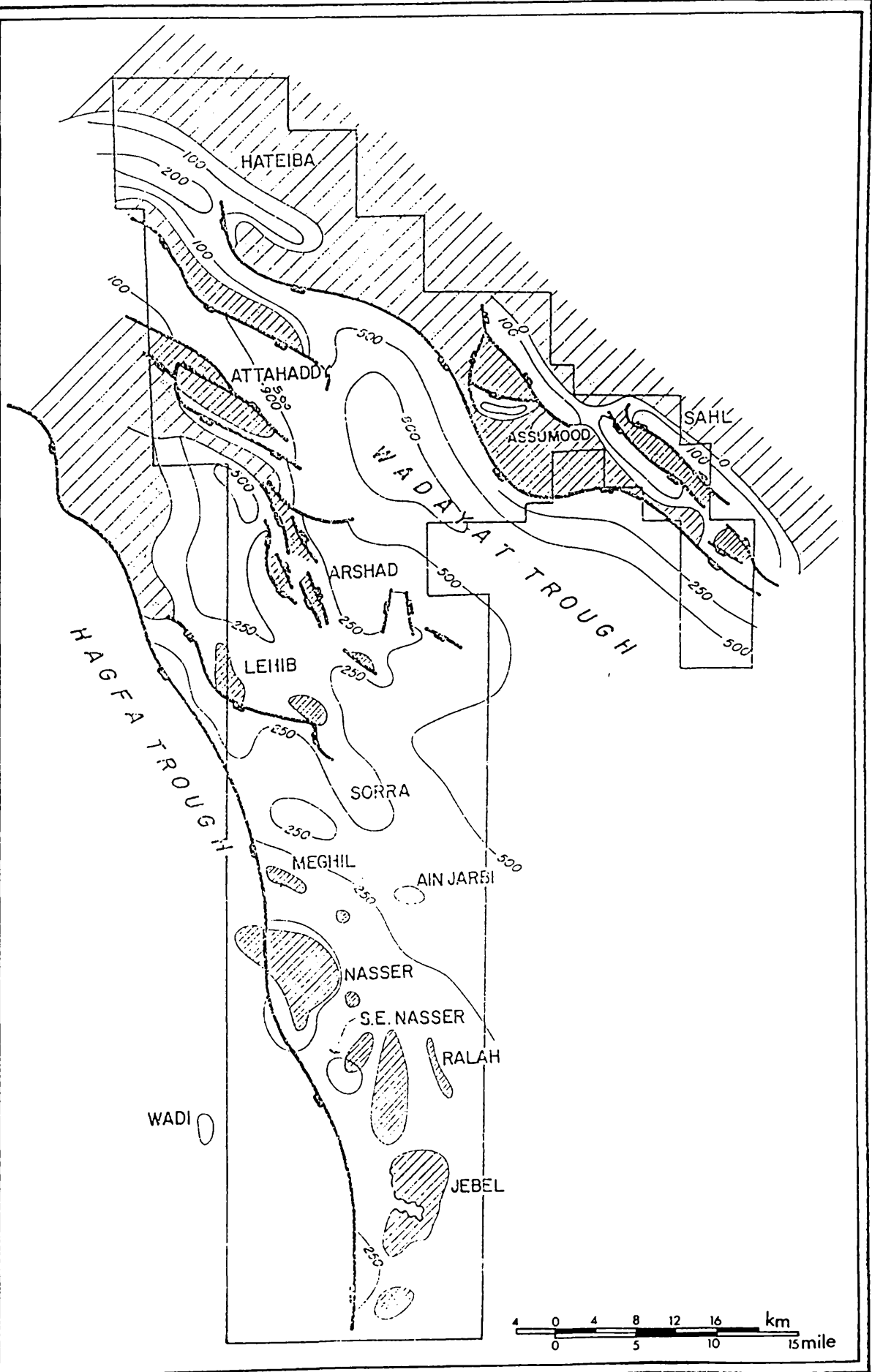


Fig. 1.8 Isopach map of Bahi Formation, (after Mc Dowell, 1988).

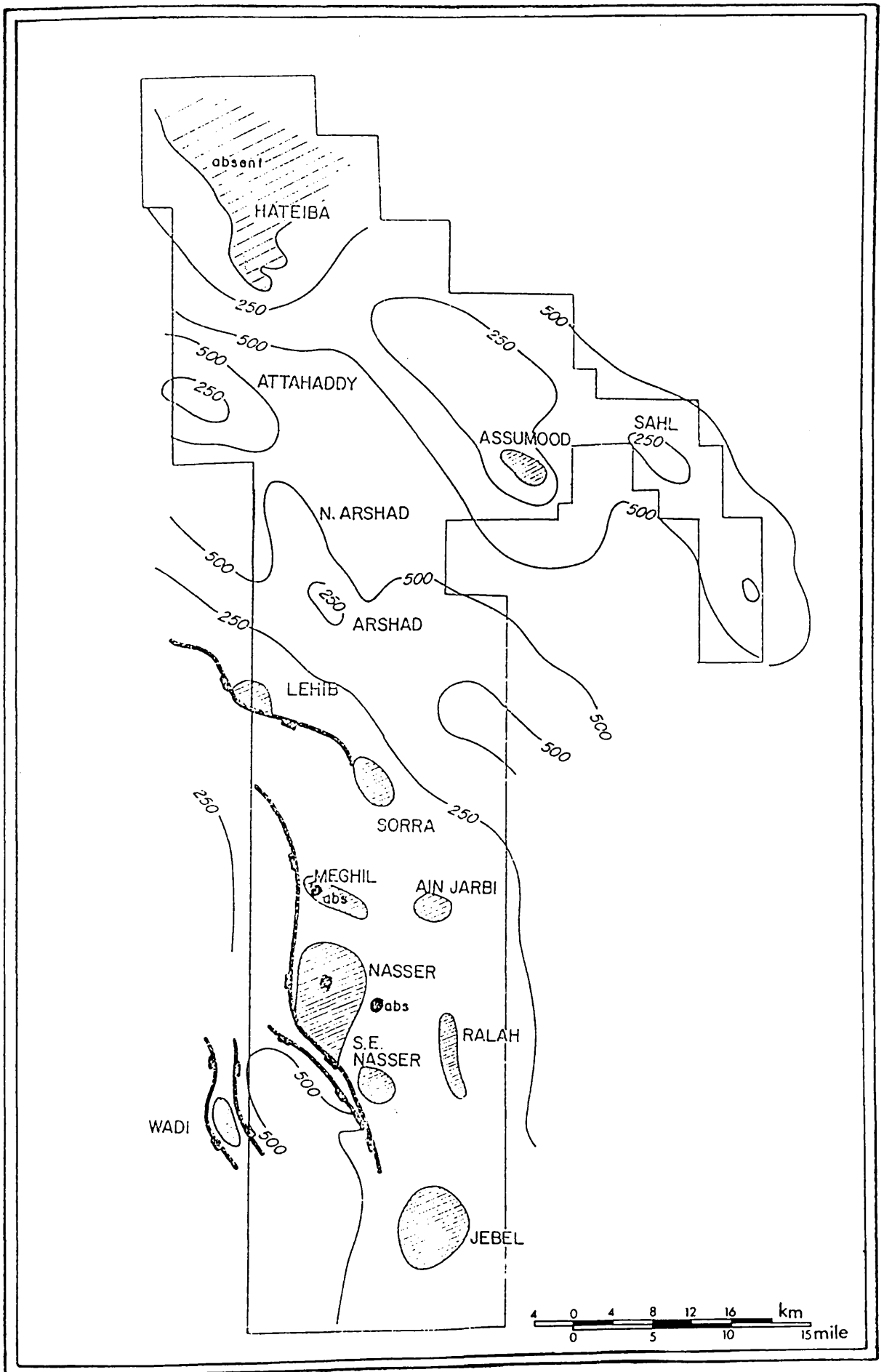


Fig. 1.10 Isopach map of Zmam Formation, (after Mc Dowell, 1988).

The project led to the conclusion that the distribution of the Socna Formation is complex, the most conspicuous structural features being the large horst blocks of Arshada and Attahaddy, where active fault movement took place during Bahi time, continuing into the Socna. Movement in the Socna was diminished, however, and little was evident by Zmam time.

(b) The reservoir blocks, as were defined by the fault planes (Kardoes, 1986), which were interpreted from the Gargaf depth structure map, as well as seismic, structural and geological cross-sections (Fig. 1.11), resulted in the discovery of a gas bearing structure extending over a distance of 28 km, connecting the Attahaddy Field with the north Arshad area, where well MMM5-6 was drilled.

(c) A comparison of reservoir characteristics in the Gargaf quartzites of the Meghil and Attahaddy gas Fields was made by Keskin (1988), resulting the following conclusions.

- (i) Matrix porosity (as detected by sonic logging) is quite common in the uppermost Gargaf section in some of the Attahaddy wells (ie FF7-6 and FF14-6).
- (ii) The calculated average porosities in the Bahi - Gargaf section of the Meghil wells are correlatable with Bahi (45 m) and the uppermost (150 m) of Gargaf section cut in well FF7-6 (Meghil : 0.062; Attahaddy : 0.0673).
- (iii) Two percent porosity limit is a confident net pay cutoff for the matrix porosity associated with fractured zones of the Bahi-Gargaf intervals.

(d) The exploration programme in the Attahaddy Field resulted in the drilling of 16 wells in order to provide some geological and structural evidence on the Field. The purpose of drilling these wells was as follows:-

FF1-6 To test the presence of gas within the Bahi Formation.

FF2-6 To investigate the presence of a down-dip oil column.

FF3-6 To drill a potential gas column, which was duly discovered to be in excess of 630 m in the Gargaf Formation.

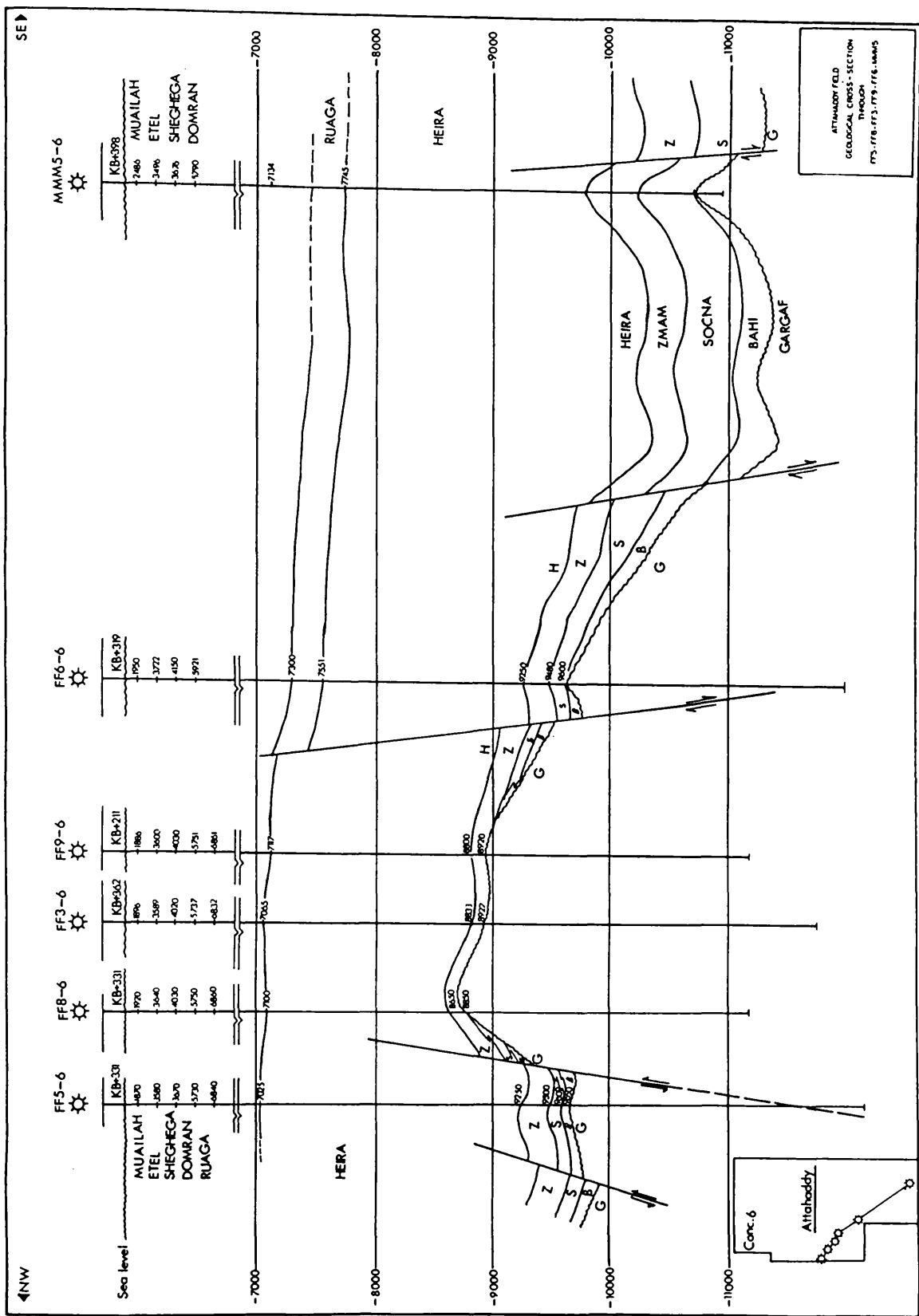


Fig. 1.11 Geological cross-section from NW to SE through Concession 6, (after Kardoes, 1986).

- FF4-6 To drill into the Gargaf Formation in a flank location on the downfaulted block 2.3 km west of FF3-6. (which drilled through the reservoir rock, and was terminated at -3242 m sub-sea).
- FF5-6 To test the NW extension of the field.
- FF6-6 To appraise the SE extension of a central anticline in the downthrown block, around 6 km south of FF3-6.
- FF7-6 To test the extension of the northern flank in a downdip location and to provide some information on the gas-water contact.
- FF8-6 Drilled to delineate the existing recoverable gas potential of the northern slope.
- FF9-6 To appraise the southeastern flank of the Attahaddy Field. The well is located rather downdip, to provide information on the area limits, as well as the gas-water contact of the field.
- FF10-6 Drilled to establish the areal extent, as well as vertical limits of the Bahi/Gargaf reservoir of the Attahaddy Field.
- FF11-6 Drilled to delineate the existing, as well as the recoverable gas potential, of the newly interpreted thick Bahi clastic fans which might have developed, especially on the northern slope of the structure.
- FF12-6 To appraise the eastern flank of the field.
- FF13-6 To test the extension of the north east flank of the field.
- FF14-6 To appraise the south extension of an anticlinal structure.
- FF15-6 To test the Gas potential in western Attahaddy Field, which is believed to be separated from the main Attahaddy horst by a significant E-W graben.
- FF16-6 To delineate the reservoir limits and the recoverable gas capacity of the least known area of the field.

1 . 6 Aims of the present research

The principal aims of this research can be summarized into the following four aspects:-

- (1) To outline the distribution of the various Upper Cretaceous-Tertiary strata within the Attahaddy Field, using the available seismic sections and geophysical logs.
- (2) To construct seismic depth structure maps and velocity maps for the Cambro-Ordovician Bahi-Gargaf Formation, which is believed to be the reservoir rock of the field, and which will also enable us to follow the depth variation of these rocks all around the field.
- (3) To study the major structure of the field by contrasting various geological and structural cross-sections.
- (4) To study the seismic stratigraphy of the field.

CHAPTER TWO

GEOPHYSICAL AND GEOLOGICAL DATA USED IN THE STUDY

2.1 Data available

Seismic coverage over the Attahaddy Field comprises an area of approximately 200 km², of 12-30 and 48 fold Vibroseis seismic data acquired in 1980, 1983, 1984 and 1985 in the Concession 6 Area. The addendum incorporates an additional 270 km² of 30 fold Vibroseis data recorded in 1987.

The final interpretation presented in this study was carried out using only the 1987 data. This is due to the unresolvable seismic time misties between the different vintages caused by the use of different acquisition and processing parameters. The 1987 data, which provides adequate coverage for mapping, forms a seismic grid with the lines oriented in a NW-SE and NE-SW direction with approximately 2.5 km line spacing.

2.2 Seismic survey and processing

2.2.1 Data acquisition

The data were recorded by Boco (party 9) in November, 1987. The field acquisition conditions were excellent, with a fairly smooth terrain over the programme area. The field acquisition parameters are similar to those used for the 1985 Sirte reconnaissance programme in Concession 6, and were based on the results of a noise study carried out in the area. The most significant parameters are :-

Fold	:	30
Station interval	:	36 metres
Source interval	:	80 metres
Spread geometry	:	2500-140-0-140-2500 metres
Sweep	:	10-40 Hz, 15 DB log, 12 sec.
Geophone type	:	SM-4 (10 Hz).

Detailed field acquisition parameters are shown on the side-label (Fig. 2.1). The data quality is good with the exception of the southwest portion of the programme area, where the data deteriorates near the fault zone.

FINAL STACK

PLATE PF-4155

JUNE 1988

FIELD PARAMETERS

RECORDED BY	BOCO PARTY 9	RECEIVERS
RECORDING DATE	SEPTEMBER 1987	PATTERN 6 STRINGS OF 12 GEOPHONES
SOURCE		ARRAY LENGTH/WIDTH 63/45 M
VIBROSEIS**	4 VIBROS. X 8 SWEEPS	STRING SPACING/FEATHER 9/6 M
VIBRATOR TYPE	LRS-311	TYPE/FREQUENCY SM-4/10 HZ
VIB. SPACING 20M.	MOVE-UP 4.5M	NO. OF GROUPS 96
VIB. IN-LINE FEATHER	10.5M	INSTRUMENT
ARRAY WIDTH/LENGTH	60M/63M	TYPE/FORMAT MDS-10/SEG-B
SWEEP FREQU.	12-48 HZ LINEAR	RECORD LENGTH/SAMPLE INT. 195/4MS
SWEEP LENGTH/TAPER	15/0.5 S	NO. OF SEISMIC CHANNELS 96
BASE PLATE PHASE CONTROL		FILTERS LC-OUT HC-62.5 HZ
LISTENING TIME	4 S	STATION AND VP INTERVAL 36M

FIELD STATICS - UPHOLE REPLACEMENT STATICS COMPUTED TO M.S.L. DATUM BY CREW



•CONOCO PTM

Fig. 2.1 Side-label showing field parameters.

2 . 2 . 2 Data processing

The data were processed by CGG in London. The selection of processing parameters was based on the results of a standard series of processing tests. Fig. 2.2 shows the processing parameters as shown on the side-label. No major processing problems were encountered.

2 . 3 Wells used for the study

As discussed in the previous chapter, 16 wells have already been drilled in the study area. The geological and geophysical data obtained from these wells are being used in this study. The general distribution of these wells in the field along with the relevant data associated are shown in Appendix 1.

2 . 4 Description of well logs

The lithological descriptions obtained from the well completion logs show 10 major formations. It is often difficult to separate the Upper Cretaceous Bahi Formation from the underlying Cambro-Ordovician Gargaf Formation, either on electric logs or in samples, due to the fact that the Bahi sands were largely derived by erosion from the underlying Gargaf. They are considered as separate formations. The contact relationships between the formations encountered were based on palaeontological aspects (faunal assemblage).

The full geological and geophysical description of these individual formations are shown in Fig. 2.3, based on data obtained from well FF6-6 completion log, while the lithological descriptions of the formations encountered are as follows.

Gargaf Formation (Cambro-Ordovician) -11267'

Consists mainly of light grey, very fine grained, transparent, very hard quartzitic sandstone and quartzite, with a minor interbedding of shale and red siltstone. This formation represents the main reservoir. The total thickness of the Gargaf Formation cannot be measured in the field, due to the fact that none of the wells drilled in the area penetrated the whole formation and none have reached the basement.

PROCESSING PARAMETERS

PROCESSED BY CCG
PROCESSING SAMPLE RATE 4MS
PROCESSING RECORD LENGTH 4S

REFORMAT SEGX TO CCG FORMAT

GEOMETRY LABELLING AND VP DISPLAY

AMPLITUDE RECOVERY - A.G.C.

MUTING -

0MS-234M 200MS-270M 620MS-1370M 1480MS-3564M

FK FILTERING OF VPS

NOTCH REJECTION 800 - 1800 M/S

SORT TO RECEIVER GATHERS

FK FILTERING OF RECEIVERS

NOTCH REJECTION 800 - 1800 M/S

CDP GATHER

FIELD STATIC CORRECTION - TO F.D.P.

SPECTRAL WHITENING (TVDEF)* -

9-48HZ 0.05 9-45HZ 1.55 9-40HZ 4.05

VELOCITY ANALYSIS* -

DISCRETE CONSTANT VELOCITY STACKS (CVS) - 15 VELOCITIES, GROUPS OF 24 CDPS

VELOCITY SPECTRA (ANVIT) - EVERY 2KM OR AT INTERSECTIONS

NORMAL MOVE-OUT*

MUTING* -

100MS-270M 250MS-306M 1200MS-1580M 1900MS-3564M

AUTOMATIC SURFACE CONSISTANT SW RESIDUALS STATICS* - SATAN I SW

DESIGN GATE: 0.55-2.55S FREQUENCY RANGE 12-35 HZ

STACK* - NOMINAL 48 FOLD

PREDICTIVE DECONVOLUTION* -

DESIGN GATE	GAP	TOTAL OP. LENGTH	PREWHITENING
-------------	-----	------------------	--------------

0.2 - 1.9 S	24 MS	120 MS	0.5 PERCENT
-------------	-------	--------	-------------

1.5 - 3.0 S	36 MS	132 MS	0.5 PERCENT
-------------	-------	--------	-------------

THREE TRACE MIX WEIGHTED 1.2.1 AND SUMMATION* - CDP INTERVAL = 36M

TIME VARIANT BAND PASS FILTER* -

TIME	BAND PASS
0.0 - 1.2 S	12 - 45 HZ
1.4 - 2.4 S	12 - 40 HZ
2.6 - 4.0 S	12 - 35 HZ

F-X DOMAIN SPECTRAL NOISE ATTENUATION* (VIZIR)

COHERENCY ENHANCEMENT* - 40 PERCENT OF ORIGINAL TRACE RETAINED

EQUALISATION* -

0.0 - 1.7 S 500 MS OPERATOR

1.7 - 4.0 S 1000 MS OPERATOR

POLARITY REVERSAL

STATIC CORRECTION - TO DATUM

DISPLAY

* TIMES REFERENCED TO FLOATING DATUM PLANE

Fig. 2.2 Side-label showing processing parameters.

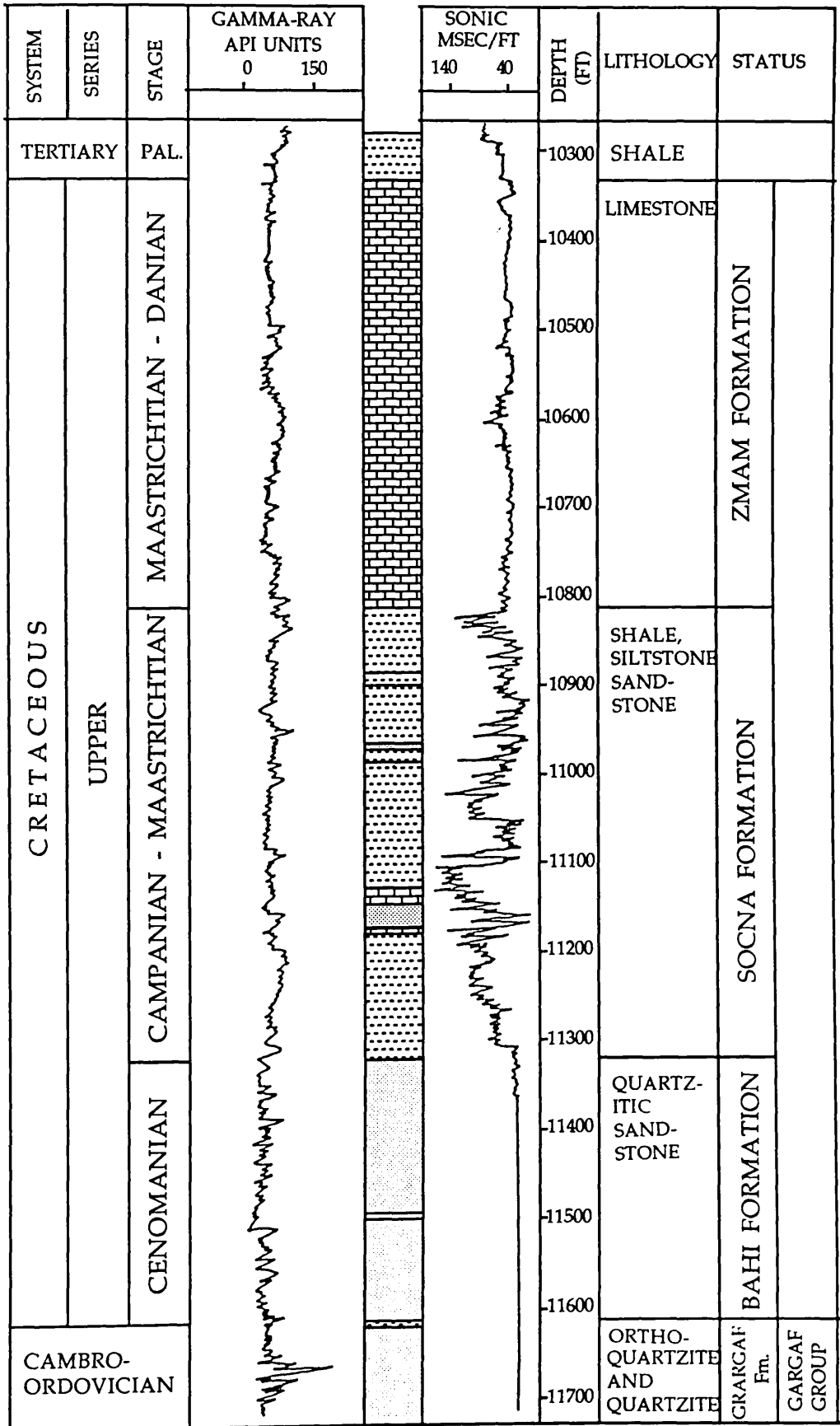


Fig. 2.3 FF6-6 Composite log (Attahaddy Field)

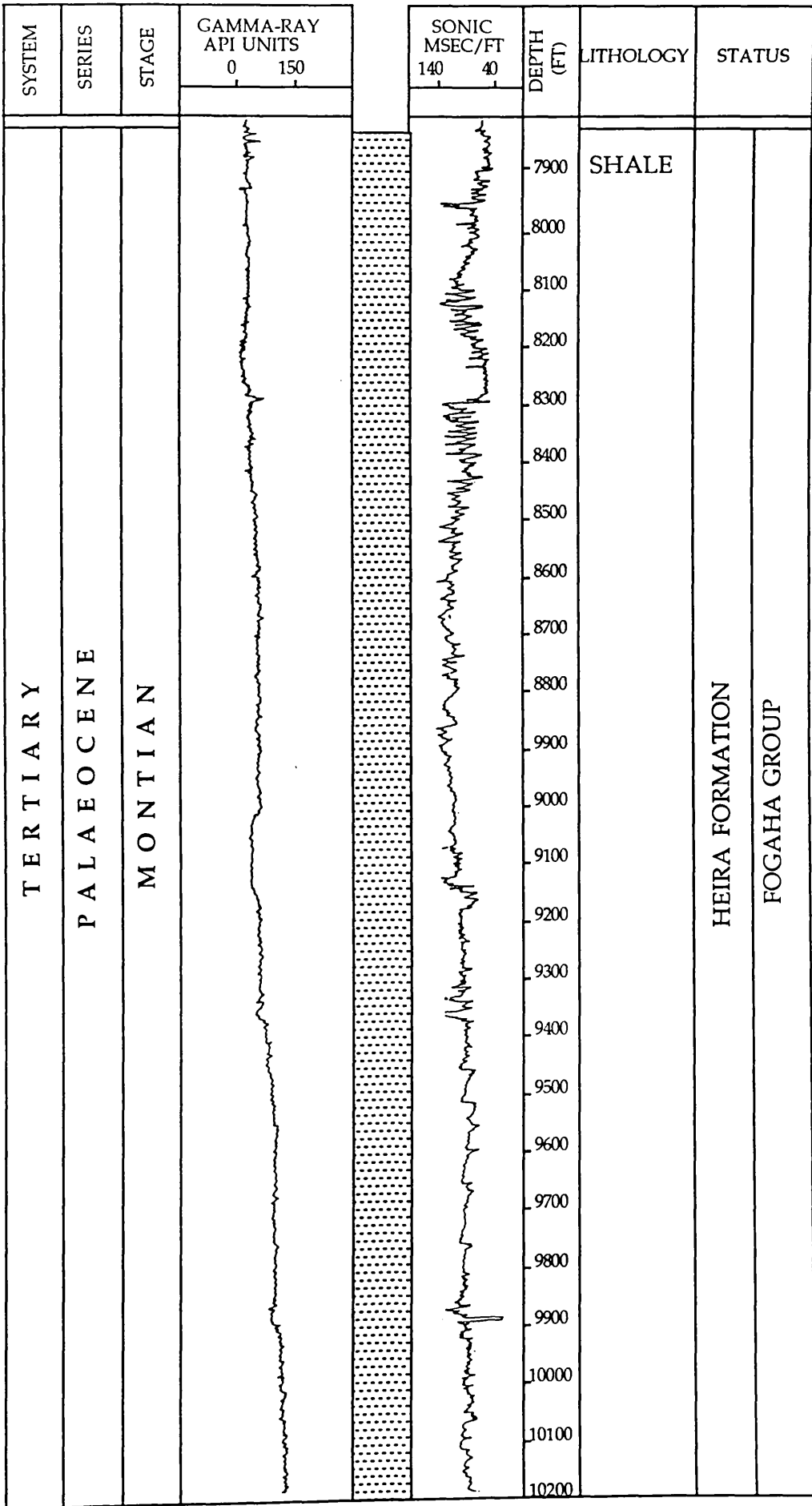


Fig. 2.3 Continued.

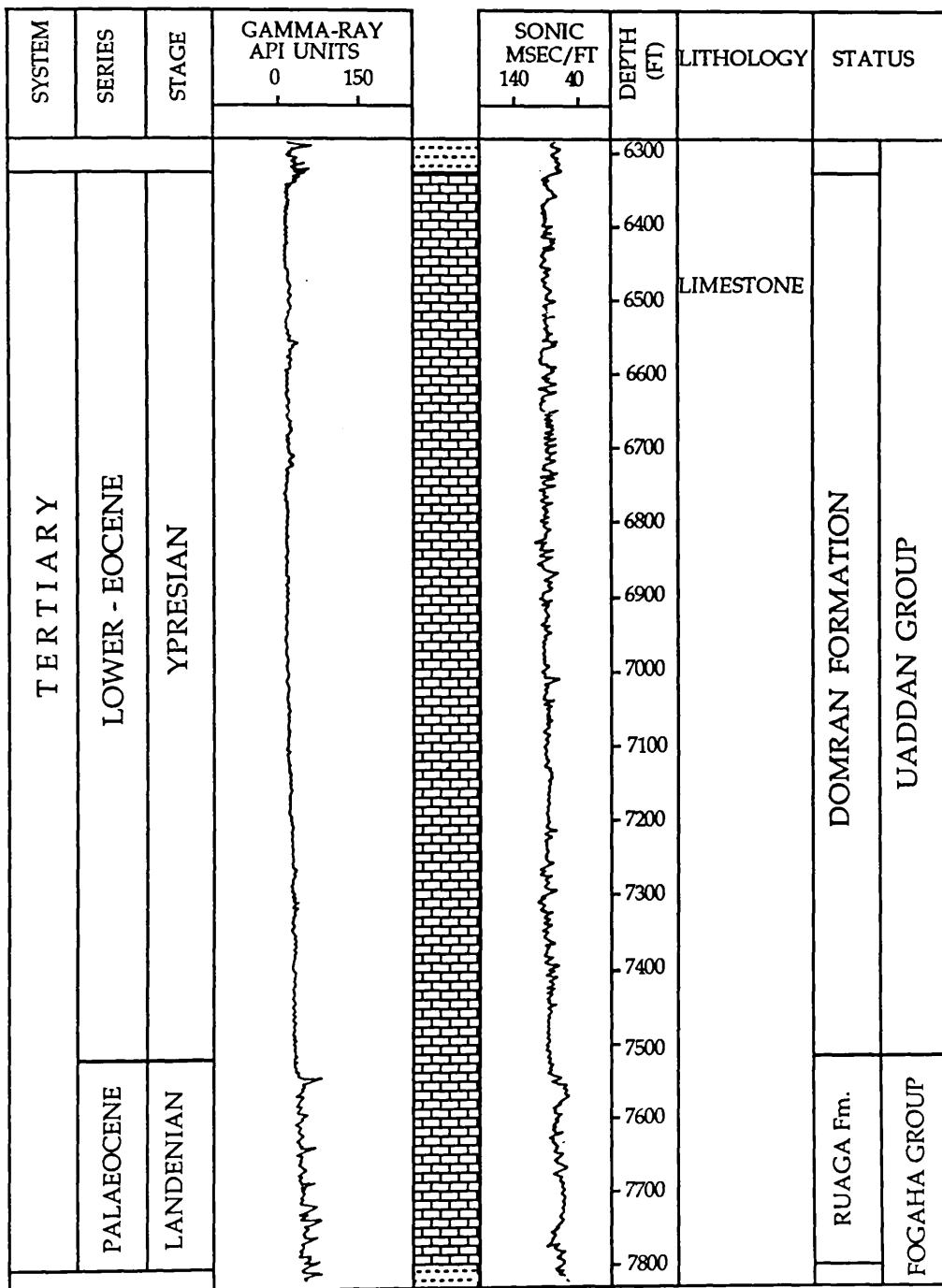


Fig. 2.3 Continued.

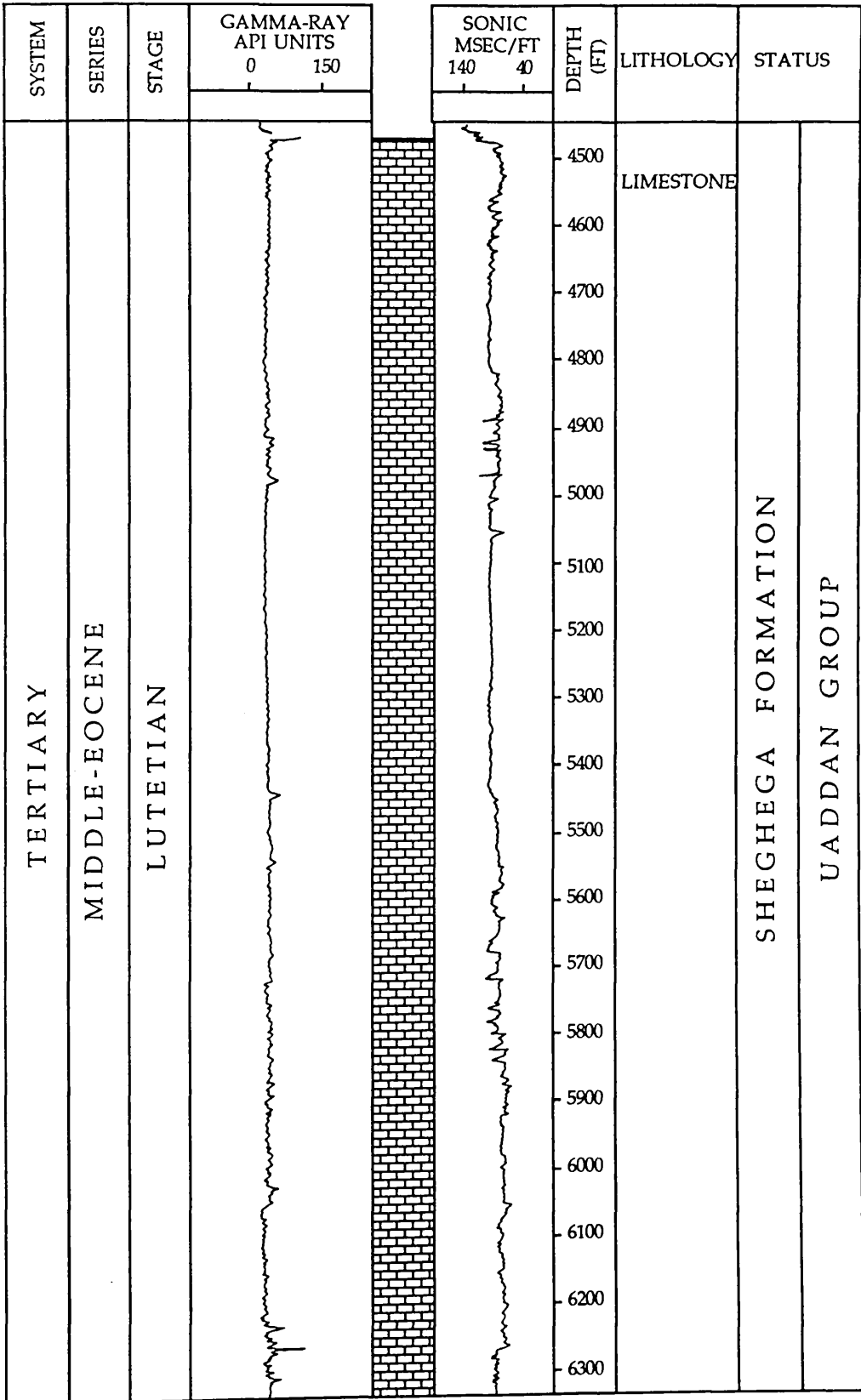


Fig. 2.3 Continued.

Bahi Formation (Upper-Cretaceous) -10984' - -11267

This formation represents the oldest upper Cretaceous age deposits, and it is considered as a secondary reservoir target. There is not much lithological variation with the underlying Gargaf Formation. It consists of a very coarse-grained sandstone of milky white colour, with very thin sandy carbonate bed intercalations.

Socna Formation (Upper-Cretaceous) -10520' - -10984'

The total thickness of this formation varies from 120-180 m. It consists mainly of silt, siltstone, sandstone and shale, with very thin beds of white to light grey colour anhydrite in the lower part of the formation.

The siltstone is light to medium grey in colour, the uppermost part is characterized by its calcareous units, while the rest of this unit is argillaceous and dolomitic at the very base. The shale beds occur at three different levels. They are light to dark grey in colour, fairly hard and characterized by having some slickensided, shiny surfaces. The variation of the shale composition can be noticed at these levels, where it varies gradually and generally from calcareous at the top to mostly argillaceous at the base.

The sandstone of Socna formation is white to light grey, very fine grained with sub-angular associated quartz grains, and are fairly well sorted. At the base the sandstone changes to more dolomitic, then to silty, sands.

Zmam Formation (Upper-Cretaceous) -10022' - -10520'

This formation represents the youngest of the Cretaceous units, and it ends the Mesozoic era. The Formation is widespread throughout the subsurface of the Sirte Basin and is stratigraphically used as a marker horizon.

It is composed mainly of light brown, microcrystalline, slightly argillaceous medium hard carbonate sequence of limestone. The upper portions of the formation occasionally contain some fossils; the amount of argillaceous material increases in the lower half, where it becomes gradually shaly, while the lowermost part of the formation is characterized by glauconitic, medium-dark beds of grey limestone.

Heira Formation (Palaeocene) -7491' - -10022'

The Heira Formation is dark grey, splintery, slightly calcareous, firm to medium hard, sometime massive shale, with occasional rare interfingers of soft medium hard limestone. The upper part of the shale is very fine grained, nearly marly and contains abundant forams, whereas the lower part of the shale is grey, medium hard, splintery and slightly silty in nature.

Ruaga Formation (Palaeocene) -5994' - -7491'

The Ruaga Formation of Fogaha Group, consists mainly of cryptocrystalline to microcrystalline limestone, which varies in colour from dark to light brown. The upper part is argillaceous, micritic and brittle, while the lower portion is characterized by abundant chert nodules. Calcite crystals are very common in the basal part of the Formation.

The lower part of the limestone is quite soft compared with the upper part and the total thickness of this formation in this well is reported to be over 96 m.

Domran Formation (Eocene) -5994' - -7172'

This is the lowest formation of the Uaddan Group. It is composed of a thick sequence of limestone, mainly of white colour, and is characterized by some chert at various levels; in the basal part the chert is more abundant.

Sheghega Formation (Eocene) -4147' - -5994'

The Sheghega Formation is composed predominantly of a carbonate sequence of cream, micritic, skeletal limestone with abundant large fossil fragments. It is characterised by abundant nummilitic beds at various levels, the upper part is slightly argillaceous, and chert and chert nodules are quite common in the middle part, whereas the lowest part of the formation shows small calcareous shaly beds averaging 3-5 metres in thickness; these shales are grey to green colour and quite firm.

Etel Formation (Oligocene) -1942' - -4147'

Consists mainly of grey to greenish, soft to very soft, firm, occasionally blocky, highly calcareous shale, the middle part of it, is slightly sandy, and none

calcareous, while the lower 60 m of this formation is characterized by a change in colour to light brown.

Muailah Formation (Oligocene) -1942' - -3642'

Consists mainly of greenish, soft, calcareous, occasionally silty shale sequence with limestone and dolomite beds intercalation, the middle 25 m is composed of mixed clastic sediments of sandstone and siltstones. The sands are white, medium dark, sub rounded, sub-angular, and highly calcareous.

Undifferentiated Miocene -1942' - surface

Composed mainly of mixed carbonate and clastic sediments, limestones of white, creamy, tan, medium hard, micaceous, chalky, vuggy types are more common within the Miocene deposits. A number of layers of greenish, very soft, gummy, calcareous shale can be observed at a various levels of the Miocene strata.

A NW-SE geological section through wells FF16-6, FF8-6, FF3-6, FF6-6, FF15-6 and FF10-6 was drawn (Enclosure 1). The section shows brief information on the geological history and the general behaviour of the formations, where it started with the deposition of the clastic sediments of Cambro-Ordovician age, changing to mixed clastics and carbonates deposit of Upper Cretaceous age, and the deposition of the thick massive sequence of shale of lower Tertiary age, ending the cycle of deposition with marine sequences of carbonate. The lower portions of the section show a break in deposition and this unconformity is marked by an erosional surface, where some Cretaceous Formations (Socna and Bahi) in some wells (FF8-6 & FF3-6) are missing. The section also shows the thickness variation as the formations were correlated.

CHAPTER THREE

SEISMIC INTERPRETATION

3.1 Number of seismic sections and examples

The seismic data base consists of 17 lines totalling 270 km in length acquired in 1987 (Fig. 3.1). In order to investigate the deep structure of the field, a seismic interpretation study is carried out on all of these sections. Selected seismic sections are reproduced as figures 3.2, 3.3, 3.4 and 3.5, along with their interpretation. Line V87-412 (Fig. 3.2) was planned to pass through the deep boreholes FF7-6, FF13-6, and FF12-6, whereas lines V87-410 (Fig. 3.3) and V87-413 (Fig. 3.4) to pass through the prognosed location of well FF16-6, which was the last well drilled in the field. The seismic survey also covers the north-west portion of the field where no wells were drilled apart from I1-6 and I2-6, but due to the lack of data for these wells no seismic ties to wells could be done. The main study was carried out in this part of the field by seismic interpretation and correlation with the north and north-eastern parts.

Line V87-407 has been included mainly to demonstrate the borehole tie to well FF4-6 (Fig. 3.6), and shows a fairly simple structure with all horizons rising south-easterly to a fault zone.

Line V87-402 (Fig. 3.7) was included principally for the purpose of the interpretation, where it represents the longest seismic profile shot in the field, and which will also help in matching the seismic horizons together to compare the behaviour of the horizons in the SE and NW parts of the field, and which will also describe the deep structure of the lower portion of the field.

3.2 Horizons used for reflection identification

There are no geological outcrops in the nearby areas, that can be used in correlation and tying. Geological identification of reflectors was initially based on well data and geological background. The events selected for horizons identification and mapping were as follows.

Horizon A: Top Sheghega Formation (Middle-Eocene). Yellow pick on sections. This is a continuous shallow event in most or all parts of the field, and is clearly defined by its good

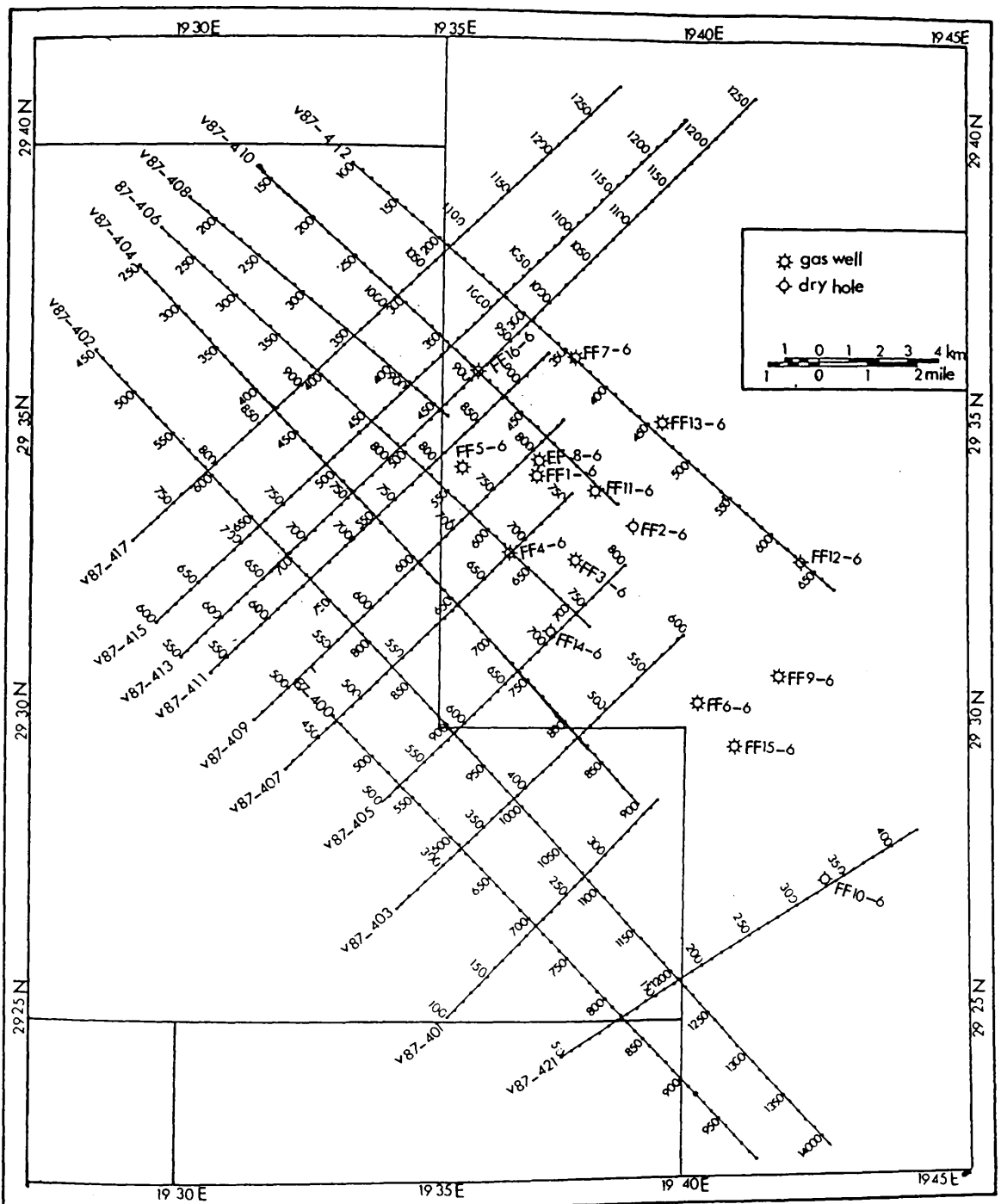


Fig. 3.1 Base map of the Attahaddy Field.

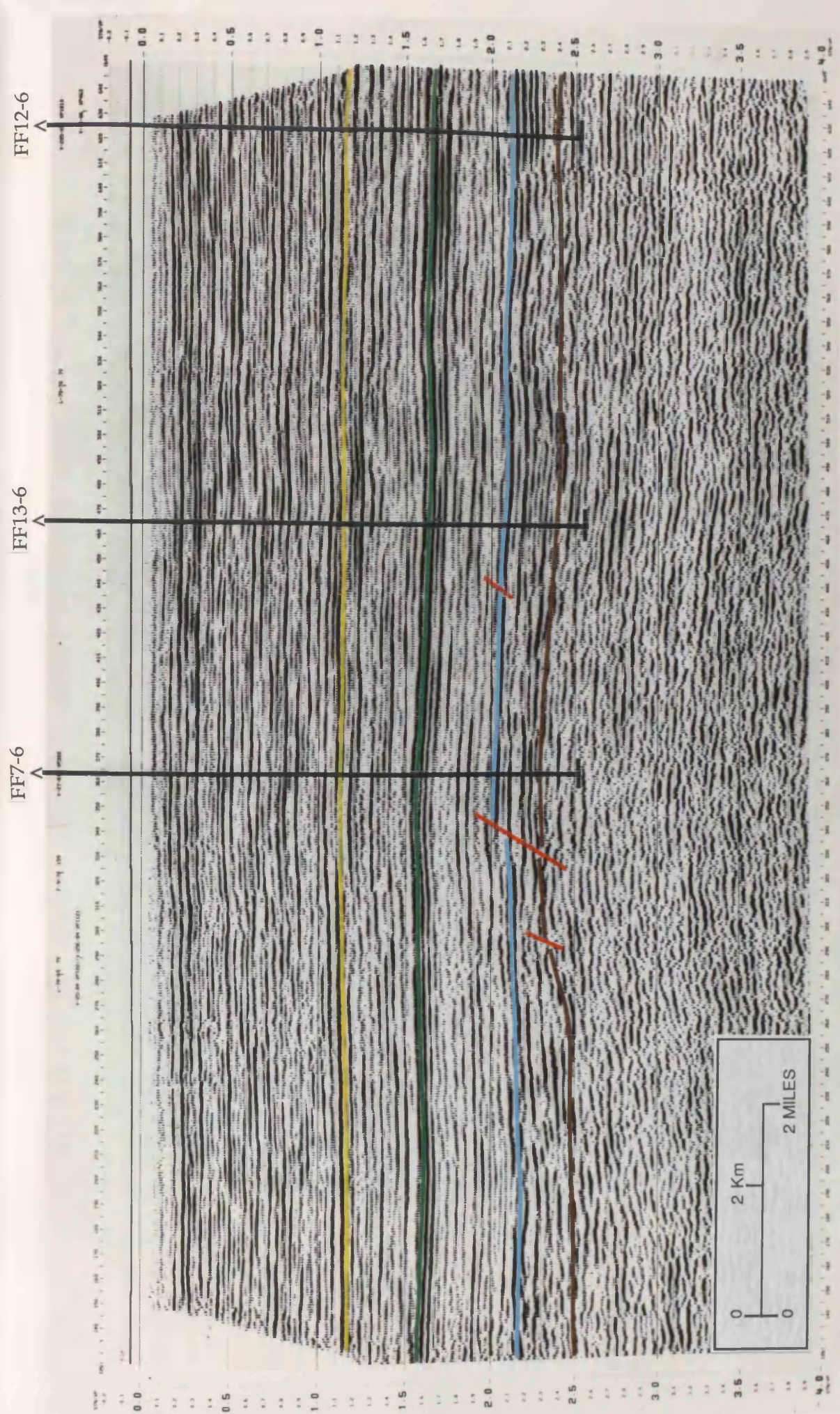


Fig. 3.2 Seismic line V87-412

FF16-6

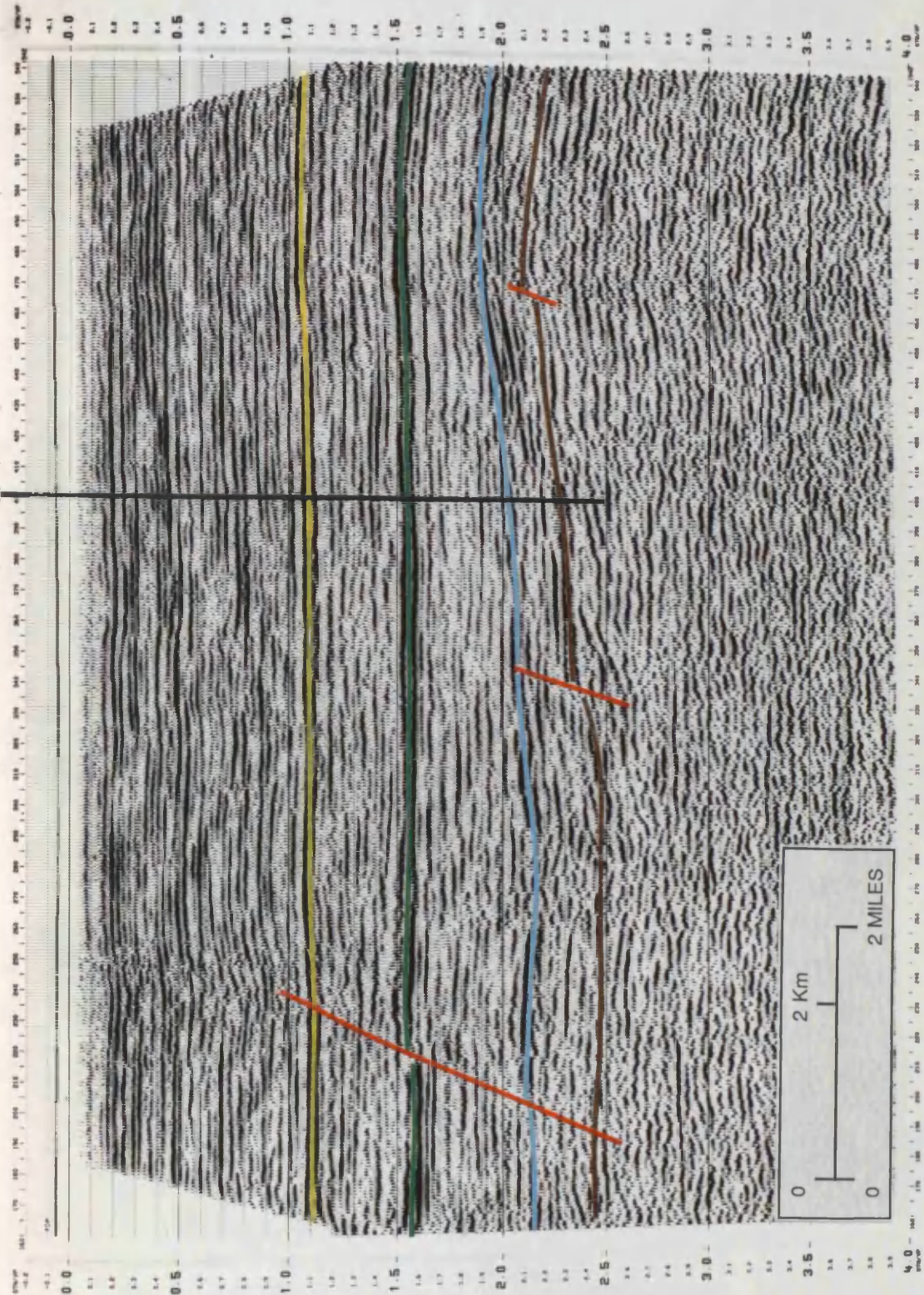


Fig. 3.3 Seismic line V87-410

FF16-6

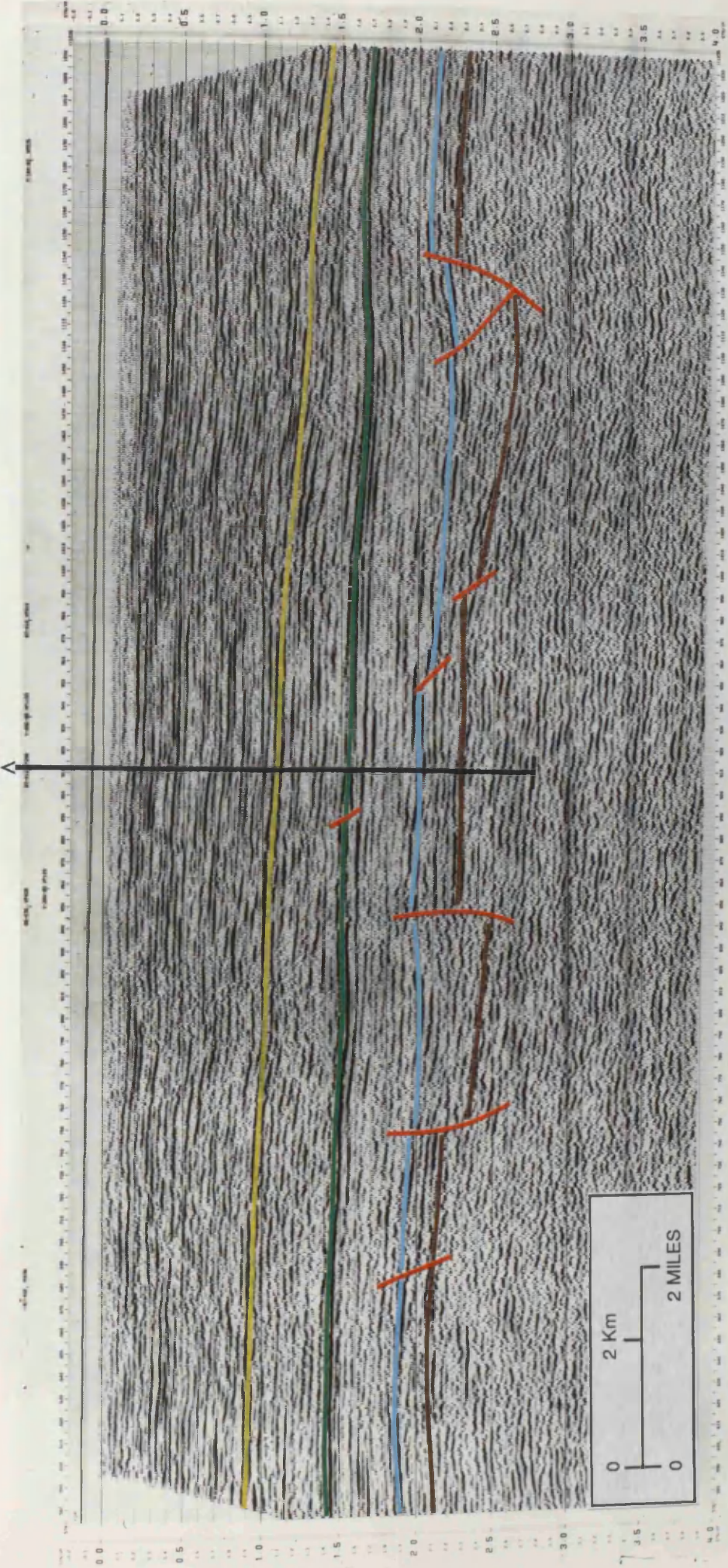


Fig. 3.4 Seismic line V87-413

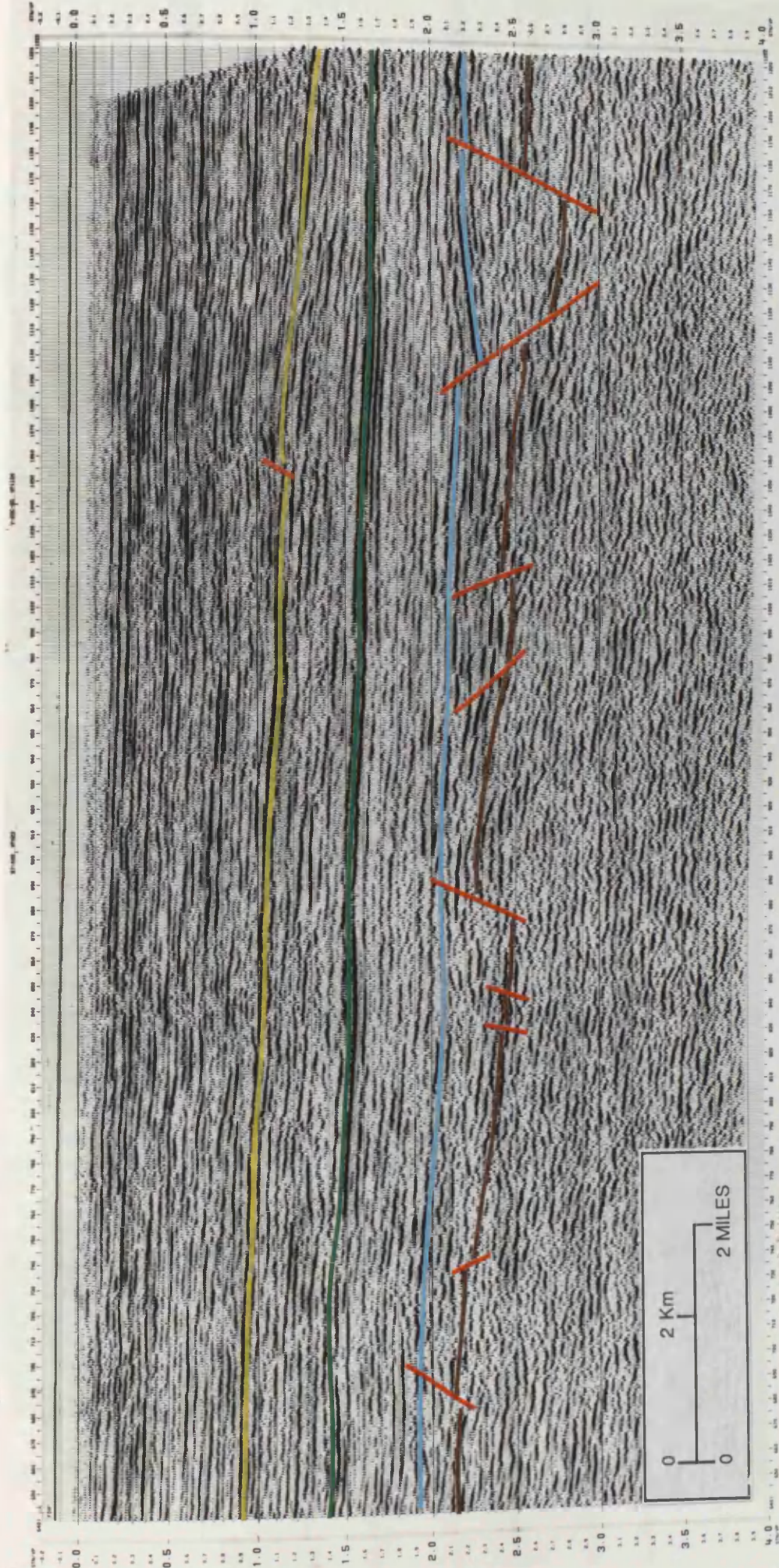


Fig. 3.5 Seismic line V87-415

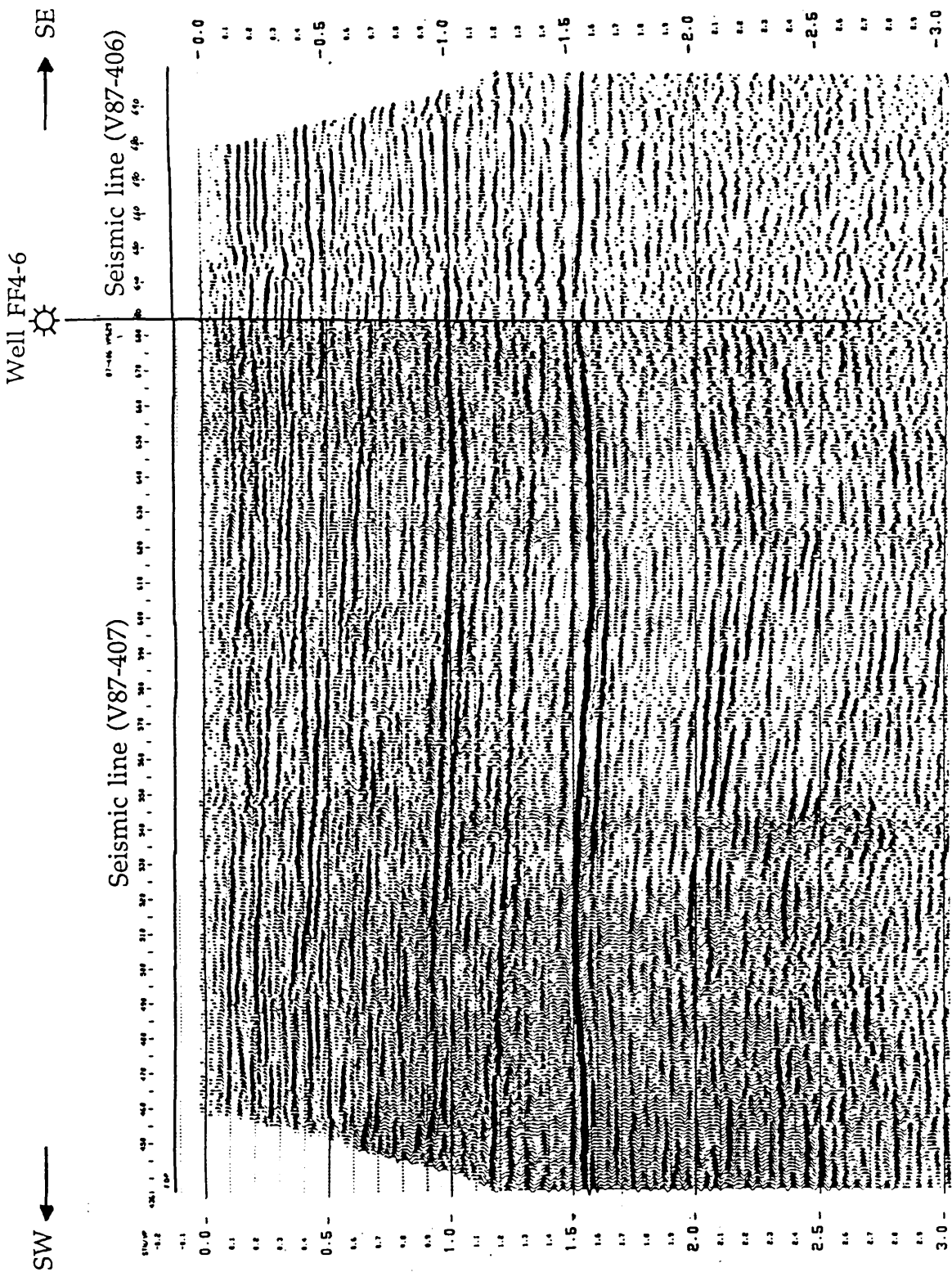


Fig. 3.6 Seismic lines V87-406 and V87-407 at the point of intersection with well FF4-6.

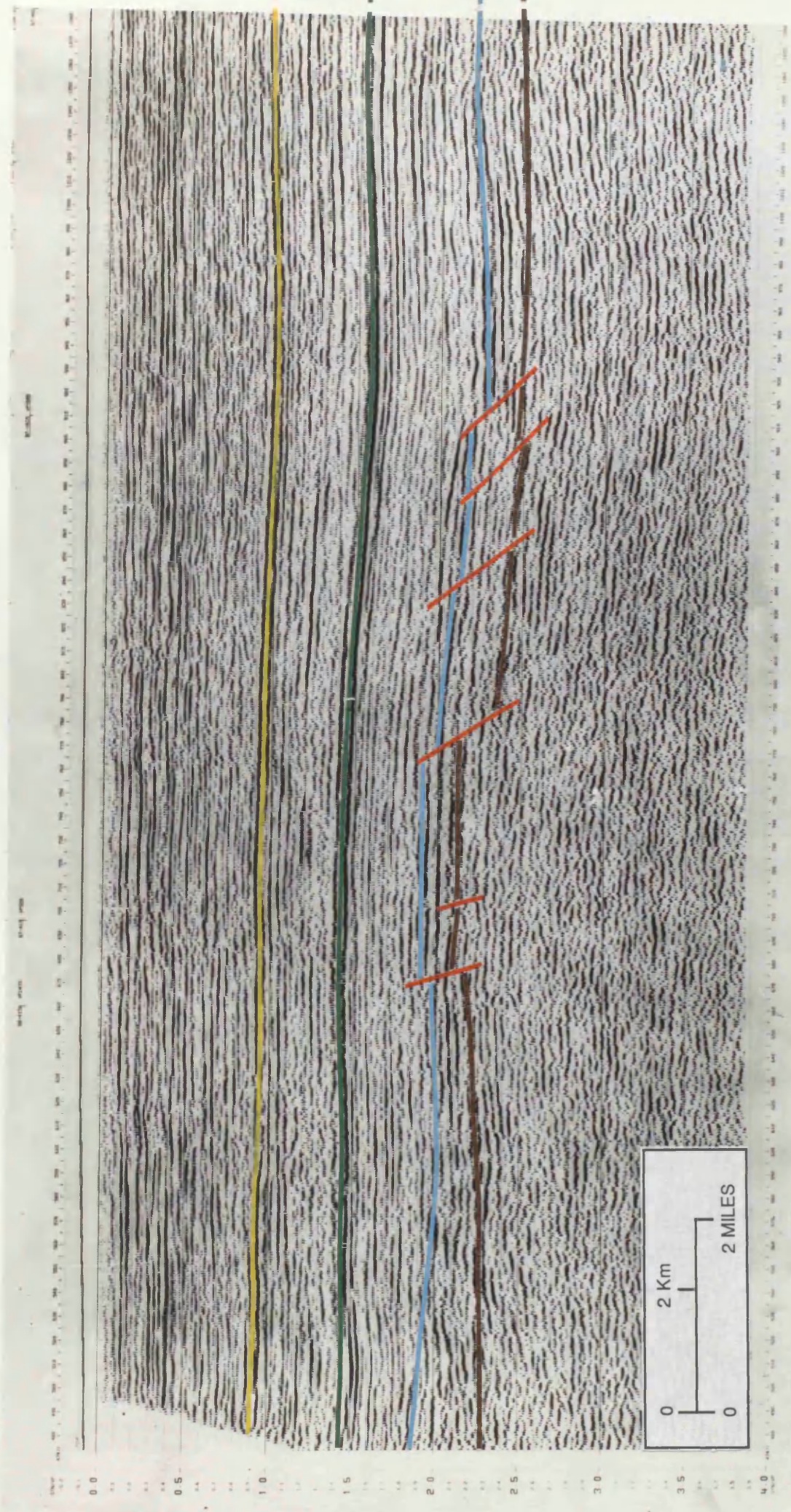


Fig. 3.7 Seismic line V87-402

strong reflector that can be matched and followed on all the sections. This horizon appears between an average two-way time of 1.17 s, and of a sub-sea depth ranging from -4000 - -5000 ft (-1200 : 1500 m) as tied to well data. No major disturbance of the horizon was noticed, but it is a horizontally continuous event, and the lithological characteristic of this event (shale to hard, massive limestone) results in a clear identification on the seismic sections.

Horizon B: Top Heira Formation (Palaeocene). Green pick on sections. This is a very strong and continuous event especially in the central part of the area, the event being interpreted at an average two-way time of 1.57 s, and of a sub-sea depth ranging from -7000 - -7500 ft (-2100 - -2250 m). The continuity of this strong event makes it very reliable in identification and mapping.

Horizon C: Top Zmam Formation (Upper Cretaceous). Blue pick on sections. Originally described as Danian, the event is not as strong as horizons A or B, but continuity is fairly good. It can be followed reliably to some extent over most of the area. There are many smaller faults which are very clearly defined at this level. The major faults are often associated with the underlying horizons, and can also be defined clearly. The event occurs at an average two-way time of 2.05 s, a sub-sea depth corresponding to -9000 - -9500 ft (-2700 - -2850 m). It is used stratigraphically as a marker bed in ending the cycle of deposition of Mesozoic era, which makes it very convenient for mapping and correlation.

Horizon D: Top Bahi/Gargaf Formations (Cambro-Ordovician). Brown pick on sections. This event shows very similar structure trends to horizon C. Although this reflector is considered the deepest reflector, it can hardly be followed due to discontinuity related to structural disturbances which makes correlation and matching across faults quite

poor. In spite of the fact that deep events are visible on some other seismic lines, the uncertainty of correlation is rather great. The lack of well data in the NE portion of the field makes it even more difficult for extension of mapping in that direction. The event is interpreted at an average two-way time of 2.45 s, at a sub-sea depth corresponding to over -9500 ft (-2850 m).

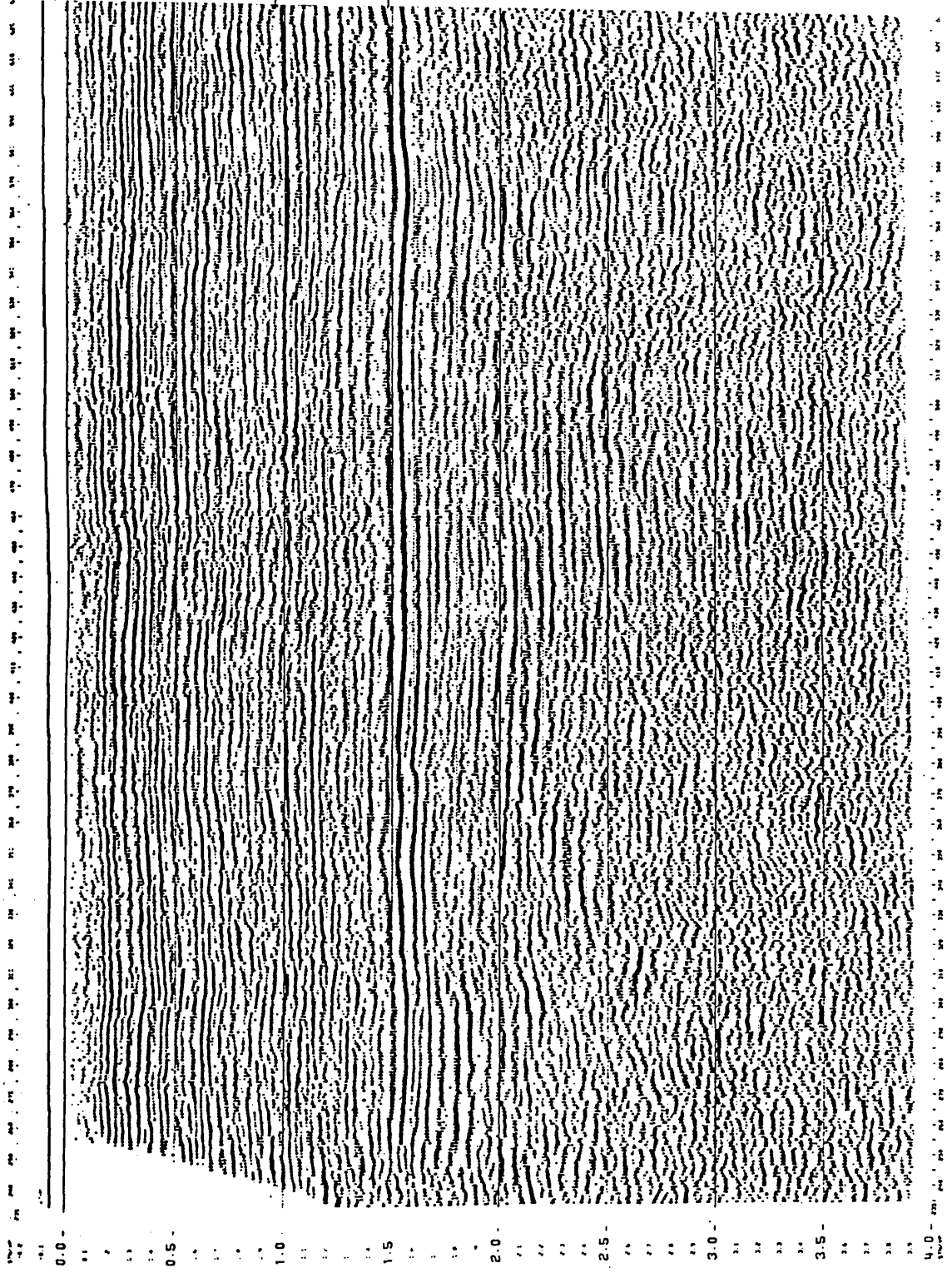
3.3 Seismic ties to well data

Two seismic sections V87-406 and V87-407, whose intersection coincides with well FF4-6 (Fig. 3.6), were used in linking between well and seismic data (Fig. 3.8 & 3.9). The seismic lines show a summary of the geological and geophysical data, where seismic reflectors being tied to both gamma-ray and sonic tools of the electric logs seem to correlate closely. The behaviour of these electric tools correlates well with lithological variation at various levels of the sub-surface strata. Generally throughout the study area at a sub-sea depth of -4020 ft (-1225 m) there is a thick sequence of limestone which marks the top of the first picked horizon A, and includes Sheghega, Domran and Ruaga Formations, these are referred to as the Eocene carbonate sequences. These sequences change gradually to shale at -7150 ft (-2145 m) marking the top of the second horizon B, and at a sub-sea depth of -8912 ft (-2716 m) horizon C appears which is represented by a thin sequence of limestone. Finally, there are the Cambro-Ordovician clastic sediments which appear at a sub-sea depth of -9015 ft (-2748 m), marking the top of horizon D.

Seismic ties around a closed loop are shown in Fig. 3.10, which was carried out using lines V87-410, V87-412, V87-413 and V87-415 (Fig. 3.2, 3.3, 3.4, and 3.5). The main four reflectors can be traced continuously all around the loops. This particular loop shows the best ties as well as the most typical two-way travel times.

3.4 Seismic mapping

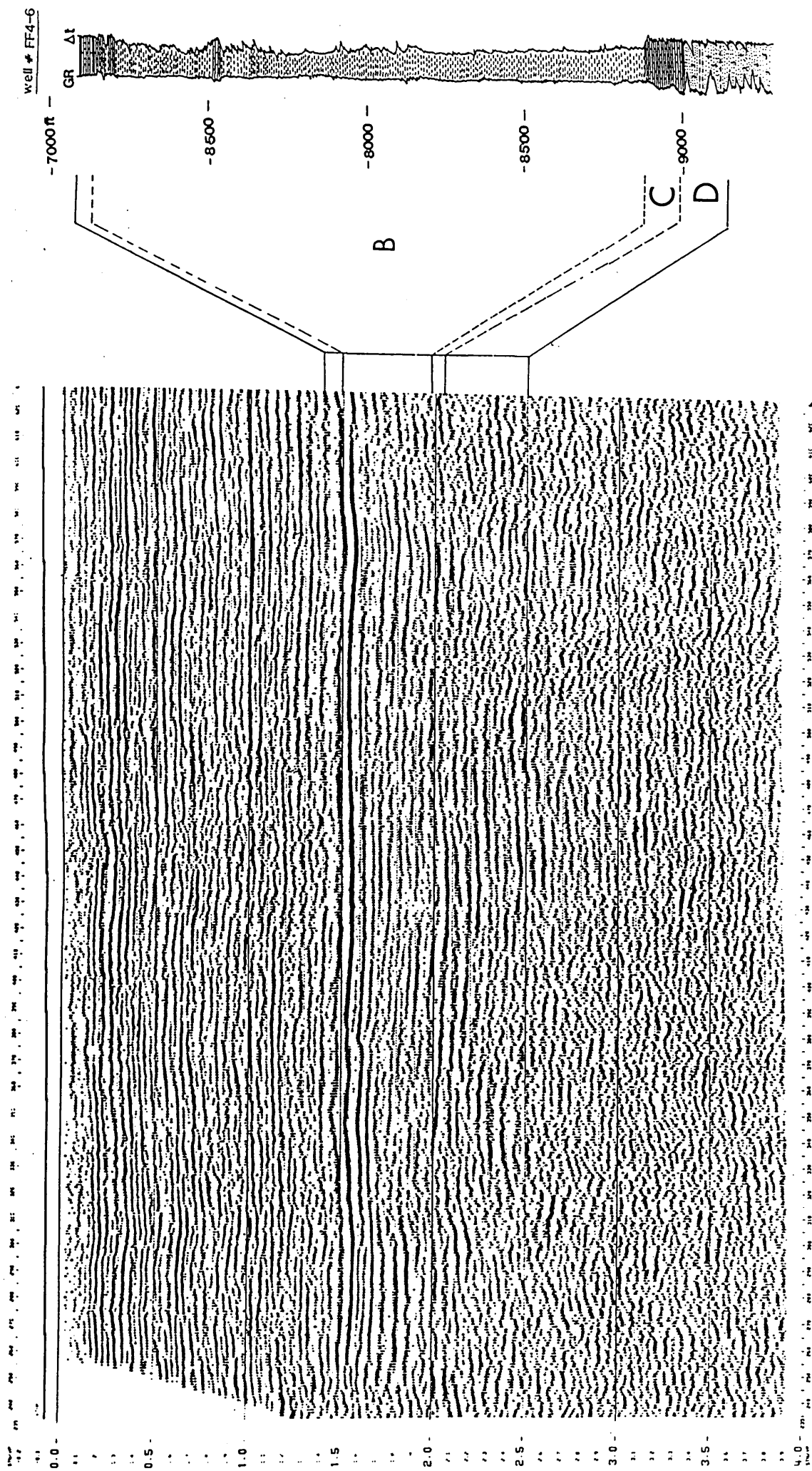
The result of the interpretation of the seismic sections was used in the construction of different types of maps, which involve two-way time (TWT), depth and velocity data. However, the reflection time maps were constructed using reflection time data that were obtained from the interpreted sections at



A- SHEGHEGA Fm.

GR - Gamma ray Δt- Sonic velocity

Fig. 3.8 Seismic lines V87-406 showing a summary of the geological and geophysical data, in linking between well and seismic data.



B- HEIRA Fm.; C- ZMAM Fm.; D- BAHJ/GARGAF Fm.

Fig 3.8 Continued.

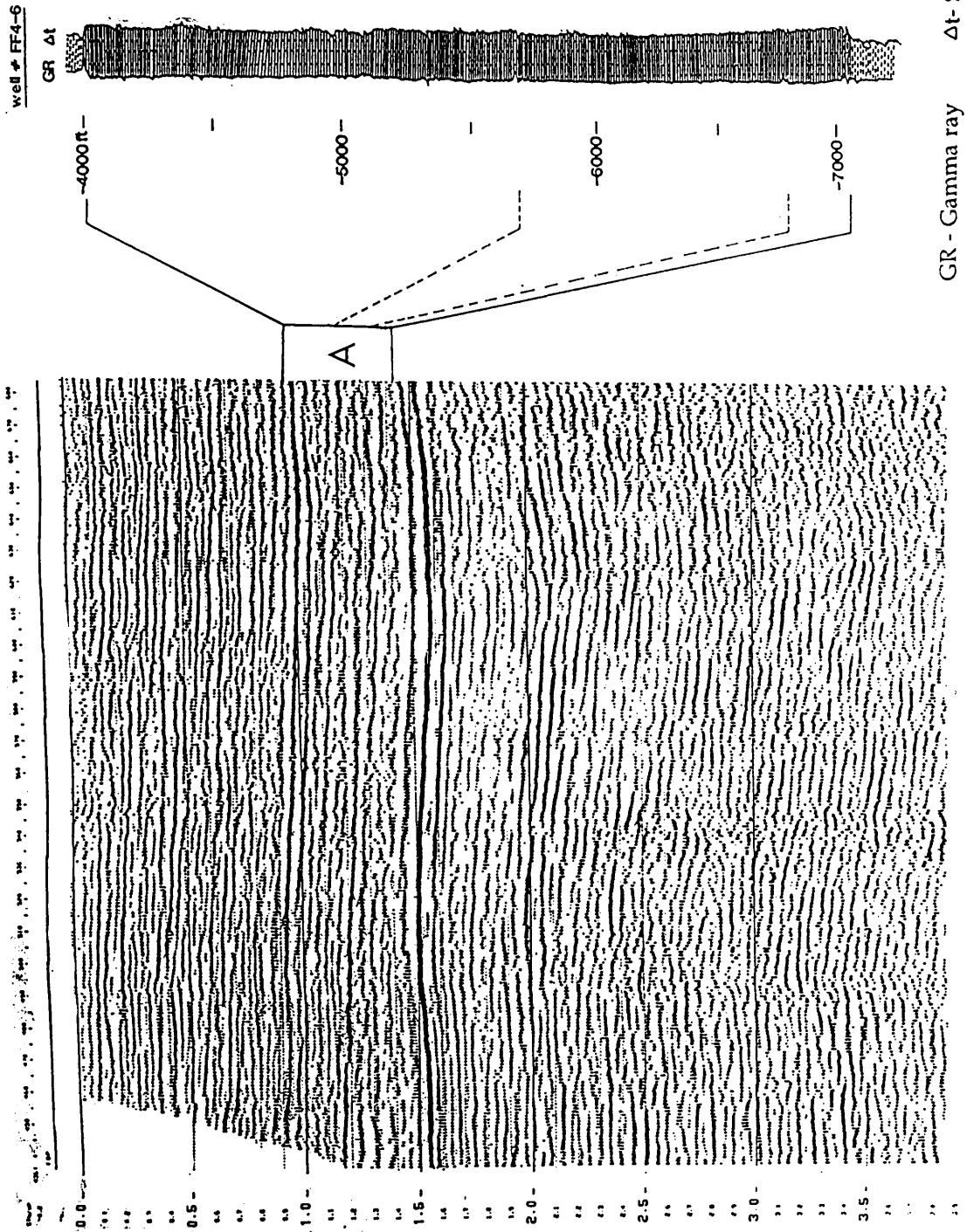
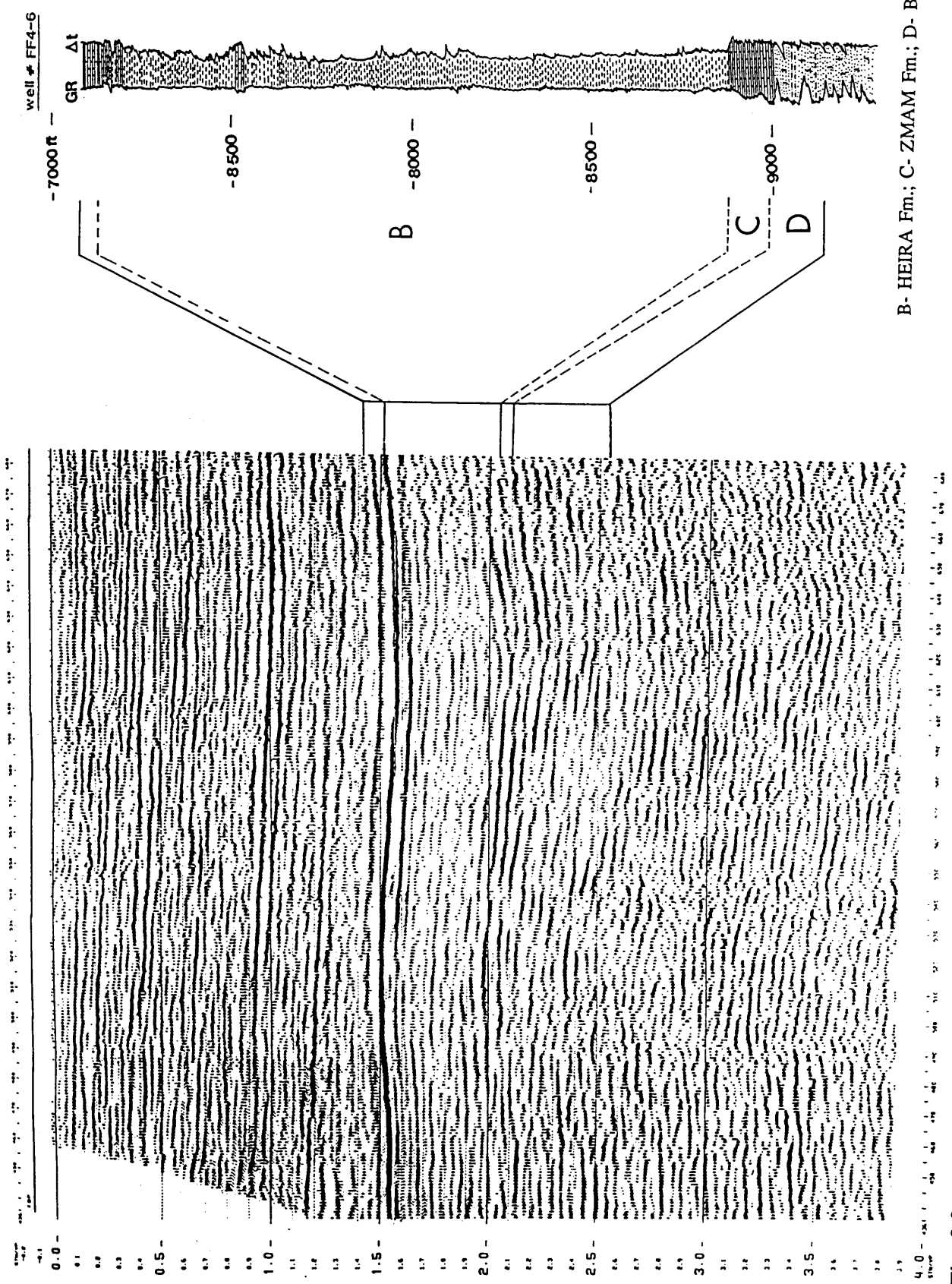


Fig. 3.9 Seismic lines V87-407 showing a summary of the geological and geophysical data, in linking between well and seismic data.



B- HEIRA Fm.; C- ZMAM Fm.; D- BAHJ/GARGAF Fm.

Fig. 3.9 Continued.

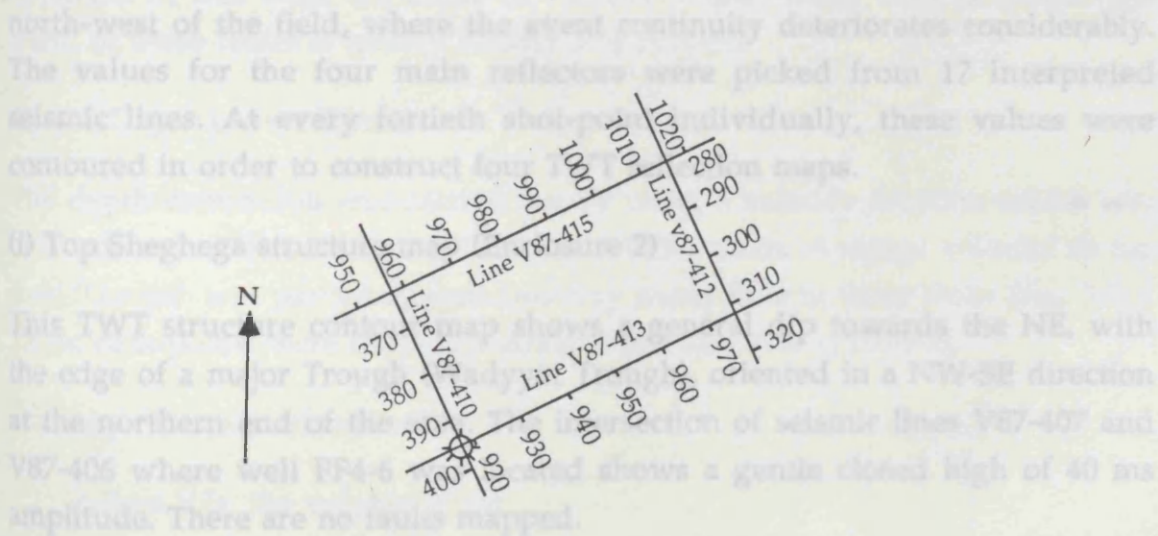
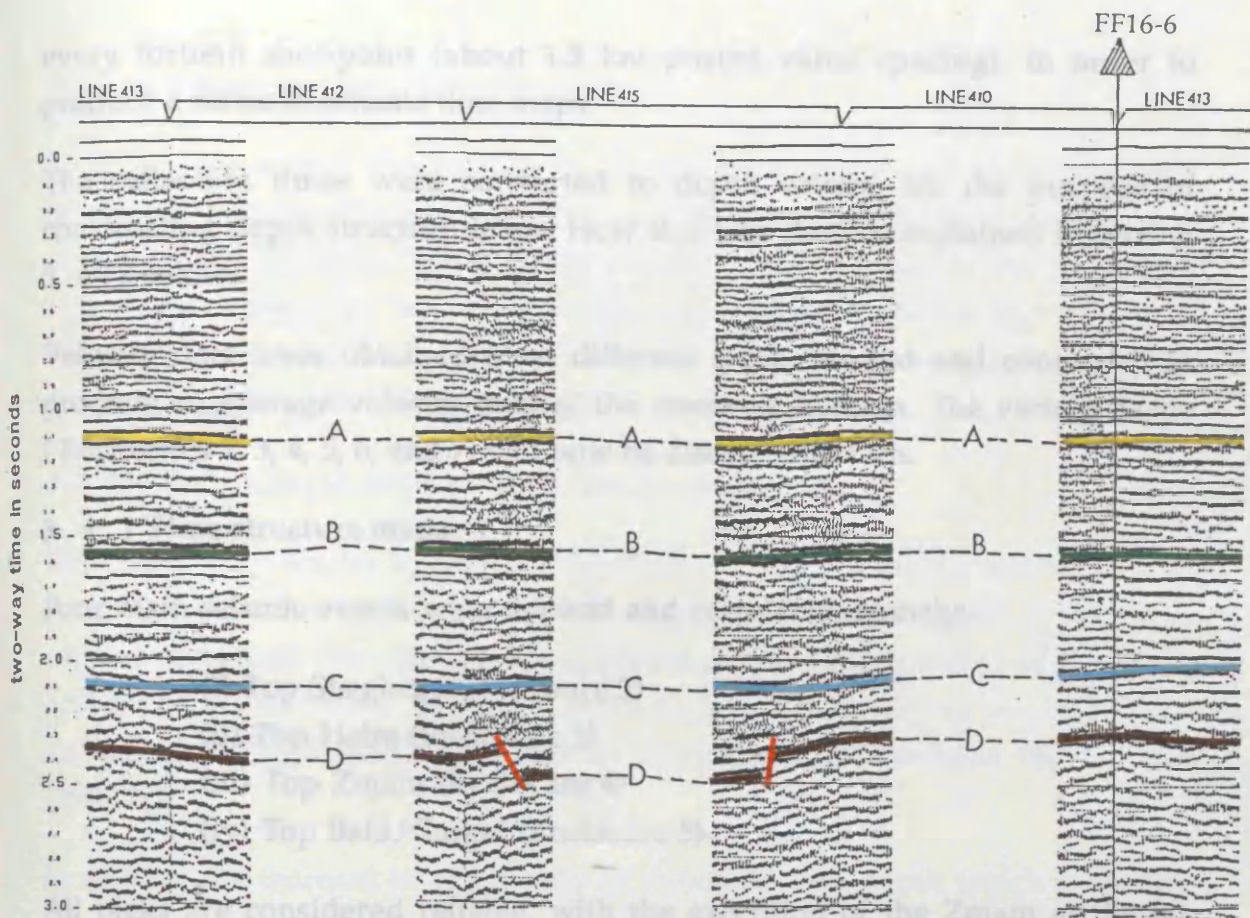


Fig. 3.10 Seismic ties around a closed loop, horizons A, B, C and D are shown at the intercepts of lines 410, 415, 412 and 413. The horizons can be traced continuously around the loop. The data quality deteriorates more at the deeper horizons.

every fortieth shot-point (about 1.5 km posted value spacing), in order to produce a series of seismic time maps.

The reflection times were converted to depth values, for the purpose of constructing depth structure maps. How this was done is explained in section 3.4.2 below.

Velocity data were obtained from different wells, plotted and contoured to produce an average velocity map of the reservoir horizon. The various maps (Enclosures 2, 3, 4, 5, 6, and 7) will now be discussed in turn.

3.4.1 Time structure maps

Four main seismic events were marked and correlated, namely:-

- (i) Top Sheghega (Enclosure 2)
- (ii) Top Heira (Enclosure 3)
- (iii) Top Zmam (Enclosure 4)
- (iv) Top Bahi/Gargaf (Enclosure 5)

All picks are considered reliable, with the exception of the Zmam at the far north-west of the field, where the event continuity deteriorates considerably. The values for the four main reflectors were picked from 17 interpreted seismic lines. At every fortieth shot-point individually, these values were contoured in order to construct four TWT reflection maps.

(i) Top Sheghega structure map (Enclosure 2)

This TWT structure contour map shows a general dip towards the NE, with the edge of a major Trough (Wadyyat Trough), oriented in a NW-SE direction at the northern end of the area. The intersection of seismic lines V87-407 and V87-406 where well FF4-6 was located shows a gentle closed high of 40 ms amplitude. There are no faults mapped.

(ii) Top Heira structure map (Enclosure 3)

The events on this map shows a gradual dip of the horizon towards the NE. A structural closed high of 30 ms amplitude against a fault trending NW-SE is apparent in the middle between FF1-6 and FF4-6 wells, in addition to another closed high of 50 ms located at the southern end of the field. Two structural low closures are also apparent in the southern part.

(iii) Top Zmam structure map (Enclosure 4)

In spite of the strong variations in the amplitude and character associated with the Zmam seismic reflector, this TWT map gives the general structural picture of the Zmam Formation as a gently dipping surface towards the N or NE. Three closed highs are apparent in this map ranging between 30 - 50 ms in amplitude, and two structural low closures. Seven faults were interpreted in this map trending NW-SE and NE-SW.

(iv) Top Bahi/Gargaf structure map (Enclosure 5)

This TWT map shows a general dip of the horizon towards the NE. Three structural high closures are present in the, central and SE parts of the field, while a structural low closure are apparent at the southern part of the field. Closure of the structural high on 2100 ms in the western part of the field is not certain, as the high seems to extend SW beyond the ends of lines V87-413 and V87-411.

In spite of the increase in complexity of structure with depth which is readily apparent in this map, six faults of various displacement were mapped. The trend of these faults is mainly NE-SW and NW-SE.

3.4.2 Depth conversion

The depth conversion was carried out by using a velocity function which was derived from FF7-6, FF11-6, FF12-6 and FF13-6 wells. Average velocity to top Bahi/Gargaf was plotted against two-way travel time in these wells (Fig. 3.11). These data points were fitted to a straight line function as follows:-

A straight line equation $V = MT + C$

where V is the velocity (ft/s)

T is the two way travel time (s)

M is the slope

C is a constant

Using the computer "S" macro for calculating least squares fits, the following result was obtained:-

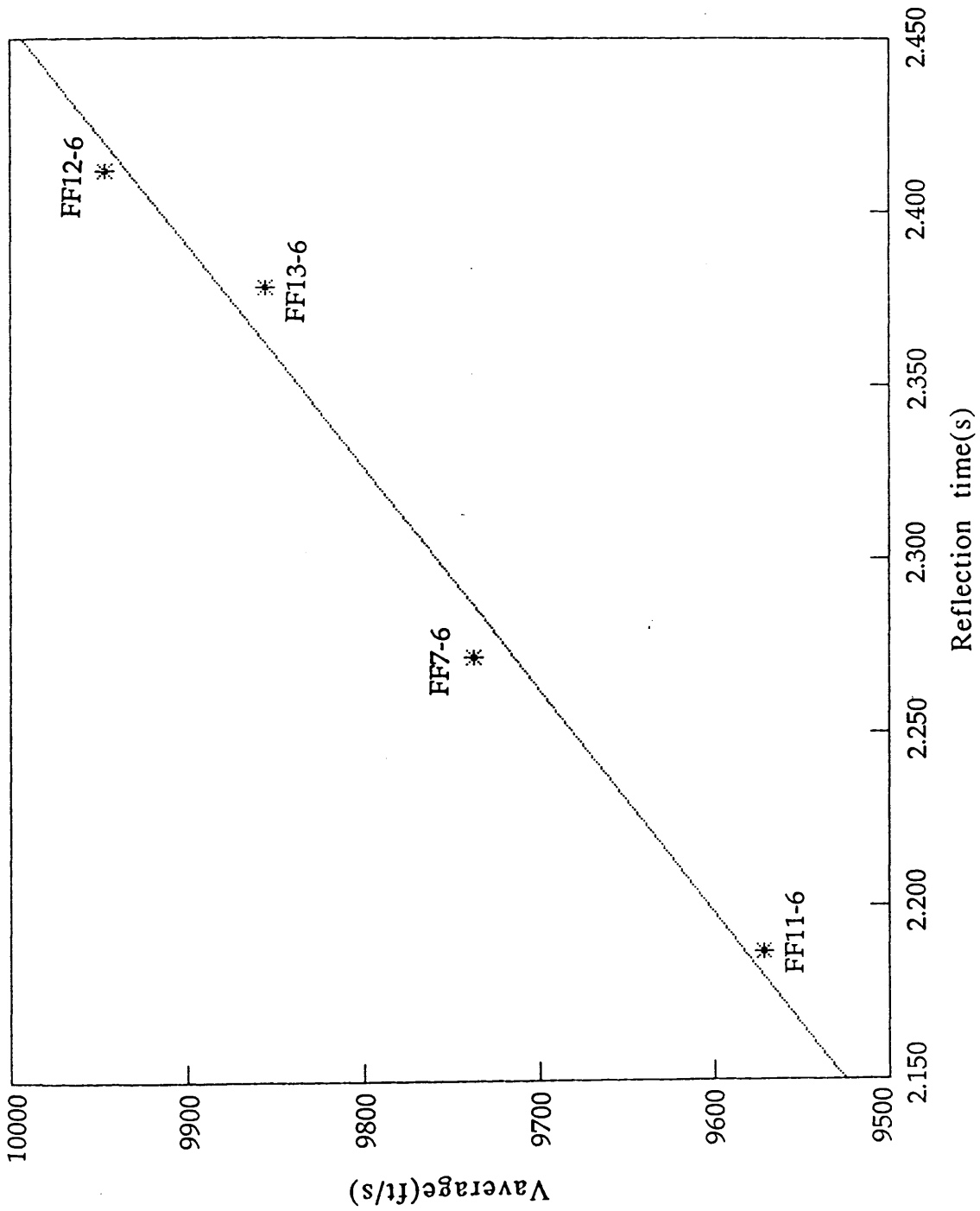


Fig. 3.11 Average velocity V to top Bahi/Gargaf as function of two-way time T.

$$M = 1562 \text{ ft/s/s} \quad C = 6167 \text{ ft/s}$$

By substituting the values of M and C and applying the equation

$$V = 1562 T + 6167$$

to the interpreted two way time T from seismic sections, velocity data were obtained for use in constructing average velocity maps.

in calculating the depth from the above relation, the following was carried out.

$$Z = V(T) \times T/2 \quad \text{where } V(T)=MT+C$$

$$Z = [1562T + 6167] \times T/2$$

$$Z = 781T.T + 3084T$$

$$Z = T(781T + 3084)$$

where Z is depth in ft, T is time in seconds.

And as a result of the application of the above, the following result was obtained.

well No.	sonic (twt) (s)	Vaverage (ft/s)	log.depth (ft)	cal.depth (ft)	z(cal)-z(log) (ft)
FF11-6	2.187	9583	-10476	-10480	+13
FF7-6	2.272	9716	-11064	-11038	-26
FF13-6	2.378	9981	-11720	-11750	+30
FF12-6	2.412	9935	-11995	-11982	-13

The difference in depth between the log data and the calculated depth is related to the location of the well points in relation to the straight line (Fig. 3.11), where FF7-6 and FF12-6 wells should be shallower than the actual log depth, whereas FF11-6 and FF13-6 are deeper.

3.4.3 Depth structure maps

A structure contour map in depth to the top Bahi/Gargaf was constructed over the Attahaddy Field (Enclosure 6). The interpretation of this map over the field and at the level of Bahi/Gargaf Formation, indicates that the north-western part is a sub-division of a larger block which includes the northern part. In fact,

The Bahi/Gargaf is shown to form a continuous reservoir with that of the northern part, down-dip of wells FF7-6 and FF16-6, but up-dip of well FF5-6.

The N-S fault which separates well FF7-6 from FF16-6 is shown to die out laterally well before reaching the practical limits of the reservoir to the north, and a vertical depth variation between the northern and the central part of the field, due to faulting, has provided more than 200 ft (60 m) of protected (not eroded) Gargaf section and/or some overlying clastics of Bahi Formation.

Generally, the map shows an increase in depth towards the NE, and two major low-relief structures separated by two sub-parallel faults trending NE-SW are clearly apparent at the SE corner and the central parts of the field, whereas the high-relief structures are spread over the northern and south western parts of the field.

3.4.4 Average velocity map

A lateral velocity variation at the level of Bahi/Gargaf horizon indicates no sudden change throughout the field (Enclosure 7). The map shows a gradual increase of velocity values towards the NE. The lowest velocity value of 9500 ft/s is represented by a low closure which is located in the north, whereas the highest values of 10500 ft/s is represented by a closed high located west of well FF14-6.

3.4.5 Isopach maps (in time)

A determination of the reflection times of the mapped horizons results in isopach maps of maximum and minimum time-difference (Enclosures 8, 9). The time variations give a broad impression of the thickness changes. In the Zmam/Heira map the time variation shows an increase towards the NE, and the highest reflection time thickness is represented by five closed low relief structures spread around the field. In the Heira/Sheghega map there seem to be little time thickness variation, but the map shows a regional increase in thickness of about 30% towards the south.

3.5 Results

The most obvious result of this study is the compilation of a suite of isopach maps that document the thickness and distribution of the Cretaceous-Tertiary sediments of the field. These maps, together with the seismic structure maps,

provide a concise geological picture of the field, and provide a base for further detailed seismic stratigraphic studies in pursuit of new leads and prospects which will be dealt with in the next chapter.

Closure on these maps is identified by two major bounding faults that maintain a sub-parallel trend. Vertical displacement along these two faults varies, and this is associated with a NE tilting of the Attahaddy main reservoir. The western major bounding fault throw ranges from 1000 ft (300 m) to 200 ft (60 m) from S to N, whilst the eastern bounding fault throw varies from 50 ft (15 m) to 200 ft (60 m) from SW to NE.

Vertical throws of faults at the Zmam level are in the range of 50 ft (15 m) to 200 ft (60 m), which suggests that the main reservoir faults existed prior to Zmam deposition. Also, the presence of a thick Socna section that ranges from 900 ft (270 m) at well FF16-6 to 1200 ft (360 m) at well FF10-6 appears to have attenuated most faults before reaching the Zmam level.

The seismic data show scattered, fairly large faults (at Zmam level) 'framing' the Zelten Platform on the south, such faults are possibly acting as 'shields' from hydrodynamic flows.

Well FF6-6 is found to be drilled in the small graben to the NW of well FF15-6, whereas well FF11-6 is drilled on the northern slope of the structure. This north easterly trending gentle slope represents palaeotopography of the continental clastic sediments of the Bahi Formation, where Bahi sands are probably derived by the considerable uplifts, and deposited in front of the major northern fault escarpment. The Bahi/Gargaf Formation is a good hydrocarbon reservoir, particularly for gas (it is considered the principal reservoir at this field). The present Bahi/Gargaf reservoirs are found primarily in alluvial fan deposits (Keskin, 1978) in proximity to Gargaf horsts and faulted highs. Thick Bahi sediments of probable fluvial origin are found off the structurally higher areas of the Zelten Platform.

The Eocene carbonate sequence are represented by the Sheghega, Ruaga and Domran Formations. These are identified to be fairly flat and represent the shallower strata in the field, and have not been affected by any significant structural movement.

The sub-surface mapping of the field can be summarised by two structural cross-sections (Enclosures 10 and 11), which show a general subsurface correlation of the formations, and indicate that the Upper Cretaceous units (Socna and Bahi) can not be locally correlated due to their absence in most of the wells, whereas the rest of the formations seem to correlate closely.

CHAPTER FOUR

SEISMIC STRATIGRAPHY

4.1 Introduction

The Attahaddy Field is a giant gas field, reservoired in the Cambro-Ordovician sands which appear to be of non-marine origin. The field is a stratigraphic trap in which closure is provided by depositional topography of these sands and minor draping over older structure (McDowell,1988).

The sub-surface geology of the field is divided into four main depositional events. Firstly, is the Eocene carbonate sequences (which consists of three lithostratigraphic units named Domran, Ruaga, and Sheghega Formations. The contact relationship between these units is based on palaeontological study and faunal aspects, whereas in this part of the study they have been assigned the name carbonate sequences). Secondly, is the Palaeocene shale deposits (which consist of a thick sequence of shale deposited in a fairly deep open sea environment). Thirdly, is the Upper Cretaceous units (which is divided into three main formations named Bahi, Socna, and Zmam respectively. The Bahi Formation consists of non-marine detrital sands deposited as alluvial fans. These sands were largely derived by erosion from the underlying Gargaf. The Socna Formation, composed primarily of shales and some limestone deposited in a deep water environment, is believed to be the principal hydrocarbon source rock for both the Bahi and Gargaf reservoirs. The Zmam Formation, a micritic limestone representing deep water carbonate deposition, is the most widespread Cretaceous sedimentary unit. Below these are the Cambro-Ordovician clastic sediments, which are predominantly non-marine quartz and quartzitic sandstone.

4.2 Relevant aspects of seismic stratigraphy

In order to investigate these depositional units, a seismic stratigraphic analysis was carried out, the aim being to analyse the depositional sequences of the Eocene carbonate shelf, to investigate the behaviour of the Palaeocene shale sequence, and finally to correlate the three lithostratigraphic units of the Upper Cretaceous age by the use of the well data.

The study will include seismic configuration and pattern analysis for each of these units mentioned. The results are summarised in seismic facies maps which are believed to give a broad impression on the sub-surface strata of the field.

By linking seismic and well data a geological model and cross section are included to support any evidence that was discussed in previous chapters. However this part of the study will include a well log correlation method to explain the separation and the contact relation between these units.

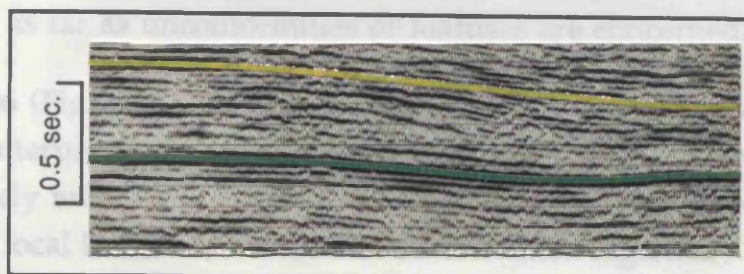
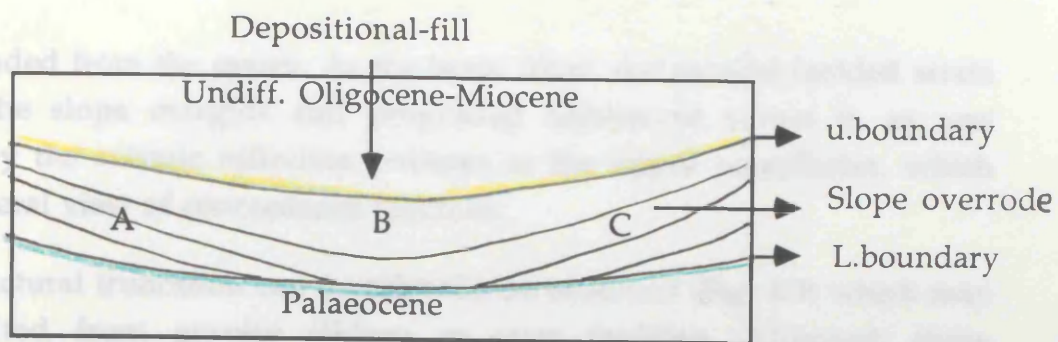
4.3 The Eocene carbonate sequence

As previously discussed, the Eocene strata are absent from most of northern Libya. However, much of the Sirte Basin contains a thick sequence of Eocene carbonate and evaporites, and the Eocene was primarily a time of carbonate deposition, but near the end of this epoch there was initiated a period of tectonic instability which peaked during the Oligocene and early Miocene. The Upper Eocene sequence is the result of a regional shallowing of the seas which brought the Eocene cycle to a close.

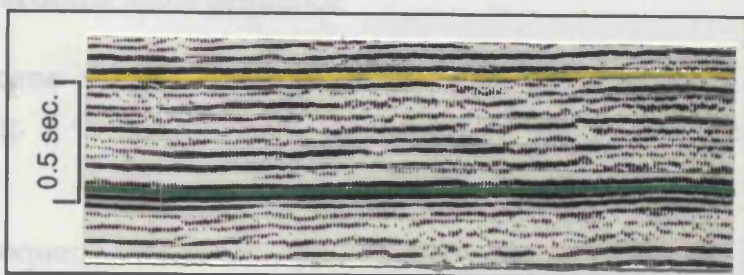
Fig. 4.1 is a seismic facies map showing the types of seismic reflection relation, and relation of strata to boundaries of depositional sequences along the upper and lower surfaces of the Eocene sequence. Despite the fact that the seismic stratigraphy is very settled at this level, the seismic reflections in the northern area of the field indicate predominantly downlap dipping north onto the deep water floor, but some apparent local onlapping westerly trending can be observed. The seismic facies pattern in the west shows a series of parallel arrows indicating low angle downlap radiating from an elongate central area, where reflections are mostly concordant to the lower surface. This pattern of downlap and concordance is interpreted as a lobe of parallel bedded strata (Fig. 4.2) which built into the central basin area from a southern source, and



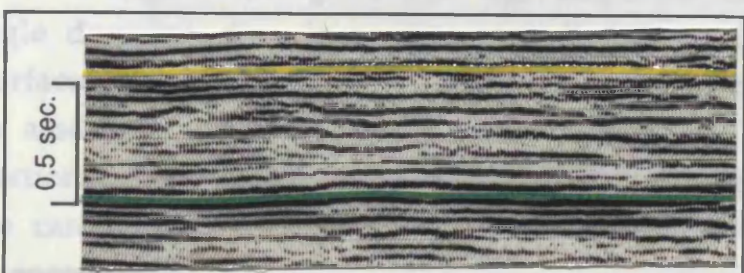
Fig. 4.1 Seismic facies map showing reflection patterns and relation to upper and lower boundaries of the Eocene carbonate sequence.



A



B



C

0 2 Km 2 MILES

Fig. 4.2 General depositional model of the Eocene carbonate sequence, with examples of reflection attitude and continuity at positions A, B and C in the model.

then prograded from the centre. As the basin filled, the parallel-bedded strata overrode the slope margins and prograded northward across it, as was indicated by the seismic reflection patterns at the upper boundaries, which show a general view of concordance relations.

A local structural truncation can occasionally be observed (Fig. 4.3) which may have resulted from gravity sliding or even faulting. Although these truncations have produced a locally discordant relation of strata to the upper sequence boundary, they have minor if non regional chronostratigraphic significance as far as unconformities or hiatuses are concerned.

Line V87-406 (Fig. 4.1) shows a toplap relation to the upper carbonate surface, this being interpreted as a result of non deposition (sedimentary by-passing) with relatively minor erosion, however, these relation types (toplap) are found to be rather local in extent, and cannot be correlated regionally.

4. 4 The Palaeocene shale sequence

The Palaeocene shale sequence displays two different generalized seismic patterns (Fig. 4.4), and accordingly, it can be subdivided into two seismic sequences.

The upper sequence consists of parallel strata where the reflection patterns are mostly parallel to slightly divergent, with high-amplitude continuous cycles and low-angle downlap dips in west-to-east direction against the lower bounding surface. The very thin limestone beds which are more common in this part in association with the shale (indicated by the high-amplitude, parallel reflection pattern) environmentally suggest that strata generating this seismic type can be interpreted as a shallow marine shelf with variable depositional energy.

The lower part of the subdivided sequence has predominantly high-angle onlap at the base (Fig. 4.5), dipping north to east, with a fairly low-amplitude and discontinuous character. However, a number of growth faults reach and often cut this part of the sequence. This is interpreted from sediment thicknesses, which are much thicker on the downthrown side of some major faults whose growth appears to have been contemporaneous with the sedimentation (see seismic line V87-412; sp 275-360: Fig. 3.2), which show how such faults affect the strata by spinning or rotating the sedimentary block, and

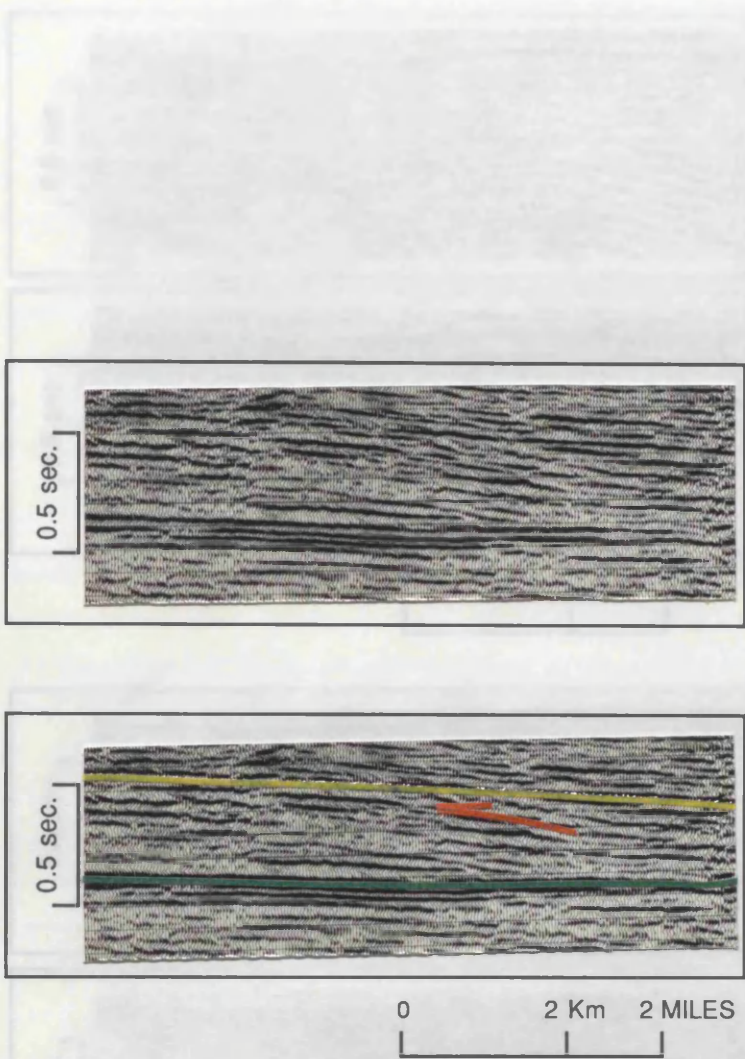


Fig. 4.3 Minor toplap at the top of the Eocene sequence.
 Lower section shows the interpretation of the data (top).

Fig. 4.4 Seismic reflection profiles of the Eocene sequence, displaying two types: (a) a parallel to subparallel type and (b) a sigmoid type illustrating an oblique-slip fault. Lower section of each panel shows interpretation.

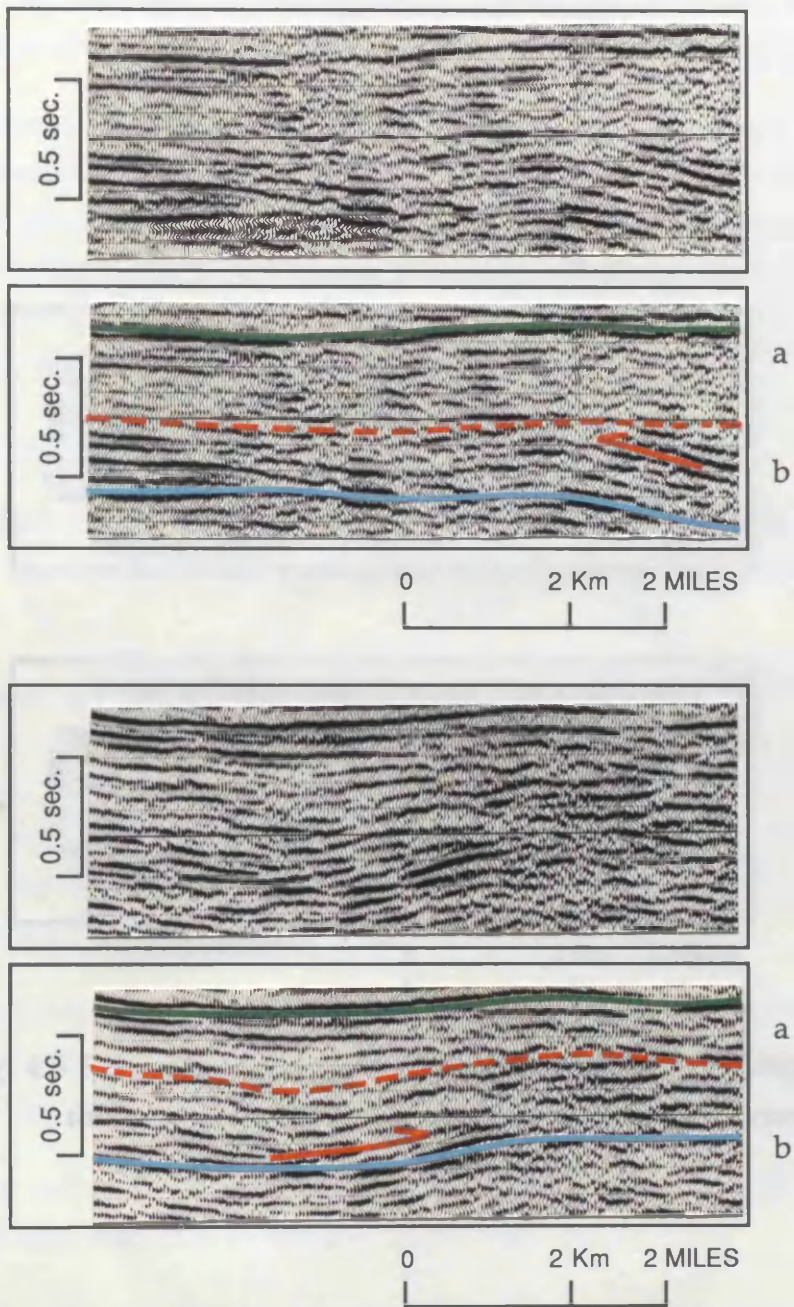


Fig. 4.4 Seismic reflection patterns of the Palaeocene shale, displaying two types: a- is a parallel to sub-parallel configuration; b- is a sigmoid type (truncating at the sequence boundary with type a). Lower section of each pair shows interpretation.

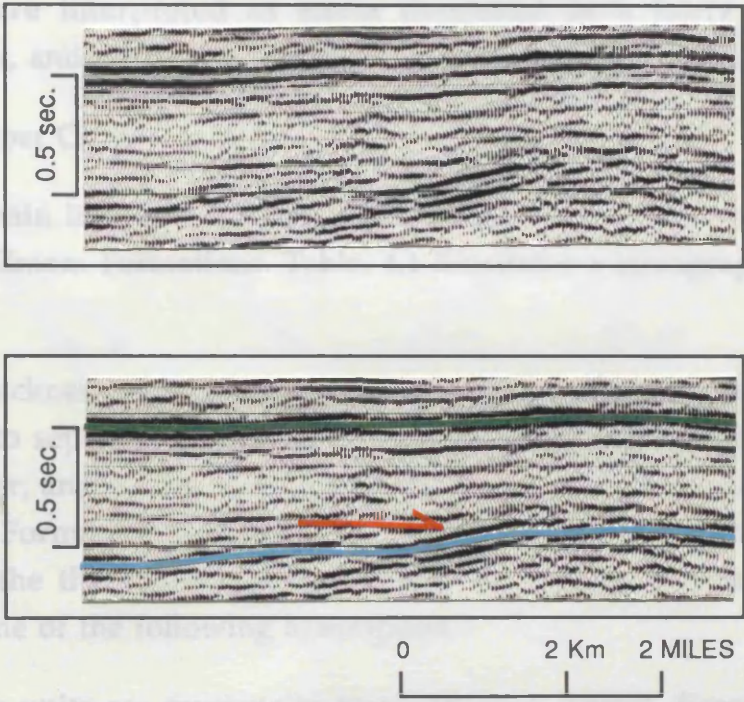


Fig. 4.5 Palaeocene lower shale sequences showing onlapping relation to the lower boundary. Second pair shows interpretation.

which also explains the discontinuity of the reflection patterns, in addition to the lithological character and variation between these two seismic sequences.

Generally, the seismic facies map (Fig. 4.6) shows a general baselap relation of the shale towards the east, with a north-east trending local truncation which is pronounced along the upper surface of the sequence in various places of the area, and is believed to have resulted from faulting and gravity sliding. These sequences are interpreted as strata deposited in a fairly deep open sea environment, and characterized by south easterly thinning out.

4. 5 The Upper Cretaceous units

The three main lithostratigraphic units in the Upper Cretaceous are the Bahi, Socna, and Zmam Formations. Table. 4.1 illustrates a stratigraphic summary of these units.

Since the thickness of these units varies from 10ft (3m) to 2000ft (600m), it is quite hard to separate them seismically, in spite of their lithological variation and character, and especially in areas where the Socna Formation is absent and the Zmam Formation is lying unconformably over the Bahi Formation. In such cases the thickness of these units does not exceed 150ft (45m). This is related to one of the following assumption:-

- a- These units are erosionally truncated in a certain direction, with minor or even major thinning out of the formation, or the strata have been tilted by structural movement (discussed in Chapter 1).
- b- These units are mainly condensed, and they seem to thin out laterally from one direction to another.
- c- These units are initially horizontal strata and onlap against an initially inclined surface, or even that they are inclined stratum that lap out updip against a surface of greater inclination.



Fig. 4.6 Seismic facies map showing reflection patterns and relation to upper and lower boundaries of the Palaeocene shale sequence.

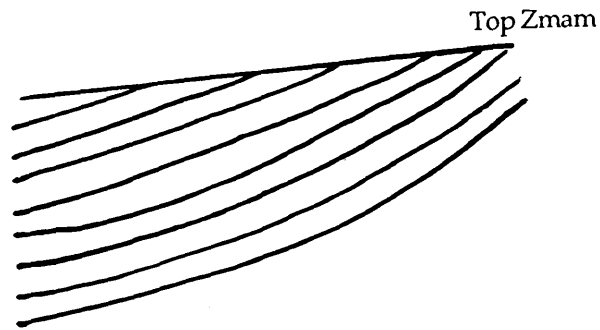
AGE	FORMATION	LITHOLOGY	THICKNESS	CONTACT RELATION	STATUS
Upper-Cretaceous	Zmam Formation	Limestone	100 - 600 Ft (30 - 180 m)	Transitional gradual change in lithology.	Widespread marker bed.
	Socna Formation	Limestone and Shale	45 - 2000 Ft (13 - 600 m)	Transitional	Principal hydrocarbon source
	Bahi Formation	Sandstone, Siltstone, Quartzite	10 - 400 Ft (3 - 120 m)	Unconformity based on abrupt change.	Secondary reservoir

Table 4.1 Stratigraphic Summary of the Upper Cretaceous units.

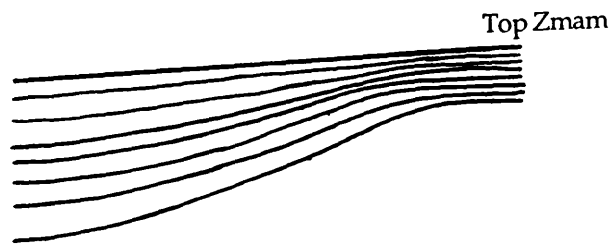
The diagrammatic illustration of these aspects is shown in Fig. 4.7. In order to analyse these models, a seismic facies map (Fig. 4.8) indicates there is a general east-west truncation of the units. This truncation is known to be of an erosional type, as it is clearly defined in some of the sections where these units are characterized by different truncational directions (Fig. 4.9). However, the folded structure (Fig. 4.9 c) has produced an irregular type of surface boundary (the upper boundary). This is mainly related to both structural disturbance and erosion of the exposed part of the strata, which is normally followed by the deposition of the overlying sequence.

In addition, we know that the Bahi Formation, which represents the oldest Upper Cretaceous unit, was originally derived by erosion from the underlying Gargaf Formation. Thus erosion is the key to the deposition of these units, and therefore it becomes obvious that all these truncation signs shown on the map have actually resulted from erosional factors.

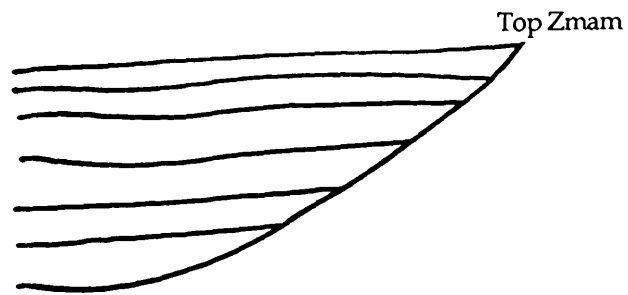
A concordant relation of the strata to the upper boundary can rarely be observed, but areas where strata do not terminate against the surface boundary, and mostly located between two truncational patterns of opposite directions, are fairly common.



a. Truncation



b. Condensed



c. Onlap

Fig. 4.7 Diagrammatic illustration showing the three models to explain the thickness variations of the Upper Cretaceous units.

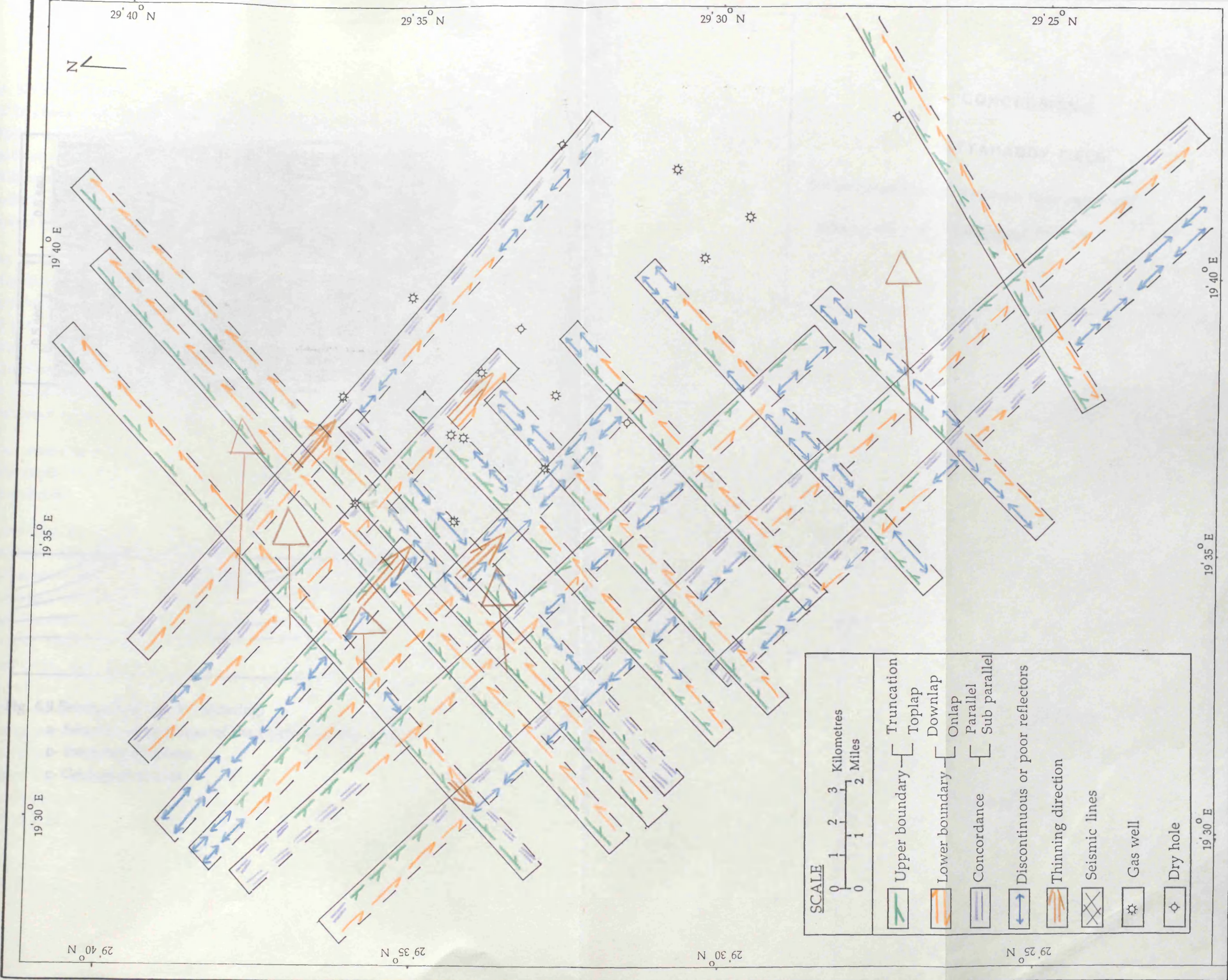


Fig. 4.8 Seismic facies map showing reflection patterns and relation to upper and lower boundaries of the Upper Cretaceous units.

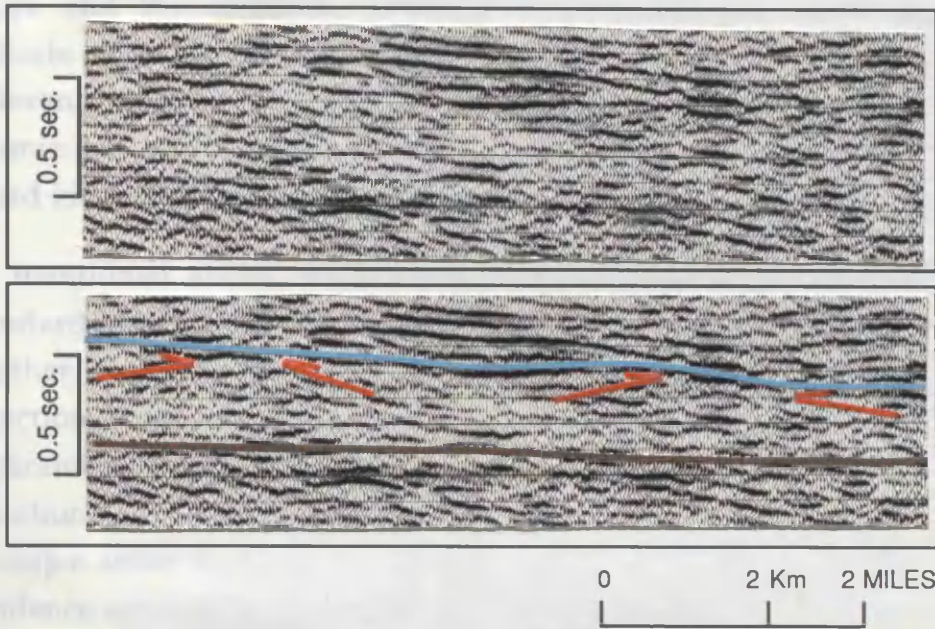


Fig. 4.9 Seismic line V87-421 showing:

- a- Seismic configuration of the Upper Cretaceous strata.
- b- Interpreted section.
- c- Geological model.

A SW-NE trending low angle baselap can be observed from area to another. This general onlap trend seems to be in common with the overlying strata of Heira and the carbonate sequences. Although this comparison does not indicate a major significant feature related to deposition, due to difficulties in differentiating between onlap and downlap relations and also to the settled seismic stratigraphy of the field which was previously explained, it still gives a broad idea on the general attitude of the whole sub-surface strata of the field.

As mentioned above, the Upper Cretaceous units are not characterized by standard uniform thickness, but their thickness varies from one location to another. The small arrows shown in some parts of the map indicate the direction of thinning, neglecting its type at this stage (where it is discussed separately in the next section). However, it appears that the general thinning direction of these units is south east, and in some areas where thinning is due to major active faulting, it is considered to be a local effect and much of this incidence appears in the north-west part of the field.

Discontinuous or poor reflections are rather common on seismic sections at this depth, making it difficult to interpret the relation of the strata to surface boundaries.

Generally, the view of the map and the overall interpretation of seismic configuration patterns on sections could lead to the fact that the Upper Cretaceous units are not uniformly spread over the study area, but the behaviour of these units suggests that in areas where the whole Socna and Bahi Formations are absent, and the Zmam Formation is underlain directly by Gargaf Formation, it seems that the whole Zmam thickness becomes negligible, and therefore these 150ft (45m) of limestone separating the Palaeocene shale from the reservoir rock cannot be analysed and studied in detail. Since it is believed that Socna Formation is the principal hydrocarbon source rock for the Bahi (the secondary reservoir in the field) and Gargaf reservoirs, it is of great importance to locate areas where this unit becomes absent. Fig. 4.10 shows the exact trend of the formation, and shows areas where the formation pinches out until it is completely absent. However, the thickness variation of this unit makes it very hard to be seismically mapped.

4.6 Electric log correlation

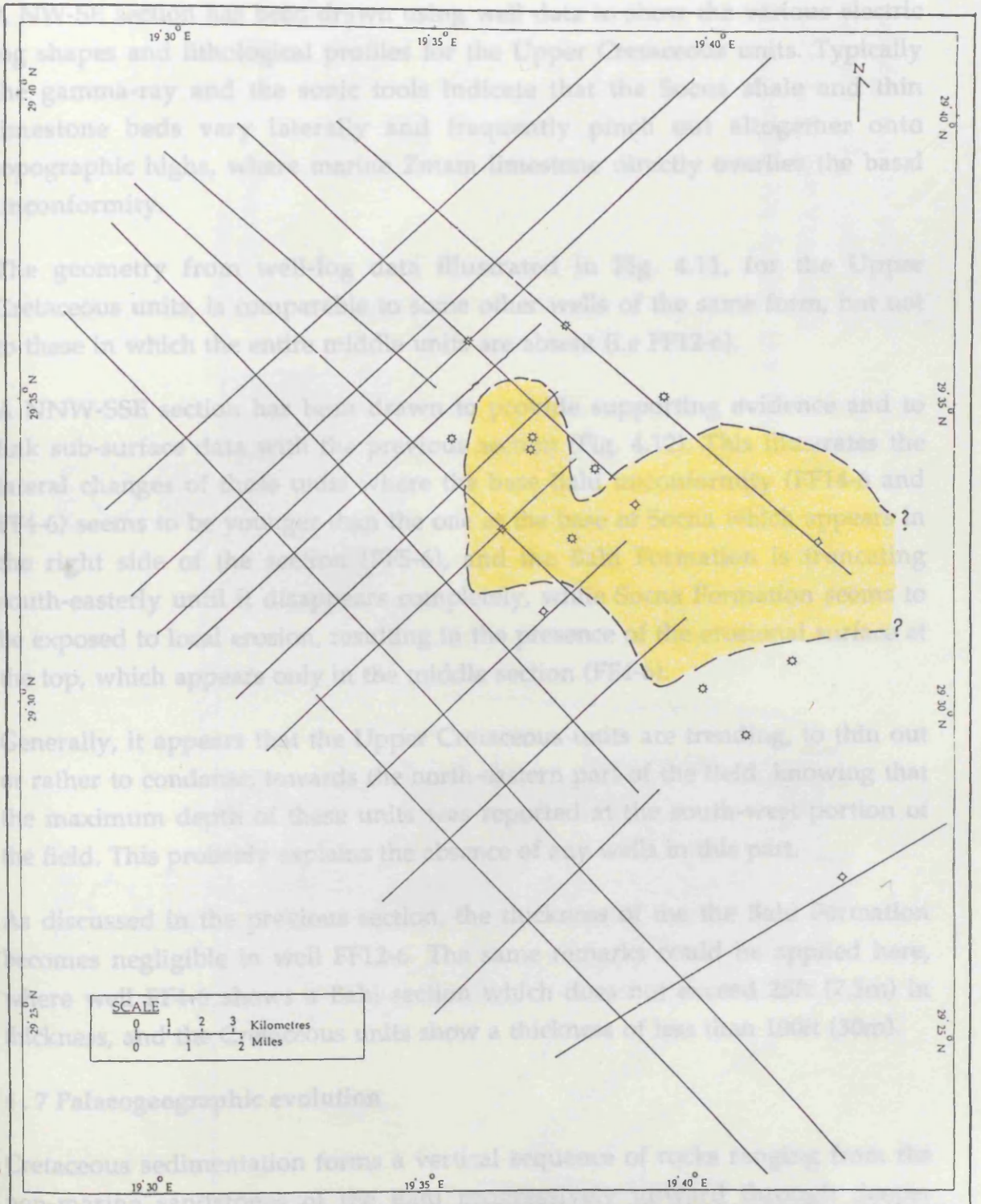


Fig. 4.10 Map showing area where Socna Formation is absent.

4.6 Electric log correlation

A NW-SE section has been drawn using well data to show the various electric log shapes and lithological profiles for the Upper Cretaceous units. Typically the gamma-ray and the sonic tools indicate that the Socna shale and thin limestone beds vary laterally and frequently pinch out altogether onto topographic highs, where marine Zmam limestone directly overlies the basal unconformity.

The geometry from well-log data illustrated in Fig. 4.11, for the Upper Cretaceous units, is comparable to some other wells of the same form, but not to these in which the entire middle units are absent (i.e FF12-6).

A NNW-SSE section has been drawn to provide supporting evidence and to link sub-surface data with the previous section (Fig. 4.12). This illustrates the lateral changes of these units where the base Bahi unconformity (FF14-6 and FF4-6) seems to be younger than the one at the base of Socna which appears in the right side of the section (FF5-6), and the Bahi Formation is truncating south-easterly until it disappears completely, while Socna Formation seems to be exposed to local erosion, resulting in the presence of the erosional surface at the top, which appears only in the middle section (FF4-6).

Generally, it appears that the Upper Cretaceous units are trending, to thin out or rather to condense, towards the north-eastern part of the field, knowing that the maximum depth of these units was reported at the south-west portion of the field. This probably explains the absence of any wells in this part.

As discussed in the previous section, the thickness of the the Bahi Formation becomes negligible in well FF12-6. The same remarks could be applied here, where well FF4-6 shows a Bahi section which does not exceed 25ft (7.5m) in thickness, and the Cretaceous units show a thickness of less than 100ft (30m).

4.7 Palaeogeographic evolution

Cretaceous sedimentation forms a vertical sequence of rocks ranging from the non-marine sandstones of the Bahi progressively upward through deeper water environments, culminating in the deep water limestone of the Zmam, as the Zelten Platform was gradually submerged by rising sea levels. Cretaceous sedimentation began with the alluvial fan and braided stream continental deposits of the Bahi (Fig.4.13). Rising sea level brought a marine invasion onto

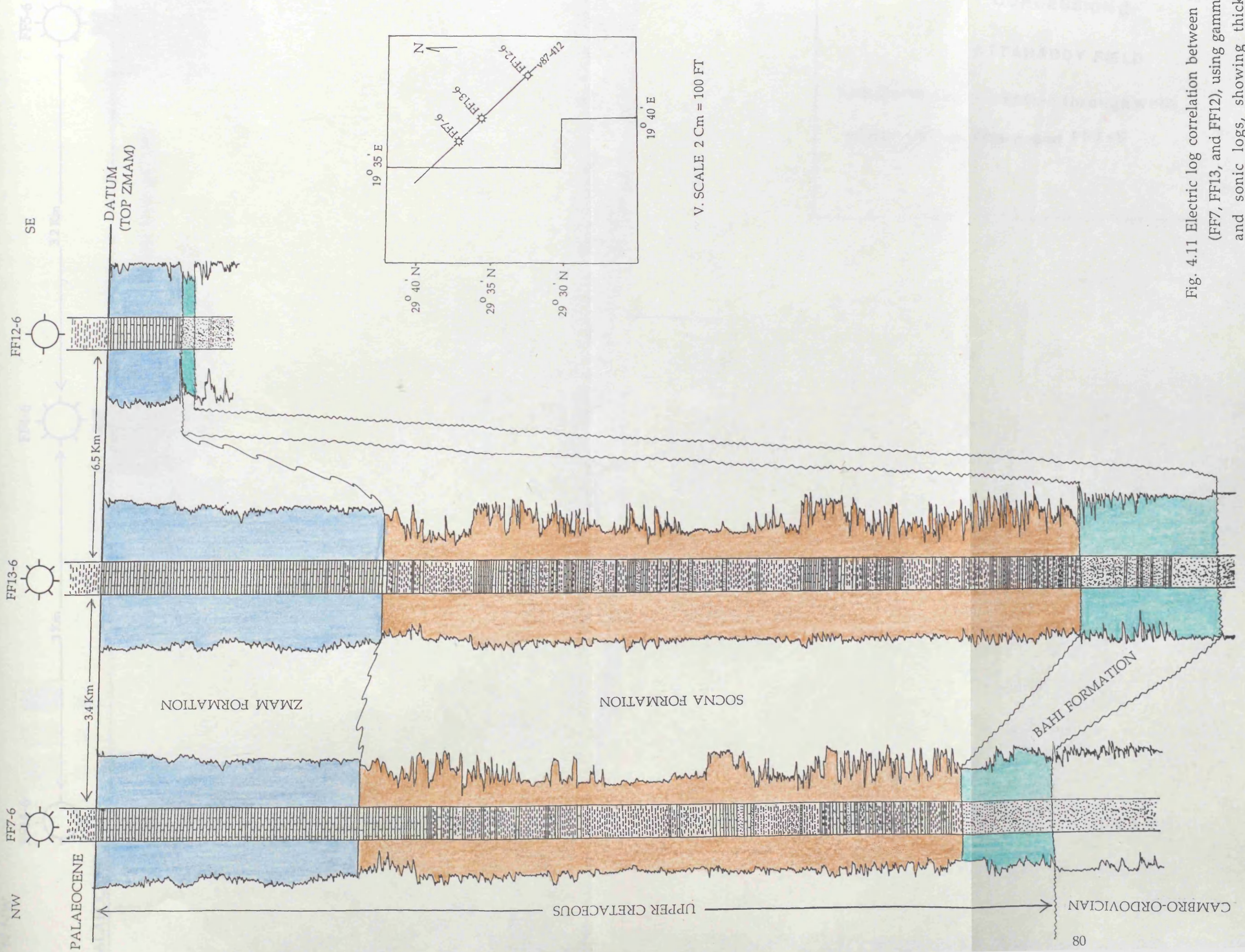


Fig. 4.11 Electric log correlation between wells (FF7, FF13, and FF12), using gamma-ray and sonic logs, showing thickness variation of the Upper Cretaceous units.

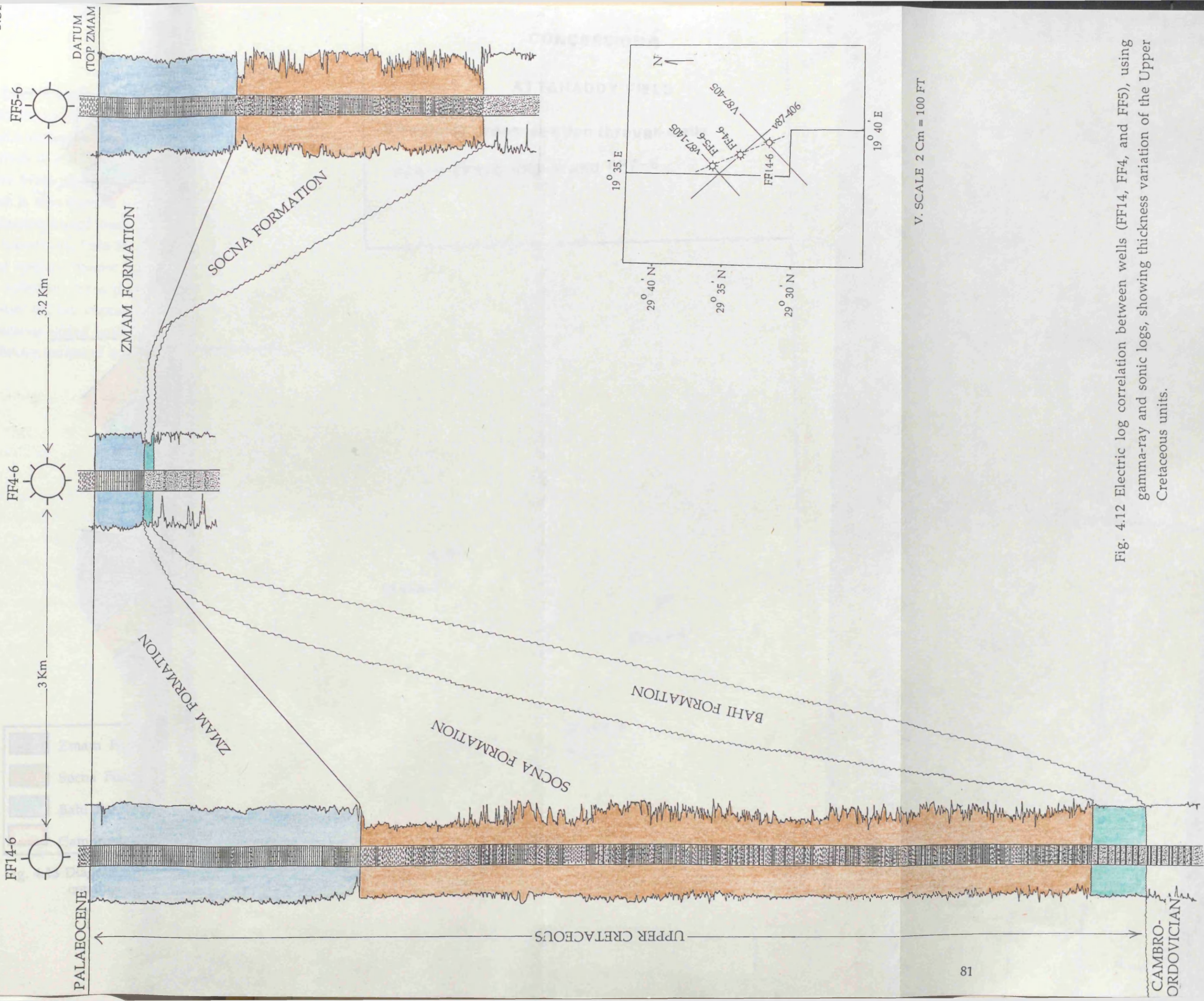
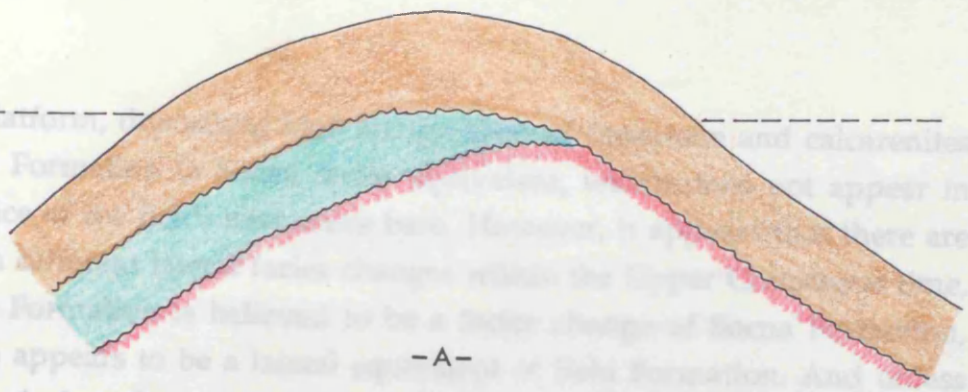


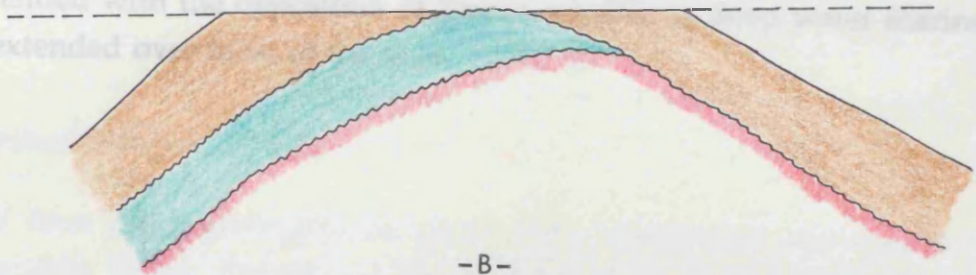
Fig. 4.12 Electric log correlation between wells (FF14, FF4, and FF5), using gamma-ray and sonic logs, showing thickness variation of the Upper Cretaceous units.

the Zmam Formation... and calcarenites of the Waha Formation... appear in the sub-surface... there are a series of a... where Waha Formation... which is also appears to be a lateral... a palaeontological study is carried out and... it is considered that Bahi Formation is older than the Socna Formation. In lower energy, deeper water environments... this was followed by a period of erosion and non-deposition... the erosion of the exposed parts of both... Cretaceous ended with the... conditions extended over



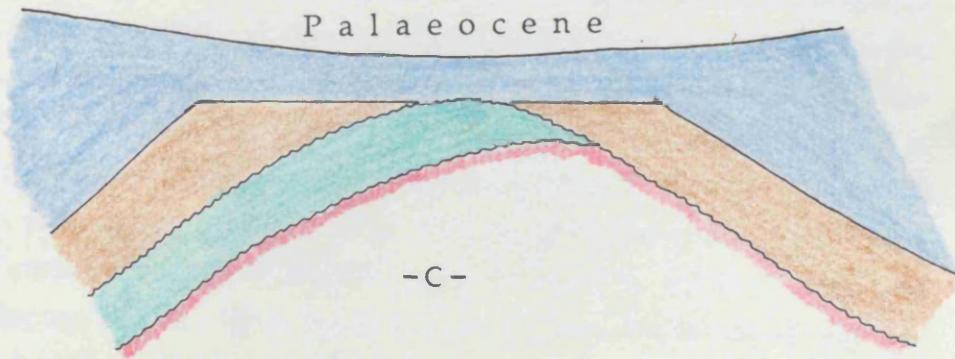
-A-

Period of erosion and non-deposition



-B-

Palaeocene



-C-

	Zmam Formation
	Socna Formation
	Bahi Formation
	Cambro-Ordovician

Fig. 4.13 Diagrammatic illustration of the erosional and depositional process creating the Upper Cretaceous units.

the Zelten Platform, depositing high energy skeletal limestone and calcarenites of the Waha Formation (a Socna facies equivalent, which does not appear in the sub-surface of the field) near wave base. However, it appears that there are a serious of a different lateral facies changes within the Upper Cretaceous time, where Waha Formation is believed to be a facies change of Socna Formation, which is also appears to be a lateral equivalent of Bahi Formation. And unless a palaeontological study is carried out and provide evidance probabeleties, it is considered that Bahi Formation is older than the overlain Socna Formation. In lower energy, deeper water environments, Socna shales were deposited, this was followed by a period of erosion and non deposition resulting in the erosion of the exposed parts of both Bahi and Socna Formations. The Cretaceous ended with the deposition of Zmam micrites as deep water marine conditions extended over most of the area.

CHAPTER FIVE

GENERAL INTERPRETATION AND CONCLUSIONS

5.1 Geophysical interpretation

The tops of four main geological horizons were interpreted and mapped, named Sheghega, Heira, Zmam and Bahi/Gargaf Formations. These events were found almost continuously over the subsurface of the field area. The Sheghega Formation represents the top of the Eocene carbonate sequences, which is characterised by a solid continuous seismic reflector that can be traced over the whole area. The Heira Formation represents the top Palaeocene shale, which can also be traced due to the continuity of its seismic reflector. The Zmam Formation represents the top Upper Cretaceous unit. This reflector is not as continuous as the overlying reflectors, but it can still be recognised and traced (although with major difficulties) on most of the seismic sections. Below these lies the Cambro-Ordovician Bahi/Gargaf Formation, which is the least continuous reflector of all. This horizon can hardly be mapped due to discontinuity and poor quality of its reflector.

The most obvious result of this study is the compilation of a suite of isopach maps that document the thickness and distribution of the sediments in the field. These maps, together with the seismic structure maps, provide a concise geological picture of the field, and could lead to the fact that closure on these maps is identified by two major bounding faults that maintain a sub-parallel trend. Vertical displacement along these two faults varies, and this is associated with a north-east tilting of the Attahaddy main reservoir.

The throw of the western major bounding fault ranges from 1000 ft (300 m) to 200 ft (60 m) from south to north, whilst the eastern bounding fault throw varies from 50 ft (15 m) to 200 ft (60 m) from south-west to north-east.

Vertical throws of faults at the Zmam level are in the range of 50 ft (15 m) to 200 ft (60 m), which suggests that the main reservoir faults existed prior to Zmam deposition. Also, the presence of a thick Socna section that ranges from 900 ft (270 m) at well FF16-6 to 1200 ft (360 m) at well FF10-6 appears to have attenuated most faults before they reach the Zmam level.

5.2 Geological interpretation

The Attahaddy Field comprises a main central block plus peripheral areas to the north and south. The field gas-water contact is present at about -12000 ft (3600 m), and the base of the reservoir is formed by a red siltstone which is present below this depth.

The Upper Cretaceous (Senomanian) Bahi Formation represents a secondary reservoir target. This formation comprises coarse to fine conglomerates, sandstones and siltstones derived from the erosion of the Gargaf orthoquartzites.

The north-west extension is the least known area of the Attahaddy Field, it is a separate fault block adjacent to that being tested by FF16-6 well. A NE-SW fault of approximately 30 ft (10 m) throw separates this area from that on which the FF16-6 is located. The NE and SW extension of this fault are not clearly defined, and the fault may not continue in these directions.

Because the Attahaddy Field is located within the south central part of the Hagfa Trough near the central part of the palae-Sirte Basin Arch, most of the Palaeozoic sections were probably eroded. The deepest wells in the field indicate that the remaining Palaeozoic section is represented by the Cambro-Ordovician, Lower Gargaf, non-reservoir red siltstone section. The actual thickness of the section is not known.

The Cretaceous section is physically divided by the mid-Cretaceous unconformity into two major parts.

The lower part represents the main Attahaddy reservoir section. This unit unconformably overlies the remaining section of the highly eroded Cambro-Ordovician Formation.

The upper part of the Cretaceous above the mid-Cretaceous unconformity (Senomanian to Maastrichtian) comprises up to 4000 ft (1200 m) of deep marine shale and limestone. This section averages about 1450 ft (435 m) over the Attahaddy Field area. The section is represented by a thick Socna shale and highly argillaceous Zmam Formations.

The Socna shale has significant stratigraphic importance in the whole Sirte Basin, as it acts as a regional, well defined, source rock for all Cretaceous and possibly for most Tertiary reservoirs. The thickest Socna as recorded in the Attahaddy area is over 1250 ft (375 m) in well FF10-6, while its minimum thickness is 371 ft (112 m) in FF6-6 well.

The Zmam Formation is a homogeneous argillaceous to micritic limestone of Upper Maastrichtian to Danian age. Regionally it is well known for having good shows but lacks good permeability. Generally, the thickest Zmam sections are to the south of the Attahaddy Field area.

The Tertiary section is predominantly shale, limestone and dolomite. Sedimentation through the section was controlled by slow tectonic movement and gradual subsidence, thus the depositional environment was mainly deep marine that laterally changed to shallow marine in localized areas.

The Palaeocene Heira Formation which underlies the lower part of the carbonate sequences (Ruaga Formation), consists of relatively thick calcareous grey-green shales that change facies vertically and laterally. Although this formation is of great importance at the very far west of the area, it is not known as a proven mature source rock in this field.

The Eocene carbonate sequence is divided into three separate carbonate units. It consists of an upper calcareous shale and carbonate called the Sheghega Formation and a lower carbonate sequence that includes Domran and Ruaga Formations.

The regional fault pattern of major tectonic rift is made up of longitudinal or curved segments that merge together to form a series of step away fault blocks (Harding, 1984). It is believed that the Attahaddy Field was developed by this mechanism during the differential subsidence of the Hagfa Trough.

Structural activity is responsible for the development of the tectonic fracture pattern, which is the main factor in developing the fracture reservoir in quartzitic formations, such as in the Bahi and Gargaf Formations of the Attahaddy Field. Tectonic fractures are by far the most important of all the types of fracture.

5.3 Conclusion

Putting together the results of this study, the following conclusions have emerged.

A) Outlining the distribution of the varies Upper Cretaceous-Tertiary strata within the subsurface of the Attahaddy Field area has led to the recognition of the following sequences:-

i) The Eocene Carbonate sequence

Comprises three main formations to include Sheghega, Domran, and Ruaga. The contact relationship between these units could not be traced seismically, due to lithological similarities, while the top and the base of these units (as one carbonate massive sequence) were traced and mapped. These sequences are present over all the area of the fields.

ii) The Palaeocene shale

This thick sequence of Heira shale is represented by a continuous seismic reflector, easy to trace and to map. The shale has been sub-divided into two seismic sequences, in which the upper sequence consists of parallel strata where the reflection patterns are mostly parallel to slightly divergent, with high-amplitude continuous cycles and low-angle downlap dips occur in east to west directions against the lower bounding surface. The lower part of the subdivided sequence has predominantly high-angle onlap at the base, dipping north to east, with fairly low-amplitude and discontinuous character. This new subdivision, which has

not previously been recognised, is mainly related to changes in the environment of deposition.

iii) The Upper Cretaceous units

The Cretaceous units in the Attahaddy Field comprise three main units named Bahi, Socna, and Zmam. The contacts between these units are defined by erosional surfaces (unconformity), as traced on seismic sections and indicated by the erosional truncation. Due to the thin stratigraphic section of the Upper Cretaceous units in the field, separation between them on seismic sections is often difficult in spite of their lithological variation, therefore these units have been mapped as one unit. Among these three units only the Socna Formation is believed to be of any great importance, being considered to be the principal hydrocarbon source rock for the underlying Bahi/Gargaf reservoir. This formation is absent in most if not all the eastern side of the field.

B) The seismic maps indicate that the Cambro-Ordovician reservoir rocks increase in depth towards the NE, and two major low relief structures separated by two sub-parallel faults trending NE-SW are apparent at the SE corner and in the central parts of the field, whereas the high-relief structures are distributed over the northern and south western parts of the field.

5.4 Recommendations for further work

1) The north-west extension of the field is due to be studied and more seismic surveys are needed to cover that part. However the lack of well data here makes subsurface correlation often difficult.

2) The recent seismic studies should be matched and correlated to all previous seismic work, particularly in analysing and investigating the Upper Cretaceous units in the field and the nearby areas. This correlation should involve the interpreted data from Concession NC130A which forms the western and southern sides of the field.

3) The currently controversial point of view is whether and how to separate the Upper Cretaceous unit (Bahi Formation) from the underlying Cambro-Ordovician Gargaf. These must be studied and analysed further both geologically and geophysically before this problem can be resolved.

4) The stratigraphical problems, caused by erroneous transcriptions of local Arabic names previously used, and the use of more than one term for the same lithostratigraphic unit by different authors, should be dealt with.

REFERENCES

- Abduladim, E. (1987) Geologic Review, Meghil- Ain Jarbi Area, Concession 6. Geologic Note 158, Sirte Oil Company, Exploration Department. Libya.
- Agoco. (1980), Geology of a Stratigraphic Giant- The Messlah Oil Field In: Symp. Geol. Libya (ed. M. Salem & M. Busrewil). Fac. Sci., Univ. Libya, Tripoli, 521-536.
- Barr, F. T. (1968), "Upper Cretaceous Stratigraphy of the Jabal al Akhdar, Northern Cyrenaica". In Geology and Archaeology of Northern Cyrenaica, Libya, F. T. Barr, ed. Petroleum Exploration. Sirte Oil Company. Libya, pp. 131-147, Tripoli.
- Barr, A. T. and Weegar, A. A. (1972), Stratigraphic nomenclature of the Sirte Basin, Libya. Petroleum Exploration. Sirte Oil Company. Libya, 179 p.
- Barr, F. and Berggren, W. (1980), Lower Tertiary biostratigraphy and tectonics. In: Symp. Geol. Libya (ed. M. Salem & M. Busrewil). Fac. Sci., Univ. Libya, Tripoli, 163-191.
- Benfield, A. and Wright, E. (1980), Post-Eocene sedimentation in the eastern Sirte Basin. In: Symp. Geol. Libya (ed. M. Salem & M. Busrewil). Fac. Sci., Univ. Libya, Tripoli, 463-499.
- Ben Saleh, F. and Ettir, O. (1975), Evaluation of Concession 5, Geol. Note. 187, Sirte Oil Company, Brega, Libya.
- Bezan, A. M. (1975), Eocene-Cretaceous rock salinity for Sirte Basin, Geol. Note. 60, Sirte Oil Company, Brega, Libya.
- Bonnefous, J. (1972), Geology of the Quartzitic "Gargaf Formation" in the Sirte Basin, Libya. Bull. Centr. Rech. Pap, 225-261.
- Brown, L. F. and Fisher, W. L. (1977), Seismic-stratigraphic interpretation of a depositional system: examples from Brazilian rift and pull-apart basins: AAPG Memoir 26, p. 213-248.

- Brown, J. E. (1981), Jahama Platform Study, Geol. Note. 141, Sirte Oil Company, Brega, Libya.
- Coffen, J. A. (1986), Seismic exploration fundamentals (Second Edition).
- Depew, D. B and Taleb, T. M (1976), Meghil Field study, Esso/NOC Concession 6, LAR, Geologic Note 186, Esso Standard Libya Inc.
- Dobrin, M. B. (1977), Seismic exploration for stratigraphic traps: AAPG Memoir 26, 329-352.
- Dunbar, C. O. and Rodgers, J. (1957), Principles of stratigraphy. Wiley International Edition, London.
- Fatmi, A. N., Eliagoubi, B. and Hammuda, S. (1980), Stratigraphic Nomenclature of the pre- Upper Cretaceous Mesozoic Rocks of Jabal Nafusah, NW Libya. In: Symp. Geol. Libya (ed. M. Salem & M. Busrewil). Fac. Sci., Univ. Libya, Tripoli, 57-66.
- Fitch, A. A. (1976), Seismic reflection interpretation. Gebruder Borntraeger, Berlin.
- Geerlings, L. B. and Suessli, P. E. (1983), Stratigraphic review of Concessions NC117B and C, Report submitted to National Oil Corporation by Shell. Pet. Dev. Co. of Libya.
- Gohrbandt, K. H. A. (1966), Upper Cretaceous and Lower Tertiary stratigraphy along the western and southern edges of the Sirte Basin, Libya, a guidebook to the geology and prehistory, J. J. Williams, ed. Petrol. Explor. Sirte Oil Company, Libya, Tripoli. 331-341.
- Hubbard, R. J., Pape, J. and Roberts, D. (1985), Depositional sequence mapping as to illustrate the evolution of a passive continental margin, in O. R. Berg and D. Woolverton, eds., Seismic stratigraphy- II: AAPG Memoir 39, 79-92.
- Keskin, C. (1988), Reservoir characteristics in the Gargaf quartzites of the Meghil and Attahaddy Fields; Geologic Note 168, Exploration Department, Sirte Oil Company.

- Keskin, C. (1988), Comments on Dr Saidi's preliminary report on the Attahaddy Field, Intercompany Correspondence, Sirte Oil Company, Exploration Department, Geology Division.
- Kleyn, A. H. (1983), Seismic reflection interpretation. Applied Science Publishers, London.
- Klilzch, E. (1971), The structural development of parts of North Africa since Cambrian time. In: Symp. Geol. Libya (ed. C. Gray). Fac. Sci., Univ. Libya, Tripoli, 253-262.
- Lyons, P. L. and Dobrin, M. B. (1972), Seismic exploration for stratigraphic traps: AAPG Memoir 16, 225-243.
- McDowell, J. E. (1988), Cretaceous study project, Geologic Note 163, Sirte Oil Company, Brega.
- McQuillin, R., Bacon, M. and Barclay, W. (1984), An introduction to seismic interpretation (Second Edition), Graham and Trotman, London.
- Megrisi, M. and Mamgain, V. D. (1980), The Upper Cretaceous-Tertiary formations of northern Libya: A synthesis. Industrial Research Centre, Tripoli.
- Mitchum, R. M. and Vail, P. R. (1977), Application of seismic reflection configuration to stratigraphic interpretation, section 2: seismic stratigraphic interpretation procedure. In seismic stratigraphy- Application to hydrocarbon exploration, C. E. Payton, ed.: AAPG Memoir 26, Tulsa, Oklahoma, 153-144.
- Mockel, R. R., Studer, M. A. and Suessli, P. E. (1984), Seismic interpretation of Concession NC117B (Marsa Brega, onshore Libya), Report submitted to Sirte Oil Company by Shell Pet. Dev. Co. of Libya.
- Payton, C. E. (1977), ed., Seismic stratigraphy- Application to hydrocarbon exploration: AAPG Memoir 26, 53-62.
- Polson, I. L. (1970), The Jahama Platform "Carbonate", Geol. Rpt. 181, Sirte Oil Company, Brega.

- Selley, R. C. (1969), Near-shore marine and continental sediments of the Sirte Basin, Libya. *Quart. Jour. Geol. Soc.*, vol. 124, pp. 419-460.
- Salem, M. J. and Spreng, A. C. (1980), Middle Miocene Stratigraphy, Al Khums Area, Northwestern Libya. In: *Symp. Geol. Libya* (ed. M. Salem & M. Busrewil). *Fac. Sci., Univ. Libya, Tripoli*, 97-116.
- Sheriff, R. E. (1980), *Seismic stratigraphy*. International Human Resources Development Corporation, Boston.
- Todd, R. G. and Mitchum, R. M. (1977), Identification of Upper Triassic, Jurassic and Lower Cretaceous seismic sequences in Gulf of Mexico and offshore west Africa: *AAPG Memoir 26*, p. 145-164.
- Wallace, F. K. (1988), Northern Jahama Platform and Environs, *Geol. Note 162*, Sirte Oil Company. Libya.
- Williams, J. J. (1968), The Sedimentary and Igneous Reservoirs of the Augila Oil Field, Libya. In *Geology and Archaeology of Northern Cyrenaica, Libya*, F. T. Barr, ed. *Petrol. Explor. Soc. Tripoli, Libya*, 197-205.
- Vail, P. R. and Mitchum, R. M. (1977), Overview of seismic stratigraphy and global changes of sea level: *AAPG. Memoir 26*, p. 49-52.
- Vail, P. R., Mitchum, R. M., Todd, R. G., Widmier, J. M., Thompson, S., Sangree J. B., Bubb, J. N. and Hatlelid, W. G. (1977), Seismic stratigraphy and global changes of sea level In *seismic stratigraphy- Application to hydrocarbon exploration*, C. E. Payton, ed.: *AAPG Memoir 26*, Tulsa, Oklahoma, 63-82.

APPENDIX I WELL DATA USED FOR THE STUDY

FF1-6**Location** : 0.5km South of well FF8-6**Co-ordinates** : 29 34' 21"N ; 19 36' 54"E.**Elevation K.B** : 322'**Classification** : D&A**Spudded date** : 26 /6 /1964**Completion date** : 17 /8/1964**Completion status** : Suspended**Total depth** : 9507'

Formation	Age	K.B depth(ft)	SS depth(ft)	Lithology
Undiff.	Miocene	surface	-	Ls, Ss, Sh.
Muailah	Oligocene	2250	-1928	Ss, Sh, Ls.
Etel	Oligocene	3980	-3658	Sh.
Sheghega	Eocene	4393	-4071	Ls.
Domran	Eocene	6060	-5738	Ls.
Ruaga	Paleocene	7172	-6850	Ls.
Heira	Paleocene	7375	-7053	Sh, Ls.
Zmam	U-Cretaceous	9138	-8816	Ls.
Bahi	U-Cretaceous	9384	-9062	conglo,Ss.
Gargaf	Camb /Ord.	9415	-9093	Orthoquartzite.

FF2-6

Location : 3.7km SE of FF1-6
Co-ordinates : 29 33' 28"N ; 19 38' 54"E
Elevation K.B : 297'
Classification : Exploration outpost
Spudded date : 6/10/1967
Completion date : 13/11/1967
Completion status : D&A
Total depth : 10035'

Formation	Age	K.B depth(ft)	SS depth(ft)	Lithology
Undiff.	Miocene	surface	—	Ls, Ss, Sh.
Muailah	Oligocene	—	—	Ss, Sh, Ls.
Etel	Oligocene	3995	-3698	Sh.
Sheghega	Eocene	4465	-4168	Ls.
Domran	Eocene	6280	-5983	Ls.
Ruaga	Paleocene	—	—	Ls.
Heira	Paleocene	7560	-7263	Sh, Ls.
Zmam	U-Cretaceous	9496	-9199	Ls.
Socna	U-Cretaceous	9920	-9623	Ss, Sh, Ls.
Bahi	U-Cretaceous	9865	-9572	conglo,Ss.
Gargaf	Camb /Ord.	9937	-9640	Orthoquartzite.

FF3-6

Location : 2.8km SE of FF1-6
Coordinates : 29 32' 52"N ; 19 37' 41"E
Elevation K.B : 362'
Classification : Exploration outpost
Spudded date : 24/4/1967
Completion date : 30/7/1967
Completion status : Gas well
Total depth : 12104'

Formation	Age	K.B depth(ft)	SS depth(ft)	Lithology
Undiff.	Miocene	surface	—	Ls, Ss, Sh.
Muailah	Oligocene	—	—	Ss, Sh, Ls.
Etel	Oligocene	3951	-3589	Sh.
Sheghega	Eocene	4328	-4020	Ls.
Domran	Eocene	6099	-5737	Ls.
Ruaga	Paleocene	7194	-6832	Ls.
Heira	Paleocene	7427	-7065	Sh, Ls.
Zmam	U-Cretaceous	9192	-8830	Ls.
Gargaf	Camb /Ord.	9289	-8927	Orthoquartzite.

FF4-6**Location** : v87-407, v87-406 intersection**Co-ordinates** : 29 33' 01"N ; 19 36' 12"E**Elevation K.B** : 362'**Classification** : Exploration outpost**Spudded date** : 24/10/1985**Completion date** : 12/2/1986**Completion status** : Gas well**Total depth** : 11170'

Formation	Age	K.B depth(ft)	SS depth(ft)	Lithology
Undiff.	Miocene	surface	-	Ls, Ss, Sh.
Muailah	Oligocene	-	-	Ss, Sh, Ls.
Etel	Oligocene	3940	-3578	Sh.
Sheghega	Eocene	4363	-4001	Ls.
Domran	Eocene	6142	-5780	Ls.
Ruaga	Paleocene	7266	6904	Ls.
Heira	Paleocene	7538	-7176	Sh, Ls.
Zmam	U-Cretaceous	9264	-8902	Ls.
Bahi	U-Cretaceous	9376	-9014	conglo,Ss.
Gargaf	Camb /Ord.	9400	-9038	Orthoquartzite.

FF5-6

Location : v87-419 SP 700
Co-ordinates : 29 34' 29"N ; 19 35' 24"E
Elevation K.B : 350'
Classification : Exploration outpost
Spudded date : 20/2/1986
Completion date : 5/5/1986
Completion status : Gas well
Total depth : 11214'

Formation	Age	K.B depth(ft)	SS depth(ft)	Lithology
Undiff.	Miocene	surface	-	Ls, Ss, Sh.
Muailah	Oligocene	-	-	Ss, Sh, Ls.
Etel	Oligocene	4014	-3664	Sh.
Sheghega	Eocene	4430	-4080	Ls.
Domran	Eocene	6218	-5868	Ls.
Ruaga	Paleocene	7243	-6893	Ls.
Heira	Paleocene	7552	-7202	Sh, Ls.
Zmam	U-Cretaceous	9678	-9328	Ls.
Socna	U-Cretaceous	10050	-9700	Ss, Sh, Ls.
Gargaf	Camb /Ord.	10653	-10285	Orthoquartzite.

FF6-6

Location : 6km SE of FF3-6
Co-ordinates : 29 30' 26"N ; 19 40' 14"E
Elevation K.B : 328'
Classification : Exploration outpost
Spudded date : 12/5/1986
Completion date : 15/9/1986
Completion status : Gas well
Total depth : 12065'

Formation	Age	K.B depth(ft)	SS depth(ft)	Lithology
Undiff.	Miocene	surface	-	Ls, Ss, Sh.
Muailah	Oligocene	2252	-1924	Ss, Sh, Ls.
Etel	Oligocene	3970	-3642	Sh.
Sheghega	Eocene	4475	-4147	Ls.
Domran	Eocene	6322	-5994	Ls.
Ruaga	Paleocene	7500	-7172	Ls.
Heira	Paleocene	7819	-7491	Sh, Ls.
Zmam	U-Cretaceous	10350	-10022	Ls.
Socna	U-Cretaceous	10850	-10522	Ss, Sh, Ls.
Bahi	U-Cretaceous	11312	-10984	conglo,Ss.
Gargaf	Camb /Ord.	11595	-11267	Orthoquartzite.

FF7-6

Location : v87-412 SP 360
Co-ordinates : 29 36' 21"N ; 19 37' 38"E
Elevation K.B : 137'
Classification : Exploration outpost
Spudded date : 23/9/1986
Completion date : 13/1 /1987
Completion status : Gas well
Total depth : 12594'

Formation	Age	K.B depth(ft)	SS depth(ft)	Lithology
Undiff.	Miocene	surface	_	Ls, Ss, Sh.
Muailah	Oligocene	2368	-2195	Ss, Sh, Ls.
Etel	Oligocene	4084	-3911	Sh.
Sheghega	Eocene	4662	-4489	Ls.
Domran	Eocene	6690	-6517	Ls.
Ruaga	Paleocene	7335	-7162	Ls.
Heira	Paleocene	7502	-7329	Sh, Ls.
Zmam	U-Cretaceous	9718	-9549	Ls.
Socna	U-Cretaceous	10132	-9959	Ss, Sh, Ls.
Bahi	U-Cretaceous	11082	-10909	conglo,Ss.
Gargaf	Camb /Ord.	11237	-11064	Orthoquartzite.

FF8-6

Location : 2.5km East of FF5-6
Co-ordinates : 29 34' 33"N ; 19 36' 57"E
Elevation K.B : 287'
Classification : Development well
Spudded date : 16/6/1986
Completion date : 2/10/1986
Completion status : Suspended Gas well
Total depth : 12018'

Formation	Age	K.B depth(ft)	SS depth(ft)	Lithology
Undiff.	Miocene	surface	-	Ls, Ss, Sh.
Muailah	Oligocene	2257	-1970	Ss, Sh, Ls.
Etel	Oligocene	3960	-3673	Sh.
Sheghega	Eocene	4392	-4105	Ls.
Domran	Eocene	6156	-5878	Ls.
Ruaga	Paleocene	7140	-6853	Ls.
Heira	Paleocene	7348	-7061	Sh, Ls.
Zmam	U-Cretaceous	9038	-8751	Ls.
Gargaf	Camb /Ord.	9220	-8933	Orthoquartzite.

FF9-6

Location : 7.5km SE of FF3-6
Co-ordinates : 29 30' 54"N ; 19 41' 15"E
Elevation K.B : 283'
Classification : Exploration outpost
Spudded date : 9/10/1986
Completion date : 21/1/1987
Completion status : Suspended Gas well
Total depth : 12000'

Formation	Age	K.B depth(ft)	SS depth(ft)	Lithology
Undiff.	Miocene	surface	-	Ls, Ss, Sh.
Muailah	Oligocene	2237	-1954	Ss, Sh, Ls.
Etel	Oligocene	3948	-3665	Sh.
Sheghega	Eocene	4485	-4202	Ls.
Domran	Eocene	6396	-6113	Ls.
Ruaga	Paleocene	7430	-7147	Ls.
Heira	Paleocene	7696	-7413	Sh, Ls.
Zmam	U-Cretaceous	9998	-9715	Ls.
Socna	U-Cretaceous	10442	-10159	Ss, Sh, Ls.
Gargaf	Camb /Ord.	10790	-10507	Orthoquartzite.

FF10-6

Location : 7.1km SE of FF6-6
Co-ordinates : 29 27' 23"N ; 19 50' 54"E
Elevation K.B : 376'
Classification : Exploration outpost
Spudded date : 23/1/1987
Completion date : 15/4/1987
Completion status : D&A
Total depth : 12630

Formation	Age	K.B depth(ft)	SS depth(ft)	Lithology
Undiff.	Miocene	surface	-	Ls, Ss, Sh.
Muailah	Oligocene	2175	-1799	Ss, Sh, Ls.
Etel	Oligocene	3966	-3590	Sh.
Sheghega	Eocene	4440	-4064	Ls.
Domran	Eocene	6256	-5880	Ls.
Ruaga	Paleocene	7451	-7075	Ls.
Heira	Paleocene	7780	-7404	Sh, Ls.
Zmam	U-Cretaceous	10593	-10217	Ls.
Socna	U-Cretaceous	11030	-10654	Ss, Sh, Ls.
Gargaf	Camb /Ord.	12345	-11969	Orthoquartzite.

FF11-6

Location : v87-410 SP 545
Co-ordinates : 29 34' 05"N ; 19 39' 53"E
Elevation K.B : 248'
Classification : Exploration outpost
Spudded date : 22/6/1987
Completion date : 18/7/1987
Completion status : Gas well
Total depth : 12753'

Formation	Age	K.B depth(ft)	SS depth(ft)	Lithology
Undiff.	Miocene	surface	-	Ls, Ss, Sh.
Muailah	Oligocene	2325	-2087	Ss, Sh, Ls.
Etel	Oligocene	4004	-2756	Sh.
Sheghega	Eocene	4578	-4430	Ls.
Domran	Eocene	6473	-6225	Ls.
Ruaga	Paleocene	7446	-7198	Ls.
Heira	Paleocene	7670	-7422	Sh, Ls.
Zmam	U-Cretaceous	9790	-9542	Ls.
Socna	U-Cretaceous	10181	-9940	Ss, Sh, Ls.
Gargaf	Camb /Ord.	10715	-10467	Orthoquartzite.

FF12-6

Location : v87-412 SP 635
Co-ordinates : 29 33' 01"N ; 19 42' 06"E
Elevation K.B : 239'
Classification : Exploration outpost
Spudded date : 24/7/1987
Completion date : 3/10/1987
Completion status : D&A
Total depth : 12607'

Formation	Age	K.B depth(ft)	SS depth(ft)	Lithology
Undiff.	Miocene	surface	—	Ls, Ss, Sh.
Muailah	Oligocene	2351	-2112	Ss, Sh, Ls.
Etel	Oligocene	4104	-3865	Sh.
Sheghega	Eocene	4738	-4499	Ls.
Domran	Eocene	6925	-6686	Ls.
Ruaga	Paleocene	7691	-7452	Ls.
Heira	Paleocene	7924	-7685	Sh, Ls.
Zmam	U-Cretaceous	10199	-9960	Ls.
Socna	U-Cretaceous	10669	-10430	Ss, Sh, Ls.
Bahi	U-Cretaceous	11908	-11689	conгло,Ss.
Gargaf	Camb /Ord.	12234	-11995	Orthoquartzite.

FF13-6

Location : v87-412 SP 455
Co-ordinates : 29 35' 18"N ; 19 39' 26"E
Elevation K.B : 190'
Classification : Exploration outpost
Spudded date : 15/10/1987
Completion date : 30/1/1987
Completion status : Suspended Gas well
Total depth : 12524'

Formation	Age	K.B depth(ft)	SS depth(ft)	Lithology
Undiff.	Miocene	surface	-	Ls, Ss, Sh.
Muailah	Oligocene	2576	-2386	Ss, Sh, Ls.
Etel	Oligocene	4114	-8924	Sh.
Sheghega	Eocene	4762	-4572	Ls.
Domran	Eocene	6788	-6598	Ls.
Ruaga	Paleocene	7558	-7368	Ls.
Heira	Paleocene	7742	-7552	Sh, Ls.
Zmam	U-Cretaceous	10028	-9838	Ls.
Socna	U-Cretaceous	10492	-10302	Ss, Sh, Ls.
Bahi	U-Cretaceous	11678	-11488	conglo,Ss.
Gargaf	Camb /Ord.	11916	-11720	Orthoquartzite.

FF14-6

Location : v87-405 SP 710
Co-ordinates : 29 31' 28"N ; 19 37' 13"E
Elevation K.B : 375'
Classification : Exploration outpost
Spudded date : 16/12/1987
Completion date : 12/4/1988
Completion status : D&A
Total depth : 13426'

Formation	Age	K.B depth(ft)	SS depth(ft)	Lithology
Undiff.	Miocene	surface	-	Ls, Ss, Sh.
Muailah	Oligocene	-	-	Ss, Sh, Ls.
Etel	Oligocene	4020	-3647	Sh.
Sheghega	Eocene	4490	-4117	Ls.
Domran	Eocene	6287	-5912	Ls.
Ruaga	Paleocene	7449	-7074	Ls.
Heira	Paleocene	8323	-7948	Sh, Ls.
Zmam	U-Cretaceous	10525	-10150	Ls.
Socna	U-Cretaceous	11156	-10781	Ss, Sh, Ls.
Gargaf	Camb /Ord.	13092	-13348	Orthoquartzite.

FF15-6

Location : 1.8km SE of FF6-6
Co-ordinates : 29 21' 42"N ; 19 40' 59"E
Elevation K.B : 328'
Classification : Exploration outpost
Spudded date : 18/4/1988
Completion date : 22/8/1988
Completion status : Gas well
Total depth : 12638'

Formation	Age	K.B depth(ft)	SS depth(ft)	Lithology
Undiff.	Miocene	surface	-	Ls, Ss, Sh.
Muailah	Oligocene	2233	-1905	Ss, Sh, Ls.
Etel	Oligocene	4013	-3685	Sh.
Sheghega	Eocene	4508	-4180	Ls.
Domran	Eocene	6298	-5970	Ls.
Ruaga	Paleocene	7357	-7029	Ls.
Heira	Paleocene	7609	-7281	Sh, Ls.
Zmam	U-Cretaceous	10175	-9847	Ls.
Socna	U-Cretaceous	10642	-10314	Ss, Sh, Ls.
Bahi	U-Cretaceous	11674	-11346	conglo,Ss.
Gargaf	Camb /Ord.	11712	-11383	Orthoquartzite.

FF16-6**Location** : v87-410, v87-413 intersection**Co-ordinates** : 29 36' 06"N ; 19 35' 42"E**Elevation K.B** : 187'**Classification** : Delineation well**Spudded date** : 28/8/1988**Completion date** : 7/12/1988**Completion status** : Gas well**Total depth** : 12256'

Formation	Age	K.B depth(ft)	SS depth(ft)	Lithology
Undiff.	Miocene	surface	-	Ls, Ss, Sh.
Muailah	Oligocene	1893	1706	Ss, Sh, Ls.
Etel	Oligocene	4043	-3856	Sh.
Sheghega	Eocene	4487	-4300	Ls.
Domran	Eocene	6387	-6200	Ls.
Ruaga	Paleocene	7207	-7020	Ls.
Heira	Paleocene	7462	-7275	Sh, Ls.
Zmam	U-Cretaceous	9627	-9440	Ls.
Socna	U-Cretaceous	10012	-9825	Ss, Sh, Ls.
Bahi	U-Cretaceous	11187	-11000	conglo,Ss.
Gargaf	Camb /Ord.	11342	-11155	Orthoquartzite.

APPENDIX II SEISMIC TWO-WAY TRAVEL TIME VALUES.

Line number - v87-400

shot-point	Two-way travel time (msec)			
	Sheghega	Heira	Zmam	Bahi/Gargaf
500	960	1540	2180	2350
520	980	1560	2190	2400
540	980	1570	2180	2410
560	980	1560	2160	2530
580	980	1560	2160	2530
600	970	1560	2140	2510
620	970	1540	2140	2520
640	970	1560	2140	2490
660	960	1550	2130	2540
680	970	1550	2130	2520
700	960	1540	2100	2450
720	950	1520	2090	2400
740	960	1510	2090	2390
760	960	1500	2080	2370
780	970	1510	2070	2400
800	980	1520	2080	2380
820	980	1520	2100	2360
840	990	1520	2130	2370
860	980	1510	2130	2400
880	980	1520	2150	2390
900	980	1530	2150	2380
920	990	1530	2160	2370
940	980	1520	2170	2380
960	980	1500	2150	2380
980	970	1500	2150	2380
1000	970	1500	2160	2400

Line number - v87-401

shot-point	Two-way travel time (msec)			
	Sheghega	Heira	Zmam	Bahi/Gargaf
140	920	1540	2030	2290
160	930	1440	2040	2310
180	940	1550	2080	2350
200	950	1500	2080	2400
220	970	1550	2100	2430
240	970	1540	2100	2440
260	980	1550	2140	2440
280	990	1550	2220	2490
300	1000	1550	2220	2520
320	1010	1550	2230	2560
340	1010	1580	2220	2600

Line number - v87-402

shot-point	Two-way travel time (msec)			
	Sheghega	Heira	Zmam	Bahi/Gargaf
480	900	1430	1870	2280
500	900	1450	1900	2290
520	920	1450	1920	2270
540	920	1440	1950	2270
560	910	1430	1970	2270
580	920	1440	2000	2270
600	950	1440	2010	2250
620	950	1440	2000	2220
640	950	1430	1980	2210
660	950	1420	1970	2190
680	940	1430	1920	2120
700	940	1420	1920	2100
720	940	1410	1910	2120
740	940	1430	1910	2120
760	940	1440	1920	2130
780	950	1460	2000	2140
800	960	1480	2030	2370
820	960	1480	2060	2410
840	970	1470	2080	2420
860	970	1520	2150	F
880	990	1540	2160	2500
900	1000	1560	2180	2470
920	1010	1010	1580	2470
940	1010	1580	2290	2530
960	1010	1580	2280	2520
980	1010	1570	2260	2580
1000	1000	1570	2250	2520
1020	980	1550	2230	2500
1040	990	1540	2220	2480
1060	970	1540	2230	2470
1080	980	1540	2240	2470
1100	990	1550	2240	2480
1120	990	1550	2240	2480
1140	990	1550	2240	2480
1160	1010	1560	2230	2480
1180	1000	1560	2230	2470
1200	990	1550	2220	2470
1220	980	1540	2220	2520
1240	980	1540	2220	2540
1260	980	1530	2210	2540
1280	980	1540	2210	2540

Line v87-402 continued

1300	990	1570	2210	2570
1320	1000	1570	2220	2580
1340	1020	1570	2220	2580
1360	1010	1570	2220	2560
1380	1000	1540	2190	2500

Line number - v87-403

shot-point	Two-way travel time (msec)			
	Sheghega	Heira	Zmam	Bahi/Gargaf
280	950	1530	2080	2480
300	960	1540	2110	2490
320	970	1540	2130	2510
340	980	1550	2170	2530
360	990	1560	2250	2560
380	1010	1570	2260	2570
400	1020	1580	2280	2610
420	1030	1580	2300	F
440	1030	1590	2230	2730
460	1040	1580	2190	2710
480	1040	1580	2180	2660
500	1040	1560	2180	2620
520	1030	1590	2180	2620
540	1050	1590	2180	2590
560	1030	1580	2160	2580

Line number - v87-404

shot-point	Two-way travel time (msec)			
	Sheghega	Heira	Zmam	Bahi/Gargaf
320	1000	1480	2050	2390
340	1020	1490	2050	2420
360	1010	1490	2040	2380
380	1010	1480	2060	2370
400	1020	1500	2050	2380
420	1010	1490	2050	2370
440	1010	1500	2060	2370
460	1020	1500	2050	2450
480	1000	1500	2050	2400
500	1010	1490	2100	2400
520	1010	1490	2020	2370
540	1000	1500	2020	2370
560	1010	1510	2040	2380
580	1020	1520	2060	2400
600	1020	1530	2080	2440
620	1020	1550	2120	2530
640	1020	1550	2130	2550
660	1030	1550	2130	2670
680	1030	1550	2140	2640
700	1040	1580	2160	2670
720	1040	1570	2130	2860
740	1040	1570	2130	2550
760	1040	1570	2120	2540
780	1040	1560	2120	2560
800	1030	1560	2130	2690
820	1040	1580	2200	2700
840	1020	1590	2200	2690
860	1030	1590	2220	2690
880	1020	1590	2220	2700

Line number - v87-405

shot-point	Two-way travel time (msec)			
	Sheghega	Heira	Zmam	Bahi/Gargaf
480	910	1510	2110	2300
500	950	1540	2150	2330
520	970	1550	2180	2400
540	990	1580	2200	2450
560	1000	1580	2200	2460
580	1000	1570	2190	2460
600	1000	1560	2180	2470
620	1010	1540	2120	2460
640	1010	1570	2120	2490
660	1020	1560	2160	2550
680	1020	1570	2130	2550
700	1040	1580	2130	2530
720	1030	1560	2120	2540
740	1030	1530	2110	2520
760	1020	1520	2090	2510

Line number - v87-406

shot-point	Two-way travel time (msec)			
	Sheghega	Heira	Zmam	Bahi/Gargaf
240	1000	1510	2120	2450
260	1050	1520	2120	2470
280	1010	1530	2100	2470
300	1060	1530	2150	2650
320	1050	1520	2100	2680
340	1040	1500	2030	2430
360	1030	1500	2080	2430
380	1030	1500	2070	2430
400	1030	1520	2080	2450
420	1040	1530	2090	2460
440	1040	1520	2100	2490
460	1040	1520	2080	2480
480	1030	1520	2010	2460
500	1030	1510	2010	2390
520	1040	1520	2020	2420
540	1020	1530	2040	2450
560	1030	1550	2050	2460
580	1020	1530	2060	2470
600	1020	1520	2050	2490
620	1010	1530	2050	2500
640	1010	1510	2040	2500
660	1020	1510	2040	2500
680	1010	1510	2030	2490
700	980	1530	2040	2490

Line number - v87-407

shot-point	Two-way travel time (msec)			
	Sheghega	Heira	Zmam	Bahi/Gargaf
440	940	1510	2120	2370
460	950	1510	2100	2360
480	950	1500	2080	2350
500	940	1480	2080	2360
520	950	1470	2070	2380
540	970	1490	2080	2400
560	990	1500	2090	2430
580	1000	1520	2120	2470
600	1010	1540	2140	2500
620	1020	1550	2180	F
640	1030	1540	2140	2720
660	1030	1530	2180	2540
680	1010	1500	2050	2510
700	1010	1490	2020	2510
720	1020	1480	2100	2520

Line number - v87-408

shot-point	Two-way travel time (msec)			
	Sheghega	Heira	Zmam	Bahi/Gargaf
200	1030	1550	2110	2420
220	1070	1550	2120	2440
240	1040	1550	2140	2450
260	1060	1550	2120	2440
280	1050	1540	2100	2440
300	1060	1530	2100	2460
320	1050	1530	2100	2500
340	1070	1530	2110	2520
360	1060	1530	2240	2760
380	1060	1540	2220	2770
400	1060	1530	2060	2310
420	1060	1540	2030	2280
440	1050	1540	2020	2310

Line number - v87-409

shot-point	Two-way travel time (msec)			
	Sheghega	Heira	Zmam	Bahi/Gargaf
500	920	1430	1970	2130
520	910	1440	1970	2110
540	910	1440	1970	2090
560	930	1440	1980	2110
580	940	1450	2000	2140
600	960	1470	2050	2380
620	980	1490	2040	2410
640	1010	1530	2080	2440
660	1030	1540	2100	2480
680	1050	1560	2140	2500
700	1030	1550	2120	2470
720	1040	1540	2080	2460
740	1030	1520	2050	2510
760	1020	1510	2030	2510
780	1040	1520	2030	2520
800	1040	1530	2060	2540

Line number - v87-410

shot-point	Two-way travel time (msec)			
	Sheghega	Heira	Zmam	Bahi/Gargaf
180	1100	1580	2160	2440
200	1120	1580	2100	2440
220	1110	1580	2110	2460
240	1120	1540	2130	2470
260	1100	1550	2150	2480
280	1090	1560	2160	2480
300	1100	1560	2130	2480
320	1100	1560	2100	2450
340	1100	1560	2080	2400
360	1090	1560	2070	2360
380	1090	1560	2060	2310
400	1090	1550	2020	2280
420	1090	1540	1990	2250
440	1050	1540	1960	2220
460	1070	1530	1910	2140
480	1050	1520	1890	2130
500	1050	1560	1980	2150
520	1050	1540	1910	2180
540	1060	1560	1950	2190

Line number - v87-411

shot-point	Two-way travel time (msec)			
	Sheghega	Heira	Zmam	Bahi/Gargaf
560	910	1410	1870	2060
580	910	1410	1870	2060
600	920	1420	1880	2080
620	920	1420	1890	2100
640	930	1430	1900	2120
660	950	1440	2050	2380
680	960	1460	2000	2420
700	980	1480	2080	2440
720	990	150	2020	2360
740	1020	1520	2040	2390
760	1030	1530	2060	2390
780	1020	1530	2050	2410
800	1040	1540	2020	2450
820	1030	1510	2020	F
840	1050	1530	2020	2190
860	1060	1530	1940	2190
880	1080	1550	1970	2220
900	1090	1540	1980	2230

Line number - v87-412

shot-point	Two-way travel time (msec)			
	Sheghega	Heira	Zmam	Bahi/Gargaf
140	1150	1570	2160	2540
160	1170	1590	2160	2540
180	1160	1600	2170	2530
200	1150	1610	2170	2510
220	1150	1610	2160	2480
240	1150	1600	2150	2460
260	1150	1590	2150	2460
280	1140	1580	2130	2410
300	1130	1570	2120	2310
320	1120	1570	2120	2300
340	1120	1560	F	2310
360	1120	1590	2020	230
380	1120	1580	2030	2300
400	1130	1600	2040	2330
420	1130	1610	2050	2360
440	1140	1620	2060	2370
460	1140	1620	2060	2390
480	1150	1630	2100	2410
500	1150	1640	2100	2380
520	1160	1630	2090	2380
540	1160	1620	2080	2400
560	1170	1630	2100	2420
580	1170	1640	2110	2410
600	1170	1640	2120	2410
620	1180	1650	2120	2410
640	1170	1650	2120	2410

Line number - v87-413

shot-point	Two-way travel time (msec)			
	Sheghega	Heira	Zmam	Bahi/Gargaf
580	900	1410	1890	2080
600	910	1420	1870	2090
620	910	1420	1870	2090
640	920	1420	1870	2090
660	930	1430	1890	2100
680	930	1430	1910	2110
700	950	1440	1920	2350
720	950	1460	1940	2170
740	980	1480	2010	2180
760	980	1480	1990	2350
780	1020	1500	2050	2380
800	1030	1520	2020	2410
820	1030	1520	2010	2430
840	1040	1510	1990	2460
860	1050	1510	2050	2270
880	1050	1520	1980	2270
900	1080	1540	2020	2270
920	1100	1560	2020	2280
940	1110	1560	2020	2300
960	1120	1570	2120	2310
980	1120	1570	2120	2320
1000	1140	1580	2160	2420
1020	1160	1600	2180	2440
1040	1190	1630	2180	2500
1060	1230	1650	2210	2540
1080	1250	1670	2220	2600
1100	1280	1670	2260	2660
1120	1280	1660	2210	2670
1140	1300	1650	2180	F
1160	1300	1650	2070	2250
1180	1330	1660	2080	2270
1200	1360	1670	2100	2290
1220	1390	1690	2120	2310

Line number - v87-415

shot-point	Two-way travel time (msec)			
	Sheghega	Heira	Zmam	Bahi/Gargaf
640	910	1410	1930	2150
660	920	1420	1930	2170
680	920	1420	1930	2170
700	930	1410	1930	2150
720	940	1420	1950	219
740	950	1430	1970	2240
760	960	1460	1990	2320
780	970	1480	2020	2320
800	990	1490	2050	2380
820	1010	1510	2080	2390
840	1030	1520	2090	2430
860	1040	1530	2080	2450
880	1040	1520	2050	2270
900	1060	1530	2040	2270
920	1060	1540	2050	2300
940	1090	1560	2070	2340
960	1110	1570	2100	2400
980	1130	1580	2120	2480
1000	1130	1580	2130	2480
1020	1130	1590	2140	2420
1040	1150	1600	2140	2450
1060	1170	1620	2150	2500
1080	1180	1630	2160	2520
1100	1200	1640	2280	2550
1120	1250	1650	2250	2720
1140	1250	1650	2220	2770
1160	1290	1650	2190	2790
1180	1280	1660	2190	2550
1200	1310	1670	2190	2560
1220	1350	1670	2190	2560

Line number - v87-417

shot-point	Two-way travel time (msec)			
	Sheghega	Heira	Zmam	Bahi/Gargaf
700	920	1440	2030	2250
720	930	1430	2030	2250
740	930	1430	2030	2260
760	930	1430	2000	2220
780	940	1440	2000	2220
800	950	1450	2000	F
820	980	1460	2040	2330
840	980	1470	2050	2340
860	1000	1480	2050	2350
880	1020	1520	2060	2380
900	1040	1520	2060	2410
920	1040	1530	2080	2430
940	1050	1530	F	2480
960	1050	1530	2260	F
980	1070	1530	2260	2760
1000	1070	1540	2120	2460
1020	1100	1550	2120	2460
1040	1120	1580	2130	2500
1060	1150	1600	2150	2490
1080	1160	1610	2170	2530
1100	1170	1630	2170	2580
1120	1200	1640	2190	2590
1140	1210	1640	2220	2660
1160	1220	1650	2260	2690
1180	1220	1650	2240	2690
1200	1250	1660	2160	2660
1220	1280	1680	2170	2660
1240	1320	1690	2190	2650
1260	1340	1740	2200	2650

Line number - v87-419

shot-point	Two-way travel time (msec)			
	Sheghega	Heira	Zmam	Bahi/Gargaf
480	950	1400	1910	2030
500	930	1420	1920	2040
520	930	1420	1950	2090
540	940	1430	1930	2110
560	950	1450	1940	2130
580	960	1470	1950	2140
600	980	1480	2020	2150
620	1000	1510	2040	2380
640	1030	1530	2070	2410
660	1020	1520	2080	2430
680	1020	1510	2010	2440
700	1030	1500	1950	2460
720	1030	1520	1950	2450
740	1040	1510	1950	2460

Line number - v87-421

shot-point	Two-way travel time (msec)			
	Sheghega	Heira	Zmam	Bahi/Gargaf
80	970	1540	2120	2320
100	990	1540	2130	2340
120	990	1540	2110	2370
140	980	1560	2190	2390
160	970	1570	2210	2430
180	970	1570	2220	2480
200	1000	1600	2240	2530
220	1020	1610	2270	2550
240	1030	1620	2280	2550
260	1040	1630	2270	2460
280	1040	1630	2290	2560
300	1040	1630	2310	260
320	1040	1630	2310	2570
340	1050	1630	2280	2540
360	1050	1630	2270	2510
380	1070	1630	2310	2550
400	1100	1640	2390	2570

**APPENDIX III AVERAGE VELOCITY AND DEPTH VALUES FOR
THE RESERVOIR HORIZON (BAHI/GARGAF).**

Line number V87-400

Shot-point	Average velocity (ft/s)	Sub-sea depth	
		feet	metre
500	8938	11560	3523
520	9916	11900	3627
540	9931	11969	3648
560	10119	12802	3902
580	10103	12731	3880
600	10088	12661	3859
620	10103	12731	3880
640	10056	12521	3816
660	10134	12872	3923
680	10103	12731	3880
700	9994	12244	3732
720	9916	11900	3627
740	9900	11832	3606
760	9869	11696	3565
780	9916	11900	3627
800	9885	11764	3586
820	9853	11628	3544
840	9869	11696	3565
860	9916	11900	3627
880	9900	11832	3600
900	9885	11764	3586
920	9869	11696	3565
940	9885	11764	3586
960	9885	11764	3586
980	9885	11764	3586
1000	9916	11900	3627

Line number V87-401

Shot-point	Average velocity (ft/s)	Sub-sea depth	
		feet	metre
140	9744	11158	3401
160	9775	11292	3442
180	9838	11560	3524
200	9916	11900	3627
220	9963	12106	3690
240	9978	12175	3711
260	9978	12175	3711
280	10056	12521	3817
300	10103	12730	38181
320	10166	13013	3966
340	10228	13298	4053

Line number V87-402

Shot-point	Average velocity (ft/s)	Sub-sea depth	
		feet	metre
480	9728	11092	3381
500	9744	11158	3401
520	9713	11025	3360
540	9713	11025	3360
560	9713	11025	3360
580	9713	11025	3360
600	9682	10893	3320
620	9635	10696	3260
640	9619	10630	3240
660	9588	10500	3200
680	9478	10048	3063
700	9447	9921	3024
720	9478	10048	3063
740	9478	10048	3063
760	9494	10112	3082
780	9510	10176	3102
800	9869	11696	3565
820	9931	11969	3648
840	9947	12037	3669
860	F	F	F
880	10072	12591	3838
900	10025	12382	3774
920	10025	12382	3774
940	10119	12802	3902
960	10103	12731	3881
980	10197	13155	4010
1000	10103	12731	3881
1020	10072	12591	3838
1040	10041	12452	3795
1060	10025	12382	3774
1080	10025	12382	3774
1100	10041	12452	3795
1120	10041	12452	3795
1140	10041	12452	3795
1160	10041	12452	3795
1180	10025	12382	3774
1200	10025	12382	3774
1220	10103	12731	3881
1240	10134	12872	3923
1260	10134	12872	3923
1280	10134	12872	3923

Line v87-402 continued

1300	10181	13084	3988
1320	10197	13155	4010
1340	10197	13155	4010
1360	10166	13013	3966
1380	10072	12591	3838

Line number V87-403

Shot-point	Average velocity (ft/s)	Sub-sea depth	
		feet	metre
280	10041	12452	3795
300	10056	12521	3817
320	10088	12661	3859
340	10119	12802	3902
360	10166	13013	3966
380	10181	13084	3988
400	10244	13369	4075
420	F	F	F
440	10431	14240	4340
460	10400	14093	4296
480	10322	13729	4185
500	10259	13441	4097
520	10228	13298	4053
540	10213	13227	4031
560	10197	13155	4009

Line number V87-404

Shot-point	Average velocity (ft/s)	Sub-sea depth	
		feet	metre
320	9900	11832	3606
340	9947	12037	3669
360	9885	11764	3586
380	9869	11696	3565
400	9885	11764	3586
420	9869	11696	3565
440	9869	11696	3565
460	9994	12244	3732
480	9916	11900	3618
500	9916	11900	3618
520	9869	11696	3565
540	9869	11696	3565
560	9885	11764	3586
580	9916	11900	3618
600	9978	12175	3711
620	10119	12802	3902
640	10150	12943	3945
660	10259	13441	4097
680	10291	13585	4141
700	10322	13802	4207
720	10353	13875	4229
740	10150	12943	3945
760	10134	12872	3923
780	10166	13013	3966
800	10369	13947	4251
820	10384	14020	4273
840	10369	13947	4251
860	10369	13947	4251
880	10384	14020	4273

Line number V87-405

Shot-point	Average velocity (ft/s)	Sub-sea depth	
		feet	metre
480	9760	11225	3421
500	9806	11426	3483
520	9916	11900	3627
540	9994	12244	3732
560	10009	12313	3753
580	10009	12313	3753
600	10025	12382	3774
620	10009	12313	3753
640	10056	12521	3817
660	19150	12943	3945
680	10150	12943	3945
700	10119	12802	3902
720	10134	12872	3923
740	10103	12731	3881
760	10088	12661	3859

Line number V87-406

Shot-point	Average velocity (ft/s)	Sub-sea depth	
		feet	metre
240	9994	12244	3732
260	10025	12382	3774
280	10025	12382	3774
300	10306	13657	4163
320	10353	13875	4229
340	9963	12106	3690
360	9963	12106	3690
380	9963	12106	3690
400	9994	12244	3732
420	10009	12313	3753
440	10056	12521	3817
460	10041	12452	3795
480	10009	12313	3753
500	9900	11832	3606
520	9947	12037	3669
540	9994	12244	3732
560	10009	12313	3753
580	10025	12382	3774
600	10056	12521	3817
620	10072	12591	3838
640	10072	12591	3838
660	10072	12591	3838
680	10056	12521	3817
700	10056	12521	3817

Line number V87-407

Shot-point	Average velocity (ft/s)	Sub-sea depth	
		feet	metre
440	9869	11696	3565
460	9853	11628	3544
480	9838	11560	3524
500	9853	11628	3544
520	9885	11764	3586
540	9916	11900	3627
560	9963	12106	3690
580	10025	12382	3774
600	10072	12591	3838
620	F	F	F
640	10572	14167	4318
660	10134	12872	3923
680	10088	12661	3859
700	10088	12661	3859
720	10103	12731	3881

Line number V87-408

Shot-point	Average velocity (ft/s)	Sub-sea depth	
		feet	metre
200	9947	12037	3669
220	9978	12175	3711
240	9994	12244	3732
260	9978	12175	3711
280	9978	12175	3711
300	10009	12313	3753
320	10072	12591	3838
340	10103	12731	3881
360	10478	14461	4408
380	10493	14535	4430
400	9775	11292	3442
420	9728	11091	3381
440	9775	11292	2442

Line number V87-409

Shot-point	Average velocity (ft/s)	Sub-sea depth	
		feet	metre
500	9494	10112	3082
520	9463	9984	3043
540	9432	9857	3004
560	9463	9984	3043
580	9509	10176	3102
600	9885	11764	3586
620	9931	11969	3648
640	9978	12175	3711
660	10041	12453	3795
680	10072	12591	3838
700	10025	12382	3774
720	10009	12313	3753
740	10088	12661	3859
760	10088	12661	3859
780	10103	12731	3881
800	10134	12872	3923

Line number V87-410

Shot-point	Average velocity (ft/s)	Sub-sea depth	
		feet	metre
180	9978	12175	3711
200	9978	12175	3711
220	10009	12313	3752
240	10025	12382	3774
260	10041	12452	3795
280	10041	12452	3795
300	10041	12452	3795
320	9994	12244	3732
340	9916	11900	3627
360	9853	11628	3544
380	9775	11292	3442
400	9728	11091	3381
420	9682	10893	3320
440	9635	10696	3260
460	9510	10176	3102
480	9494	10112	3082
500	9525	10240	3121
520	9572	10435	3181
540	9588	10500	3200

Line number V87-411

Shot-point	Average velocity (ft/s)	Sub-sea depth	
		feet	metre
560	9385	9667	2947
580	9385	9667	2947
600	9416	9794	2985
620	9447	9921	3024
640	9478	10048	3063
660	9885	11763	3586
680	9947	12037	3669
700	9978	12175	3711
720	9853	11628	3544
740	9900	11832	3606
760	9900	11832	3606
780	9931	11969	3648
800	9994	12244	3732
820	F	F	F
840	9588	10500	3200
860	9588	10500	3200
880	9635	10696	3260
900	9650	10761	3280

Line number V87-412

Shot-point	Average velocity (ft/s)	Sub-sea depth	
		feet	metre
140	10134	12872	3923
160	10134	12872	3923
180	10119	12802	3902
200	10088	12661	3859
220	10041	12452	3795
240	10009	12313	3753
260	10009	12313	3753
280	9931	11969	3648
300	9775	11292	3442
320	9760	11225	3421
340	9775	11292	3442
360	9760	11225	3421
380	9760	11225	3421
400	9806	11426	3483
420	9853	11628	3544
440	9885	11696	3565
460	9900	11832	3606
480	9931	11969	3648
500	9885	11764	3586
520	9885	11764	3586
540	9916	11900	3627
560	9947	12037	3669
580	9931	11969	3648
600	9931	11969	3648
620	9931	11969	3648
640	9931	11969	3648

Line number V87-413

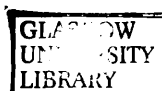
Shot-point	Average velocity (ft/s)	Sub-sea depth	
		feet	metre
580	9416	9794	2985
600	9432	9857	3004
620	9432	9875	3004
640	9432	9857	3004
660	9447	9921	3024
680	9463	9984	3043
700	9838	11560	3524
720	9557	10370	3161
740	9572	11426	3483
760	9838	11560	3524
780	9885	11764	3586
800	9931	11969	3565
820	9963	12106	3690
840	10009	12313	3753
860	9713	11025	3360
880	9713	11025	3360
900	9713	11025	3360
920	9728	11091	3381
940	9760	11225	3421
960	9775	11292	3442
980	9791	11359	3462
1000	9947	12037	3669
1020	9978	12175	3711
1040	10072	12591	3838
1060	10134	12872	3923
1080	10228	13298	4053
1100	10322	13729	4185
1120	10338	13802	4207
1140	F	F	F
1160	9682	10893	3320
1180	9713	11025	3360
1200	9744	11158	3401
1220	9775	11292	3442

Line number V87-415

Shot-point	Average velocity (ft/s)	Sub-sea depth	
		feet	metre
640	9525	10241	3121
660	9557	10370	3161
680	9557	10370	3161
700	9225	10241	3121
720	9588	10500	3200
740	9666	10827	3300
760	9712	11359	3462
780	9791	11359	3462
800	9885	11764	3586
820	9900	11832	3606
840	9963	12106	3690
860	9994	12244	3732
880	9713	11025	3360
900	9713	11025	3360
920	9760	11225	3421
940	9822	11493	3503
960	9916	11900	3627
980	10041	12452	3795
1000	10041	12452	3795
1020	9947	12037	3669
1040	9994	12244	3732
1060	10072	12591	3838
1080	10103	12731	3881
1100	10150	12943	3945
1120	10416	14167	4318
1140	10494	14535	4430
1160	10525	14684	4476
1180	10150	12943	3945
1200	10166	13013	3966
1220	10166	13013	3966

Line number V87-417

Shot-point	Average velocity (ft/s)	Sub-sea depth	
		feet	metre
700	9682	10893	3320
720	9682	10893	3320
740	9697	10959	3340
760	9635	10696	3260
780	9635	10696	3260
800	9728	11091	3381
820	9806	10935	3333
840	9822	11493	3503
860	9838	11560	3524
880	9885	11764	3586
900	9931	11969	3648
920	9963	12106	3690
940	10041	12452	3795
960	F	F	F
980	10478	14461	4408
1000	10009	12313	3753
1020	10009	12313	3753
1040	10072	12591	3838
1060	10056	12521	3817
1080	10119	12802	3902
1100	10197	13155	4009
1120	10213	13227	4031
1140	10322	13729	4185
1160	10369	13947	4251
1180	10369	13947	4251
1200	10322	13729	4185
1220	10322	13729	4185
1240	10306	13657	4163
1260	10306	13657	4163



Line number V87-419

Shot-point	Average velocity (ft/s)	Sub-sea depth	
		feet	metre
480	9338	9479	2890
500	9353	9542	2908
520	9432	9857	3004
540	9463	9984	3043
560	9494	10112	3082
580	9560	10176	3102
600	9525	10241	3121
620	9885	11764	3586
640	9931	11969	3648
660	9963	12106	3690
680	9978	12175	3711
700	10009	12313	3753
720	9994	12244	3732
740	10009	12313	3753

Line number V87-421

Shot-point	Average velocity (ft/s)	Sub-sea depth	
		feet	metre
80	9791	11359	3462
100	9822	11493	3503
120	9869	11696	3565
140	9900	11832	3606
160	9963	12106	3680
180	10041	12452	3795
200	10119	12802	3902
220	10150	12943	3945
240	10150	12943	3945
260	10009	12313	3753
280	10166	13013	3966
300	10228	13298	4053
320	10181	13084	3988
340	10134	12872	3923
360	10088	12661	3859
380	10150	12943	3945
400	10181	13084	3988